I hereby certify that this correspondence is being deposited with the United States Postal Service as first class mail in an envelope addressed to: Commissioner of Patents and Trademarks, Box AF, Washington, D.C. 20231, on _____

By _____

PATENT

Attorney Docket No. 16243-1-5

IN THE UNITED STATES PATENT AND TRADEMARK OFFICE

In re application of:	
Richard H. Tullis	Examiner: J. Martinell
Serial No.: 08/078,768	DECLARATION OF JERRY L. RUTH
Filed: June 16, 1993	
For: OLIGONUCLEOTIDE THERAPEUTIC AGENT AND METHODS OF MAKING SAME	

Box AF
Commissioner of Patents and Trademarks
Washington, D.C. 20231

Sir:

I, Dr. Jerry L. Ruth, being duly warned that willful false statements and the like are punishable by fine or imprisonment or both, under 18 U.S.C. § 1001, and may jeopardize the validity of the patent application or any patent issuing thereon, state and declare as follows:

1. All statements herein made of my own knowledge are true and statements made on information or belief are believed to be true. The Exhibits attached hereto are numbered 1-9. They are each incorporated herein by reference.

2. I have previously submitted a declaration in support of this patent application. My scientific credentials are presented therein.

3. As I understand the Examiner's remaining rejection, he believes that the pending claims should be restricted to the phosphotriester-modified nucleic acids that are stated as a preferred embodiment representing a class of stabilized nucleic acids for *in vivo* applications. The Examiner reasons that the pending claims inclusive of *in vivo* uses are too broad. More specifically, the Examiner states that no other suitable nucleic acid analogs were available as of the filing date in October of 1981, that unmodified nucleic acids would not be adequately stable to have biological activity under *in vivo* conditions, and that the means for administering the antisense molecules would require undue experimentation.

The purpose of this declaration is to address each of the above issues. More specifically, I will explain: (1) that as of the priority filing date, those of skill were aware of other analogs of nucleic acid that were modified to enhance stability against nuclease activity and which were suitable for *in vivo* use; (2) that the stability of natural (unmodified) nucleic acid under *in vivo* conditions is sufficient to permit the observation of its biological activity, *i.e.*, to inhibit expression of specific protein; and, (3) given the level of skill in the art, there is nothing but routine experimentation involved in the *in vivo* use of the claimed method.

A. PRIOR TO THE FILING DATE OF THE PARENT APPLICATION ON OCTOBER 23, 1981, A NUMBER OF STABILIZED NUCLEIC ACID ANALOGUES WERE AVAILABLE FOR USE IN THIS INVENTION.

The alkylphosphotriester DNA analogs described in the application as an example of a stabilized oligonucleotide were described in the literature in 1974 by Miller *et al.* (A1). These analogs have a phosphate bearing four oxygens, three of which are substituted with carbon-based substituents. The following discussion presents other references that describe chemically modified nucleic acids that were available prior to October of 1981 and were used intracellularly. Collectively, they present uncontestable evidence that a variety of stabilized nucleic acids were known and available for use in the claimed invention as of the original filing date.

A second chemically modified nucleic acid was the methylated ribonucleic acids described by Befort *et al.*(1974). Befort is already of record as reference A27. In Befort, the authors reported uptake of their stabilized RNA into fibroblasts and the subsequent inhibition of viral multiplication. The stabilized nucleic acid was a methylated RNA that complemented a portion of the viral genome.

In Tennant *et al.* (1974), the authors describe the *in vivo* effects of an alkylated homopolymer of ribonucleic acid on virally induced oncogenesis. Tennant is already of record as reference A47.

In Kunkel *et al.* (Exhibit 1), *P.N.A.S. USA* 78(11):6734 (1981). The authors describe work conducted and published before 1981 using thio-substituted deoxynucleosides. On column 2 of page 6734, the authors describe that their analogs were previously reported as incorporated into oligonucleotides using DNA polymerase and nuclease resistant.

Finally, Miller *et al.* reported on the *in vivo* effects of a DNA analog in March 1981. This reference is already of record as A2. Attached to this declaration as Exhibit 2 is a true copy of the Medline abstract entry for this reference. The entry clearly identifies its publication date as March 1981, seven months before applicant's filing date. The analog described by Miller in 1981 was an alkyl phosphonate which differs from the phosphotriester of their earlier work by the direct attachment of the alkyl substituent to the phosphate. The Examiner is asked to review page 1879, second column, where a discussion of the intracellular half-lives of the phosphonates and the triesters are compared.

Thus, it is clear that as of the priority filing date of the present application, those of skill would have understood the applicant's reference to stabilized nucleic acid to have included more than the phosphotriester compounds that were specifically identified. Moreover, and because the use of stabilized nucleic acids was a mere example in a universe where both stabilized and natural oligonucleotides would function to downregulate expression of protein under *in vivo* conditions, it was, in my opinion, unnecessary to identify for those of skill all the stabilized nucleic acids that were available for use in the invention as of October of 1981.

B. UNMODIFIED RNA AND DNA HAVE A HALF-LIFE *IN VIVO* THAT IS SUFFICIENT TO PERMIT ITS UPTAKE INTO CELLS.

The Examiner questions whether unmodified nucleic acid will actually survive under *in vivo* conditions for a sufficient length of time to actually be taken up by the cells. There are numerous studies that should convince the Examiner that his concerns are without foundation. Unmodified nucleic acid does survive in the body for a fairly long period. While its susceptibility to degradation make more stable forms of nucleic acid a preferred embodiment, susceptibility to degradation does not render unmodified nucleic acid useless. It is merely a matter of dosage with unmodified nucleic acid requiring higher amounts and/or longer administration to see the equivalent effects of stabilized nucleic acid.

While most articles report on the use of DNA, unmodified RNA will also survive under *in vivo* conditions. In Michelson *et al.* (1985) "Poly(A)·Poly(U) as Adjuvant in Cancer Treatment Distribution and Pharmacokinetics in Rabbits (42082)," *Proc. Soc. Exp. Biol. & Med.* 179:180-186 (Exhibit 3). In Michelson *et al.*, the authors describe the half-life of synthetic polyribonucleotides as measured in days. Its uptake into cells was also reported on page 184, 1st Col. A second report of long term survival of RNA appeared in Wolff *et al.* (1990) "Direct Gene Transfer into Mouse Muscle in Vivo," *Science*, 247:1465-1468 (Exhibit 4). In Michelson, purified RNA and DNA were simply injected into the muscle of mice and their respective gene products measured. The authors clearly state in their abstract that, "protein expression was detected in all cases and **no special delivery system was required**...."

Reports involving the use of purified DNA are more numerous than of RNA. Illustrative reports of DNA expression of plasmids directly injected into animals are provided in Lin *et al.* (1990) "Expression of Recombinant Genes in Myocardium In Vivo After Direct Injection of DNA," *Circulation*, 82:2217-2221 and Wolff *et al.* (1992) "Long-Term Persistence of Plasmid DNA and Foreign Gene Expression in Mouse Muscle," *Human Mol. Genet.* 1(6):363-369 which are Exhibits 5 and 6,

respectively. The DNA may be linear or circular (see Exhibit 4 at page 368, 2nd Col.)

C. UNMODIFIED ANTISENSE OLIGONUCLEOTIDES HAVE BEEN DEMONSTRATED TO BE USEFUL IN A VARIETY OF DIFFERENT ORGANS.

Naked, natural phosphodiester, antisense oligodeoxynucleotides have been reported as sufficiently stable to downregulate gene expression when directly injected into an animal. For example, Phillip *et al.* (1994) "Antisense Inhibition of Hypertension: A new strategy for Renin-Angiotensin Candidate Genes," *Kidney Intern.,* 46:1554-1556 (Exhibit 7) reports on the direct injection of an antisense DNA (unmodified) for reducing hypertension in mice. The DNA was merely injected into the mouse carotid artery using a saline solution.

Others have reported that antisense DNA will work when directly injected into the brain. For example, in Akabayashi *et al.* (1994) *Mol. Brain Res. 21:55-61,* the authors dissolved the antisense DNA in saline and simply injected it into the brain to inhibit production of a neuropeptide (Exhibit 8). At page 56, 1st Col., the authors state that theirs is the third such report.

As stated above, the use of stabilized DNA was merely a preferred embodiment. The use of unmodified DNA was less preferred, but similar results could be achieved by merely using more DNA or RNA to accommodate instability. Given the level of skill of those practicing molecular biology, this is an intuitively apparent solution to an obvious problem. The use of high levels of DNA is described in Exhibit 9, Hijya *et al.* (1994) *Proc. Natl. Acad. Sci., U.S.A.* 91:4499-4503. Hijya *et al.* report on the use of an unmodified phosphodiester oligonucleotide for controlling the expression of a gene which is involved in skin cancer. The authors applied the antisense oligonucleotide via a subcutaneous route and used constant-infusion pumps to ensure that the oligonucleotide was adequately administered.

D. THERE IS NO UNDUE EXPERIMENTATION INVOLVED IN THE ADMINISTRATION OF ANTISENSE OLIGONUCLEOTIDES.

The level of skill of those in the art of antisense technology is quite high. Most of the artisans are like myself and hold doctorates in a relevant biological science. To achieve a measurable downregulation of protein expression, one need only contact the target cells with an adequate amount of antisense oligonucleotides. The infusion techniques are conventional and were fully known in 1981. The technique is merely the injection of a saline solution containing the antisense oligonucleotides into the appropriate organ. There is simply no basis to conclude that such a experimental step was anything but routine and intuitively apparent to those of skill.

In summary, the relative stability of unmodified antisense oligonucleotides compared to stabilized oligonucleotides does not render the *in vivo* use of unmodified DNA or RNA without utility for the purpose of downregulating protein expression. The attached Exhibits 3-9 clearly document to one of skill that the claimed methods are operable under *in vivo* conditions. Furthermore, there is nothing beyond routine experimentation required to administer the antisense oligonucleotides under *in vivo* conditions and detect a downregulation in the expression of a specific protein.

The declarant has nothing further to state.

Dated: _____ By: _____

Dr. Jerry L. Ruth

Attachments: Exhibits 1-9

14/9/2
DIALOG(R)File 155:MEDLINE(R)
(c) format only 1995 Knight-Ridder Info. All rts. reserv.

04418862 81246862
Development in the phosphite-triester method of synthesis of oligonucleotides.
Finnan JL; Varshney A; Letsinger RL
Nucleic Acids Symp Ser (ENGLAND) 1980, (7) p133-45, Journal Code: O8N
. Contract/Grant No.: GM 10265
Languages: ENGLISH
Document type: JOURNAL ARTICLE
JOURNAL ANNOUNCEMENT: 8111
Subfile: INDEX MEDICUS
Tags: Support, U.S. Gov't, P.H.S.
Descriptors: *Indicators and Reagents; *Oligodeoxyribonucleotides --Chemical Synthesis--CS; *Oligonucleotides--Chemical Synthesis--CS; *Organophosphorus Compounds; Base Sequence; Methods
CAS Registry No.: 0 (Indicators and Reagents); 0 (Oligodeoxyribonucleotides); 0 (Oligonucleotides); 0 (Organophosphorus Compounds); 60010-51-7 (2,2,2-trichloroethyl phosphorodichloridite)

14/9/3
DIALOG(R)File 155:MEDLINE(R)
(c) format only 1995 Knight-Ridder Info. All rts. reserv.

04356488 81184488
Biochemical and biological effects of nonionic nucleic acid methylphosphonates.
Miller PS; McParland KB; Jayaraman K; Ts'o PO
Biochemistry (UNITED STATES) Mar 31 1981, 20 (7) p1874-80, ISSN 0006-2960 Journal Code: A0G
Contract/Grant No.: GM 166066-12
Languages: ENGLISH
Document type: JOURNAL ARTICLE
JOURNAL ANNOUNCEMENT: 8109
Subfile: INDEX MEDICUS
Oligodeoxyribonucleoside methylphosphonates with base sequences complementary to the anticodon loop of tRNALys and to the -ACCA-OH amino acid accepting stem of tRNA were prepared by chemical synthesis. Oligodeoxyadenosine methylphosphonates form stable, triple-stranded complexes with both poly(U) and poly(dT). These analogues selectively inhibit cell-free aminoacylation of tRNALys (E. coli) but have no effect on aminoacylation of tRNALys (rabbit). The extent of inhibition is temperature dependent and parallels the ability of the oligomer to bind to poly(U), which suggests that inhibition occurs as a result of oligomer binding to the -UUUU- anticodon loop of tRNALys (E. coli). The failure of the oligodeoxyadenosine methylphosphonates to inhibit tRNALys (rabbit) amino-acylation suggests that there may be a difference between the structure of tRNALys or its interaction with aminoacyl synthetase in the Escherichia coli and rabbit systems. The oligodeoxyadenosine analogues also effectively inhibit polyphenylalanine synthesis in cell-free translation systems derived from both E. coli and rabbit reticulocytes. The extent of inhibition parallels the Tm values of the oligo(A) phosphonate-poly(U) complexes and suggests that the inhibition is a consequence of complex formation with the poly(U) message. Tritium-labeled oligodeoxyribonucleoside methylphosphonates with a chain length of up to nine nucleotidyl units are taken up intact by mammalian cells in culture. All the oligomer analogues tested inhibited, to various extents, colony formation by bacterial, hamster, and human tumor cells in culture.

EXHIBIT
1

Proc. Natl. Acad. Sci. USA
Vol. 78, No. 11, pp. 6734–6738, November 1981
Biochemistry

Deoxynucleoside [1-thio]triphosphates prevent proofreading during *in vitro* DNA synthesis

(phosphorothioate nucleotides/fidelity of DNA synthesis/DNA polymerases)

THOMAS A. KUNKEL*, FRITZ ECKSTEIN†, ALBERT S. MILDVAN‡, R. MARLENE KOPLITZ*, AND LAWRENCE A. LOEB*§

*The Joseph Gottstein Memorial Cancer Research Laboratory, Department of Pathology SM-30, University of Washington, Seattle, Washington 98195; †The Max Planck Institut für Experimentelle Medizin, Abteilung, Chemie, Hermann-Rein Strasse 3, D-3400 Göttingen, Federal Republic of Germany; and ‡Department of Physiological Chemistry, Johns Hopkins University, School of Medicine, Baltimore, Maryland 21205

Communicated by Edwin G. Krebs, July 27, 1981

ABSTRACT **The contribution of proofreading to the fidelity of catalysis by DNA polymerases has been determined with deoxyribonucleoside [1-thio]triphosphate substrates. These analogues, which contain a sulfur in place of an oxygen on the α phosphorus, are incorporated into DNA by DNA polymerases at rates similar to those of the corresponding unmodified deoxynucleoside triphosphates. The fidelity of DNA synthesis was measured with φX174 *am*3 DNA; reversion to wild type occurs most frequently by a single base substitution, a C for a T at position 587. By using avian myeloblastosis virus DNA polymerase and DNA polymerase β (enzymes without a proofreading 3′→5′ exonucleolytic activity), substitution of deoxycytidine thiotriphosphate in the reaction mixture did not alter fidelity. In contrast, with DNA polymerases from *E. coli* (DNA polymerase I) and bacteriophage T4 (enzymes containing a proofreading activity), fidelity was markedly reduced with deoxycytidine [1-thio]triphosphate. DNA containing phosphorothioate nucleotides is insensitive to hydrolysis by the exonuclease associated with these prokaryotic DNA polymerases. These combined results indicate that the deoxynucleoside [1-thio]triphosphates have normal base-pairing properties; however, once misinserted by a polymerase, they are not excised by proofreading. Proofreading of a C:A mismatch at position 587 is thereby found to contribute 20-fold to the fidelity of *E. coli* DNA polymerase I and a greater amount to the fidelity of bacteriophage T4 DNA polymerase.**

The ability to correct errors during DNA replication has long been recognized as one important mechanism by which an organism can potentially achieve the highly accurate replication of its genetic information. This concept stems from the observation that prokaryotic DNA polymerases contain an integrally associated 3′→5′ exonuclease activity, which can selectively remove mistakes as they occur during polymerization (1). Biochemical support for this concept was obtained by Brutlag and Kornberg (2), who demonstrated that the 3′→5′ exonuclease of *Escherichia coli* DNA polymerase I (Pol I) preferentially removes mismatched bases at primer termini before initiation of polymerization. Support for proofreading *in vivo* comes from studies with certain mutator (3) and antimutator (4) bacteriophage T4 DNA polymerases. These studies (5–8) correlated spontaneous mutation rates of bacteriophage T4 with the ratio between the polymerization reaction and the excision of a noncomplementary nucleotide at the primer terminus. Also, differences in discrimination between adenosine and its base analogue 2-aminopurine by mutant T4 DNA polymerase (9) can be accounted for by proofreading. Based on the kinetic data with substrate analogues, a number of mathematic models for proofreading have been proposed (10–13).

Our continuing interest in determining the relative importance of the several mechanisms available to the cell to achieve high fidelity (14) has led us to assess the contribution of proofreading to accuracy by direct measurements of misincorporati n *in vitro*. The excision of noncomplementary bases does not occur with purified eukaryotic DNA polymerases (15), avian myeloblastosis virus (AMV) DNA polymerase (16), or possibly RNA polymerase, indicating that proofreading does not occur with these enzymes. It remains to be determined whether separate exonucleases work in concert with those polymerases during replication or transcription. We have shown that proofreading has a minimal contribution to the accuracy with which purified Pol I copies poly[d(A-T)] (17) but has a much greater contribution with natural DNA (18). Also, proofreading may be significant in multienzyme systems that function with natural DNA, as recently suggested by studies with *E. coli* DNA polymerase III holoenzyme (19). In this report, we make use of the φX174 fidelity assay (20, 21) to measure the fidelity of several purified DNA polymerases, using a substrate analogue that contains a sulfur atom in place of an oxygen on the α phosphorus of the deoxynucleoside triphosphate. This analogue is incorporated normally (22, 23), but the phosphorothioate diester bond is not hydrolyzed by the 3′→5′ exonuclease of Pol I. By comparing fidelity with a normal substrate versus this deoxynucleoside [1-thio]triphosphate analogue, we assess the contribution of proofreading to the fidelity of different DNA polymerases.

MATERIALS AND METHODS

Materials. Unlabeled 2′-deoxynucleoside 5′-*O*-([1-thio]triphosphate) derivatives (dNTPαS) were prepared as described (22). In all experiments, the A isomer of dATPαS was used, whereas dGTPαS and dCTPαS consisted of both the A and B isomers. Because the B isomer is not incorporated by Pol I (23), it was not considered in quantitating substrate concentrations. All other reagents including [α-^{32}P]dTTP were obtained from sources as described (24). The φX174 single-stranded viral DNA (template) and restriction endonuclease *Hae* III fragment Z-5 (primer) were prepared as described (24), as was homogeneous Pol I. AMV DNA polymerase was a gift of J. W. Beard (Life Sciences Research Laboratories), and homogeneous DNA polymerase β from rat (Novikoff) hepat ma was a gift of R. Meyer (University of Cincinnati). M. F. Good-

The publication costs of this article were defrayed in part by page charge payment. This article must therefore be hereby marked "*advertisement*" in accordance with 18 U. S. C. §1734 solely to indicate this fact.

Abbreviations: dNTPαS, 2′-deoxynucleoside 5′-*O*-([1-thio]triphosphate) derivatives; AMV, avian myeloblastosis virus; Pol I, *E. coli* DNA polymerase I.

§ To whom reprint requests should be addressed.

EXHIBIT 2

man (University of Southern California), and P. Englund (Johns Hopkins University) provided samples of highly purified wild-type T4 DNA polymerase.

DNA Polymerase Assays. Reaction mixtures (50 μl) contained 20 mM Tris·HCl (pH 8.0); 2 mM dithiothreitol; 10 mM $MgCl_2$; 0.2 μg of φX174 *am*3 viral DNA primed at a 5:1 molar ratio with Z-5 primer; Pol I (7 units, 25:1 molar ratio of enzyme to template) (1), AMV DNA polymerase (10 units) (16), phage T4 DNA polymerase (0.5 unit) (10), or DNA polymerase β (0.8 unit) (25); and 5 μM [α-^{32}P]dTTP (200–1000 cpm/pmol). The concentration of dATP, dCTP, dGTP, or the corresponding phosphorothioate derivative (A isomer) was 5 μM unless otherwise indicated. Incubation was at 37°C for 5 min (Pol I and T4 polymerase), 10 min (AMV polymerase), or 30 min (polymerase β), by which time synthesis had proceeded past the amber mutation (83 nucleotides) for all conditions reported here. Reactions were terminated by addition of EDTA to 15 mM, and duplicate aliquots were processed to determine acid-insoluble radioactivity.

Exonuclease Assays. The φX174 DNA substrates used for exonuclease digestion were prepared with Pol I in reactions scaled up to copy 10 μg of Z-8 primed φX174 DNA. Two synthetic reactions were performed with 5 μM [α-^{32}P]dTTP (5000 cpm/pmol) and either 5 μM dATP, dCTP, and dGTP or 5 μM dATPαS, dCTPαS, and dGTPαS. The reactions were incubated for 15 min at 37°C and then stopped by adding EDTA to 15 mM. The DNA was separated from nonincorporated deoxyribonucleotides on a Sephadex G-100 column (0.5 × 60 cm), preequilibrated and eluted with 0.5 M KCl/0.05 M Tris·HCl, pH 7.4. Approximately 0.05 μg of each DNA was used as a substrate for hydrolysis by the exonuclease activities associated with Pol I or T4 DNA polymerase. Reaction mixtures (50 μl) contained, in addition to the DNA, 30 mM Tris·HCl (pH 7.4), 2 mM dithiothreitol, 6 mM $MgCl_2$, and either 5 units of Pol I or 0.70 unit of phage T4 DNA polymerase. Reactions were incubated at 37°C for the times indicated in Fig. 1 and stopped by addition of 200 μl of 10% (wt/vol) trichloroacetic acid, followed by addition of 50 μl of calf thymus DNA (1.0 mg/ml) as a carrier. Acid-insoluble DNA was removed by centrifugation, and the acid-soluble radioactivity in the supernatant was quantitated by counting in a liquid scintillation counter.

Transfection Assay for Determination of Error Rate. The reversion frequency of the amber mutation in the copied DNA was determined by transfecting the copied DNA into *E. coli* spheroplasts and measuring the titer of the resultant progeny phage on bacterial indicators either permissive or nonpermissive for the amber mutation. A detailed account of the methodology for this assay has been published (24). All reversion frequency values are the average of duplicate determinations after subtracting the background reversion frequency of uncopied DNA from reactions not incubated at 37°C (typically 2.0–2.5 × 10^{-6}). The procedure for measuring phage titer gives results that fluctuate 2- to 3-fold from day to day; however, within an experiment, the average variation of duplicate samples is about 20%. For error rate determinations, only reversion frequencies at least 2 SD above background were considered significant.

RESULTS

Incorporation and Excision of dNTPαS. The ability of three purified DNA polymerases to incorporate dNTPαS approached that obtained with normal nucleotide substrates (Table 1). This was true for each of the three different dNTPαS used and confirmed previous observations with Pol I (22, 23). In all cases, incorporation was more than sufficient to copy past the amber mutation for determination of error rates. The simultaneous use of these same three dNTPαS, together with [α-^{32}P]dTTP, also yielded relatively normal incorporation (not shown). When this phosphorothioate-substituted DNA was used as a substrate for hydrolysis by the exonucleases associated with Pol I or wild-type phage T4 DNA polymerase, no release of acid-soluble nucleotides was observed (Fig. 1, closed symbols) in a 4-hr incubation. In this experiment, the amount of DNA polymerase was ≈10-fold greater than that of the DNA substrate. When compared to the substantial digestion observed under these same conditions with DNA synthesized with unmodified deoxynucleotide substrates (Fig. 1, open symbols), the results suggest that dNTPαS, once incorporated, cannot be excised by the 3′→5′ exonuclease activity. This conclusion is further substantiated by the recent study of Brody and Frey (26), who observed that the phosphorothioate diester bond in poly [d(A-T)] is completely resistant to the action of the exonuclease activities associated with Pol I.

Table 1. Incorporation of dNTPαS into φX174 DNA by purified DNA polymerases

DNA polymerase	% of control incorporation		
	dATPαS	dCTPαS	dGTPαS
AMV	69	95	100
Pol I	80	70	80
T4	43	68	67

Controls represent incorporation in the presence of all four normal substrates with [α-^{32}P]dTTP. Where indicated, dNTPαS was used in place of the corresponding normal dNTP. The 100% incorporation values were as follows: AMV DNA polymerase, 105 nucleotides per template (2.1 pmol); Pol I, 686 nucleotides per template (13.0 pmol); and T4 DNA polymerase, 339 nucleotides per template (7.0 pmol).

Fidelity Measurements with dNTPαS. The normal rates of synthesis and lack of hydrolysis led us to measure the effect of the phosphorothioated substrates on fidelity.

The assay (21) uses a single-strand circular φX174 DNA containing a TAG amber codon (amber 3, in gene *E*) in place of the TGG wild-type codon. Because the same sequence codes for the gene *D* protein in a different reading frame, the number of possible substitutions is limited. Synthesis was initiated at a single fixed point on the template, using as a primer a DNA restriction endonuclease fragment whose 3′-OH terminus is 83 nucleotides away from the *am*3 site. The accuracy of *in vitro* DNA synthesis was quantitated by transfecting the copied DNA into *E. coli* spheroplasts and measuring the titer of the resultant progeny phage on permissive and nonpermissive indicator bacteria. Because the mRNA and gene E proteins are coded for by the *in vitro* synthesized minus strand, an error rate for the DNA polymerase *in vitro* at the *am*3 site can be calculated from the reversion frequency of the phage (21). We have shown by DNA sequencing that those substitutions which produce wild-type phage occur at position 587, opposite the template A of the TAG amber codon (21). The most frequent error in Mg^{2+}-activated Pol I reactions is misincorporation of C, which produces the original wild-type DNA sequence (21). Therefore, we carried out polymerization reactions with purified DNA polymerases using either normal dCTP or dCTPαS in the presence of the other three normal dNTP substrates. The error rates of AMV DNA polymerase and DNA polymerase β, which lack associated 3′→5′ exonuclease activity (15, 16, 25), were the same with either substrate (Table 2). Two conclusions are evident from this result. First, the DNA synthesis-dependent increase in reversion frequency observed with these enzymes shows that the phosphorothioate-substituted minus strand DNA is biologically active (i.e., it is expressed in the transfection assay). Second, because dCTPαS is not more mutagenic than normal dCTP, the

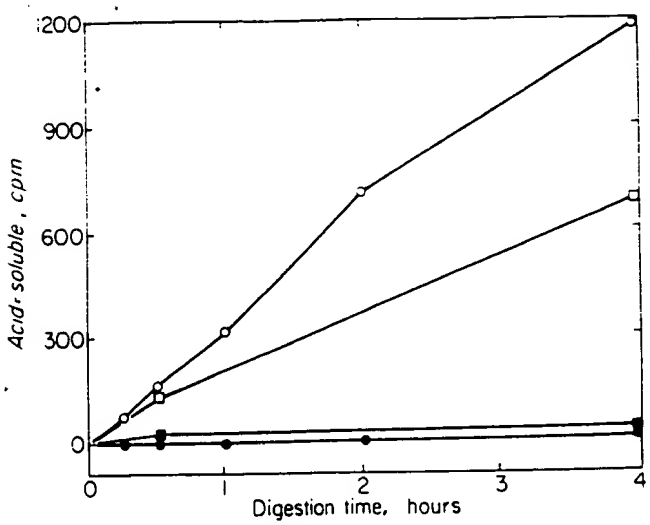

FIG. 1. DNA polymerase-associated exonuclease digestion of normal versus phosphorothioate-substituted ϕX174 DNA. ○, Pol I with dNTP; □, phage T4 DNA polymerase with dNTP; ●, Pol I with dNTPαS; ■, T4 polymerase with dNTPαS. In digestion experiments with ϕX174 DNA, in which only one of four deoxynucleotide substrates was a phosphorothioate (dCTPαS), we did observe some degradation, although at a slower rate than with unmodified DNA. Presumably, this represents cleavage of normal phosphodiester bonds releasing oligonucleotides and is not hydrolysis of phosphorothioate diester bonds.

analogue is not mutagenic by any unexpected mechanism, such as a change in base-pairing specificity.

The critical experiments were those with Pol I and phage T4 DNA polymerase (Table 2). Both of these enzymes contain associated 3′→5′ exonuclease activities, and both showed substantially reduced accuracy with dCTPαS. As previously reported (21), Pol I is highly accurate; in this experiment (with 5 μM dNTP), the error rate was 1/2,000,000 as determined from the reversion frequency obtained by increasing the normal dCTP concentration 50-fold over the other three dNTPs. However, with dCTPαS, a significant increase in reversion frequency of copied DNA was seen, even without any pool bias, and the effect was approximately 10-fold greater with a 10-fold dCTPαS bias (50 μM). This calculates to an error rate of approximately 1/100,000 and represents a 20-fold decrease in accuracy. The mutagenic effect of dCTPαS was even greater with T4 DNA polymerase. With normal dCTP, no enhancement in mutagenicity was observed, even with a 500-fold bias. However, with dCTPαS, even with an unbiased substrate condition, the reversion frequency of copied DNA was several-fold greater than background. The increase in the reversion frequency was in proportion to the concentration of dCTPαS in the reaction mixture. Therefore, the change in fidelity was from <1/10,000,000 with dCTP to approximately 1/20,000 with dCTPαS, or >500-fold.

Absence of "Next-Nucleotide Effect" with dCTPαS. A recent study of the *E. coli* DNA polymerase III holoenzyme (17) has provided kinetic evidence that proofreading activity is accompanied by what may be referred to as the "next nucleotide effect." Intuitively, the amount of time available to excise a misinserted base at the primer terminus can be decreased by increasing the rate of incorporation of the next correct nucleotide after the mistake. This will move the enzyme forward along the template and remove the incorrect nucleotide from the catalytic site for excision. In our assay, the relevant template DNA sequence, in order of synthesis from the provided Z-5 primer is ...GAT... Thus, an incorrect substitution at position 587 is followed by the next correct nucleotide, an A, opposite the template T at position 586. Once incorporation of A occurs at 586, any mistake made at position 587 will be less accessible to excision by a 3′→5′ exonuclease and more likely to remain as a stably misincorporated base. Thus, for an enzyme that is actively proofreading mistakes, the error rate should show a dependence on the dATP concentration in the polymerization reaction such that, at low dATP, few mistakes are stably misincorporated, whereas at high dATP, stable misincorporation increases.

We have shown that in Mg^{2+}-activated Pol I reactions C is misincorporated at least 10 times more frequently than A (21). Furthermore, DNA sequence analysis has shown that the increase observed with increasing dATP is, in fact, due to misincorporation of C at position 587 (18). The control experiment to demonstrate this next nucleotide effect is shown in Fig. 2. With normal dCTP, the reversion frequency increased as much as 25-fold with increasing dATP concentration (open circles). When a similar experiment was performed with dCTPαS rather than dCTP (Fig. 2, closed circles), the dATP-dependent enhancement in mutagenesis was not observed. These results support the conclusion that the use of dNTPαS substrates reduces or eliminates proofreading during polymerization.

DISCUSSION

In this paper, we describe experiments to quantitate the contribution of proofreading to the fidelity with which purified polymerases synthesize DNA *in vitro*. The approach is unique in that natural DNA is used as a template for directly measuring the stable misincorporation of a substrate with normal base-pairing properties. The analogue used is one of the well-characterized dNTPαS, which have been used previously to probe the stereochemistry of the reaction catalyzed by Pol I (23). Pol I has been shown to incorporate the S-diasteroisomer of dATPαS (isomer A) with normal kinetics *in vitro* (23) and with stereochemical inversion at phosphorus to yield a phosphorothioate diester with the *R*-configuration. When used in permeabilized *E. coli* cells or crude cell extracts, these modified dNTPs are incorporated into ϕX174 DNA (22). Similarly, in the experiments shown here, *in vitro* incorporation is relatively normal for three different DNA polymerases (Table 1). Moreover, AMV polymerase and phage T4 DNA polymerase, like Pol I, use the S_p-diastereoisomer of dCTPαS.

Table 2. Effect of normal dCTP versus dCTPαS on fidelity of DNA polymerases *in vitro*

DNA polymerase	dCTP or dCTPαS, μM	dCTP		dCTPαS	
		$\nu_{rev} \times 10^{-6}$	Unbiased error rate	$\nu_{rev} \times 10^{-6}$	Unbiased error rate
AMV	10	11.4	1/17,100	11.0	1/17,700
β	500	18.9	1/10,300	17.3	1/11,300
Pol I	5	0.11	—	1.61	1/121,000
	50	—	—	17.6	1/111,000
	250	4.47	1/2,180,000	—	—
T4	5	<1.50	—	6.69	1/29,100
	50	<1.50	—	82.2	1/23,700
	250	<1.50	—	588.0	1/16,600
	2500	<1.50	$<1/10^7$	—	—

Duplicate DNA polymerase reactions were performed with dATP, dGTP, and [α-^{32}P]dTTP at 10 μM (AMV DNA polymerase), 500 μM (DNA polymerase β), or 5 μM (Pol I and phage T4 DNA polymerase) and the indicated concentration of either dCTP or dCTPαS. Error rates were calculated as described (21) and unbiased (Pol I and T4 polymerase) by dividing the calculated error rate by the ratio of the incorrect (dCTP) nucleotide to the correct (dTTP) nucleotide in the reaction mixture. ν_{rev}, Reversion frequency.

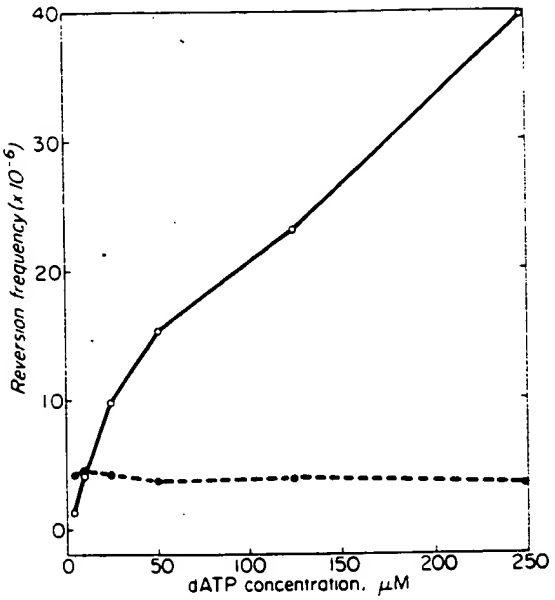

FIG. 2. Effect of concentration of "next nucleotide" on the error rate of Pol I with normal and phosphorothioated substrates. Duplicate DNA polymerase reactions were performed with Pol I and the following substrate concentrations: ○——○, 5 μM dGTP and TTP, 250 μM dCTP, and increasing dATP; ●---●, 5 μM dGTP and dTTP, 25 μM dCTPαS (A isomer), and increasing dATP. The reversion frequencies shown were determined in the transfection assay and are minus the background for uncopied DNA (1.79×10^{-6}).

Although incorporation of this analogue is normal, excision by exonucleases clearly is not. This was first demonstrated with Pol I-synthesized phosphorothioate-substituted poly (dA). The rate of snake venom phosphodiesterase-catalyzed hydrolysis of the R_p-configuration of the phosphorothioate polymer is approximately 10-fold less than that of the S_p-configuration, which is estimated to be 20,000-fold less than that of unsubstituted poly (dA) (23). More importantly, when an alternating copolymer containing normal T and phosphorothioate A is subjected to hydrolysis by the exonuclease activities of Pol I, only dinucleotides are obtained, and these retain the phosphorothioate-diester linkage intact (26). This bond in the R_p-configuration is thus refractory to the proofreading exonuclease of Pol I. The digestion experiment described here (Fig. 1) supports this conclusion and extends the observation to natural DNA and to the 3′→5′ exonuclease of wild-type phage T4 DNA polymerase. Because no degradation of the αS-substituted DNA is observed with either prokaryotic polymerase, there is—at the very least—a large difference in the rate of hydrolysis of the phosph rothioate-diester bond.

The lack of hydrolysis of substituted DNA by proofreading exonucleases led us to perform the fidelity measurements with the φX assay. When dCTPαS is used as an incorrect nucleotide, enhanced mutagenesis is observed specifically for those enzymes with an associated proofreading exonuclease activity. A comparison of error rates with the two different substrates demonstrates that the accuracy of Pol I and phage T4 DNA polymerase is increased 20-fold and greater than 500-fold, respectively, due to proofreading of misinserted bases. The contribution of proofreading by Pol I, assessed with the [1-thio]triphosphate, is in accord with an estimate of 25-fold using the next-nucleotide effect (18). The absence of the next-nucleotide effect with dCTPαS (Fig. 2) adds further support to the conclusion that the phosphorothioate analogue is n t proofread.

A final estimate of the fidelity of phage T4 DNA polymerase with normal substrates will require further analysis of the product of the reaction. However, the higher ratio of 3′→5′ exonuclease to polymerase in phage T4 DNA polymerase (1, 17) compared to Pol I argues that T4 DNA polymerase is more accurate. It should be noted that our estimate of accuracy with purified wild-type T4 DNA polymerase is the same or less than that reported by Hibner and Alberts (27) for the entire T4 replication complex. This similarity may result from the methods of assay employed or may reflect the nature of the mismatch being measured. Alternatively, the DNA polymerase may be the primary contributor to accuracy by the T4 replicating complex. With either enzyme, the absolute values (20-fold and >500-fold) are with respect to a single mismatch at a single position and may differ in other situations, since proofreading may be affected by position or the nature of the mismatch (18). If we assume that proofreading is negligible when the analogue is misinserted, then the misinsertion frequency of these enzymes becomes equivalent to the misincorporation frequency. Thus, the error rate with the phosphorothioate analogues is a direct measure of the error prevention (base-selection) capabilities for these DNA polymerases. With dCTPαS, the error rates for T4 DNA polymerase and Pol I are, respectively, 2 and 3 orders of magnitude lower than predicted by Watson–Crick base-pairing alone (28)—a value possibly obtained due to an active role of the enzyme in base discrimination.

We have suggested a structural mechanism for error prevention, based on NMR studies of the conformation of bound purine and pyrimidine substrates on Pol I (29, 30) and on fluorescence polarization studies of the moblity of the bound substrate (28, 30). Pol I was found to change the conformation of the bound nucleotide substrate to one that fits more precisely into double helical B DNA (29) and to immobilize the purine ring (30). Such orientation and immobilization of the substrate by the enzyme could prevent errors to the extent observed with dCTPαS. This fidelity is then further increased 20-fold due to correction of misinserted bases at the primer terminus during ongoing polymerization. Interestingly, the phage T4 DNA polymerase is less accurate than Pol I for error prevention (error rate approximately 1/20,000), but the overall accuracy of this enzyme is greater than that of Pol I, presumably due to a much more highly active proofreading activity for correcting errors (1).

The phosphorothioated dNTPαS can be used to probe the contribution of proofreading in a number of systems. For example, those mutator and antimutator phage T4 DNA polymerases that have altered exonuclease-to-polymerase ratios (7) should exhibit similar fidelity with the phosphorothioate substrates. The analogue can be used to address questions on the frequency of misinsertions of different incorrect bases and of excision of different mismatches during proofreading. Finally, these substrates should be a powerful probe to search for proofreading activities in eukaryotic cells.

We thank Elizabeth A. James for expert technical assistance and Shirley M. Kunkel and Mary T. Whiting for typing the manuscript. This work was initiated while Fritz Eckstein was on sabbatical leave at the Department of Pharmacology, University of Washington. This study was supported by grants from the National Institutes of Health (CA 11525; CA 12818) and the National Science Foundation (PCM 76-80439).

1. Kornberg, A. (1980) *DNA Replication* (Freeman, San Francisco).
2. Brutlag, D. & Kornberg, A. (1972) *J. Biol. Chem.* 247, 241–248.
3. Speyer, J. F., Karam, J. D. & Lenny, A. B. (1966) *Cold Spring Harbor Symp. Quant. Biol.* 31, 693–697.
4. Drake, J. W., Allen, E. F., Forseberg, S. A., Preparata, R. M. & Greening, E. O. (1969) *Nature (London)* 221, 1128–1130.
5. Muzyczka, N., Poland, R. L. & Bessman, J. (1972) *J. Biol. Chem.* 247, 7116–7122.
6. Hershfield, M. S. (1973) *J. Biol. Chem.* 248, 1417–1423.

7. Bessman, M. J., Muzyczka, N., Goodman, M. F. & Schnaar, R. L. (1974) *J. Mol. Biol.* **88**, 409–421.
8. Galas, D. J. & Branscomb, E. W. (1978) *J. Mol. Biol.* **124**, 653–687.
9. Goodman, M. F., Hopkins, R. & Gore, W. C. (1977) *Proc. Natl. Acad. Sci. USA* **74**, 4806–4810.
10. Clayton, L. K., Goodman, M. F., Branscomb, E. W. & Galas, D. J. (1979) *J. Biol. Chem.* **254**, 1902–1912.
11. Hopfield, J. J. (1974) *Proc. Natl. Acad. Sci. USA* **71**, 4135–4139.
12. Ninio, J. (1975) *Biochimie* **57**, 587–593.
13. Bernardi, F., Saghi, M., Dorizzi, M. & Ninio, J. (1979) *J. Mol. Biol.* **129**, 93–112.
14. Loeb, L. A., Weymouth, L. A., Kunkel, T. A., Gopinathan, K. P., Beckman, R. A. & Dube, D. K. (1977) *Cold Spring Harbor Symp. Quant. Biol.* **43**, 921–927.
15. Chang, L. M. S. & Bollum, F. J. (1973) *J. Biol. Chem.* **248**, 3398–3404.
16. Battula, N. & Loeb, L. A. (1976) *J. Biol. Chem.* **251**, 982–986.
17. Loeb, L. A., Dube, D. K., Beckman, R. A. Koplitz, M. & Gopinathan, K. P. (1981) *J. Biol. Chem.* **256**, 3978–3987.
18. Kunkel, T. A., Schaaper, R., Beckman, R. A. & Loeb, L. A. (1981) *J. Biol. Chem.*, in press.
19. Fersht, A. R. (1979) *Proc. Natl. Acad. Sci. USA* **76**, 4946–4950.
20. Weymouth, L. A. & Loeb, L. A. (1978) *Proc. Natl. Acad. Sci. USA* **75**, 1924–1928.
21. Kunkel, T. A. & Loeb, L. A. (1980) *J. Biol. Chem.* **255**, 9961–9966.
22. Vosberg, H.-P. & Eckstein, F. (1977) *Biochemistry* **16**, 3633–3640.
23. Burgers, P. M. & Eckstein, F. (1980) *J. Biol. Chem.* **254**, 6889–6893.
24. Kunkel, T. A. & Loeb, L. A. (1979) *J. Biol. Chem.* **254**, 5718–5725.
25. Stalker, D. M., Mosbaugh, D. W. & Meyer, R. R. (1976) *Biochemistry* **15**, 3114–3121.
26. Brody, R. S. & Frey, P. A. (1981) *Biochemistry* **20**, 1245–1252.
27. Hibner, U. & Alberts, B. M. (1980) *Nature (London)* **285**, 300–305.
28. Mildvan, A. S. & Loeb, L. A. (1979) *C.R.C. Crit. Rev. Biochem.* **6**, 219–244.
29. Sloan, D. L., Loeb, L. A., Mildvan, A. S. & Feldman, R. J. (1975) *J. Biol. Chem.* **250**, 8913–8920.
30. Mildvan, A. S., Stein, P. J., Abboud, M. M., Koren, R. & Bean, B. L. (1978) in *Protons and Ions Involved in Fast Dynamic Phenomena* (Elsevier, Amsterdam), pp. 413–433.

PROCEEDINGS OF THE SOCIETY FOR EXPERIMENTAL BIOLOGY AND MEDICINE 179, 180–186 (1985)

Poly(A)·Poly(U) as Adjuvant in Cancer Treatment Distribution and Pharmacokinetics in Rabbits (42082)

A. M. MICHELSON,* D. SHAOOL,† AND F. LACOUR†

*Institut de Biologie Physico-Chimique, 13, rue P. et M. Curie, 75005 Paris, and †CNRS, GR No. 8, Institut Gustave Roussy, Rue Camille Desmoulins, 94805 Villejuif, France

Abstract. Rabbits were injected with poly(A)·poly(U) and the metabolic fate and stability studied using scintigraphic techniques, radioactive counting, and subcellular fractionation. The complex has a very long lifetime (measured in days) in both liver and spleen, the major locations of concentration in the animal, with about nine times more per gram of tissue in the spleen compared with the liver. In spleen cells the material is about equally divided between nuclei and cytoplasm. The polymer is slowly degraded to shorter molecules in these cells but, even 1 week after injection, significant amounts of apparently intact polynucleotide complex can be detected in both cellular fractions.

Polyadenylic·polyuridylic acid poly(A)·poly(U), a double-stranded complex of synthetic polyribonucleotides, has shown significant antitumor effects in a number of tumor systems: as an adjuvant to surgery (1) in spontaneous mammary tumor and transplanted hamster melanoma, in Rausher MuLV-induced BALB/c mouse ascites (2), and as prophylactic therapy in spontaneous AKR mouse leukemia (3) and in spontaneous C_3H/He mouse mammary tumor (4). A synergistic inhibition of established transplantable mammary tumor in C_3H/He mice by combined treatment with poly(A)·poly(U) and cyclophosphamide has also been reported (5). Recently, in a randomized therapeutic trial on 300 operable breast cancer patients, a significant beneficial effect was observed in patients treated with the complex (6, 7). No toxic symptoms could be evidenced (8) in mice injected with very high doses (250 mg/kg) of poly(A)·poly(U).

The mechanisms governing the antitumor action of poly(A)·poly(U) have been discussed with respect to various biological effects such as immunomodulation for both humoral and cell-mediated immune response (9, 10), induction of interferon in rabbits (11), mice, and humans (12), and enhancement of natural killer (NK) cell activity (5). Few *in vitro* studies have been reported on the cellular properties of the complex. Shell (13) has demonstrated that poly(A)·poly(U) penetrated Ehrlich ascites tumor cells, without separation of the two strands. Fenster *et al.* (14) have shown that uptake of the complex by mouse ascites tumor cells and by human lymphocytes in culture occurred and that the material migrated rapidly into the cell nucleus and remained intact for 2 hr. In contrast, Mutchnich *et al.* (15) presented evidence indicating that 80% of thymocytes bound poly(A)·poly(U) on the cell membrane *in vitro*. However, no studies on the organ localization, cellular penetration, and metabolic lifetimes of poly(A)·poly(U) (or other polynucleotide complexes) after injection into animals of any kind (including man) have been reported.

We now present *in vivo* results on the fate of poly(A)·poly(U) after injection into rabbits as a complement to earlier studies with cell cultures which do not always reflect observations obtained with living animals.

Materials and Methods. *Polynucleotides.* Poly(A)·poly(U) was prepared as previously described (16). The material had a mean sedimentation constant of $s_{w,20} = 10.01$ with an average molecular weight of about half a million, but was polydisperse with polynucleotide complexes ranging from 250,000 to several million daltons. These preparations are stable for more than $2\frac{1}{2}$ years when stored as a sterile solution in physiological saline at 4°C.

^{51}Cr-labeled poly(A)·poly(U). A solution containing 2 mCi of $^{51}Cr^{3+}$ (NEN, sp act 72.23 mCi/mmole) in 1 ml of 0.1 *N* HCl was adjusted to pH 7 with 1 ml of 0.1 *N* NaOH and 0.1 ml of 0.1 *M* Tris–HCl, pH 8.2, and

was added to a solutio
of poly(A)·poly(U) in 2
0.01 *M* Tris, pH 7.4, 0.
sulfate (SDS). After 30
66°C, NaCl was adjust
solution was incubated
then left at 4°C overnig

Separation of polyn
$^{51}Cr^{3+}$ was obtained by p
through a Sephadex 100
in 5×10^{-3} *M* Tris, pH
the same buffer for eluti
tions were pooled and
and radioactivity (RA)
specific RA was betwee
cpm/μg for different pr

^{51}Cr-labeled poly(A)·
beled poly(A)·poly(U)
0.2 *M* NaCl with 2 vol
in 0.15 *M* NaCl, 0.01
SDS, and centrifuged
gradient at 20,000 rp
The ^{51}Cr-labeled poly
of 16–18 S were poole
2 vol of ethanol.

Subcellular studies.
^{51}Cr-labeled poly(A)·p
1500 μg of unlabele
physiological saline
injected intravenously
dose of 500 μg of poly

Rabbits were sacri
hr, 76 hr, and 7 day
liver collected. Male
bits weighing 3 to 3.5
120 days) for these
graphy.

Nuclear and cytopl
gans were frozen in
homogenized for 20
Waring blender. Tis
lysed in the presence
in 0.01 *M* Tris HCl,
M $MgCl_2$, 0.25 *M* s
degree of liberation
with a phase contras
ute. The lysis was
10 min. Nuclei were
15 min at 3000*g* at
was collected.

Nuclei were sus
HCl, pH 7.4, NT bu
SDS, and 200 μg/r

0037-9727/85 $1.50

EXHIBIT

ibution and

OUR†

id †CNRS. GR No. 8, f, France

fate and stability fractionation. The spleen, the major am of tissue in the y divided between in these cells but, ucleotide complex d Medicine.

uptake of the complex or cells and by human e occurred and that the dly into the cell nucleus for 2 hr. In contrast, 5) presented evidence of thymocytes bound the cell membrane *in* studies on the organ penetration, and meta-/(A)·poly(U) (or other xes) after injection into (including man) have

vivo results on the fate er injection into rabbits earlier studies with cell t always reflect obser-living animals.

thods. *Polynucleotides.* prepared as previously material had a mean rt of $s_{w,20}$ = 10.01 with weight of about half a isperse with polynucle-ging from 250,000 to ns. These preparations n 2½ years when stored in physiological saline

)·poly(U). A solution $^{51}Cr^{3+}$ (NEN, sp act 1 ml of 0.1 *N* HCl was 1 ml of 0.1 *N* NaOH Tris–HCl, pH 8.2, and was added to a solution containing 800 μg of poly(A)·poly(U) in 2 ml of 0.1 *M* NaCl, 0.01 *M* Tris, pH 7.4, 0.3% sodium dodecyl sulfate (SDS). After 30 min of incubation at 66°C, NaCl was adjusted to 0.3 *M* and the solution was incubated at 37°C for 8 hr and then left at 4°C overnight.

Separation of polynucleotides from free $^{51}Cr^{3+}$ was obtained by passage of the solution through a Sephadex 100 column (30 × 1 cm) in 5×10^{-3} *M* Tris, pH 7, 0.1% SDS using the same buffer for elution. Appropriate fractions were pooled and the OD at 260 nm and radioactivity (RA) were measured. The specific RA was between 1×10^5 and 2×10^5 cpm/μg for different preparations.

^{51}Cr-labeled poly(A)·poly(U), 16–18 S. Labeled poly(A)·poly(U) was precipitated in 0.2 *M* NaCl with 2 vol of ethanol, redissolved in 0.15 *M* NaCl, 0.01 *M* Tris, pH 7.4, 0.1% SDS, and centrifuged on a 5–20% sucrose gradient at 20,000 rpm for 20 hr at 17°C. The ^{51}Cr-labeled poly(A)·poly(U) fractions of 16–18 S were pooled and precipitated with 2 vol of ethanol.

Subcellular studies. About 3×10^7 cpm of ^{51}Cr-labeled poly(A)·poly(U) was mixed with 1500 μg of unlabeled poly(A)·poly(U) in physiological saline and the mixture was injected intravenously in adult rabbits at a dose of 500 μg of poly(A)·poly(U)/kg.

Rabbits were sacrificed after 90 min, 24 hr, 76 hr, and 7 days and the spleens and liver collected. Male New Zealand white rabbits weighing 3 to 3.5 kg were used (age 100–120 days) for these studies and for scintigraphy.

Nuclear and cytoplasmic extracts. The organs were frozen in liquid nitrogen, then homogenized for 20 sec three times in a Waring blender. Tissue homogenates were lysed in the presence of 0.5% Nonidet P-40 in 0.01 *M* Tris HCl, pH 7.4, 0.2 *M* KCl, 0.02 *M* $MgCl_2$, 0.25 *M* sucrose at 0°C, and the degree of liberation of nuclei was controlled with a phase contrast microscope every minute. The lysis was usually complete within 10 min. Nuclei were separated by centrifuging 15 min at 3000*g* at 0°C and the supernatant was collected.

Nuclei were suspended in 0.01 *M* Tris HCl, pH 7.4, NT buffer, 0.015 *M* NaCl, 0.1% SDS, and 200 μg/ml of Pronase (Sankyo). The mixture was left 20 min at room temperature; then 1% SDS was added and the solution was extracted with phenol–chloroform–isoamyl alcohol (1/1/24, v/v) 10 min at 4°C and then centrifuged for 10 min at 10,000*g*. A mitochondria-free cytoplasmic phase was obtained by centrifuging the supernatants for 20 min at 12,000*g*. They were then adjusted to 0.2 *M* NaCl, 0.1% sarcosyl, and 200 μg/ml of Pronase, left for 30 min at room temperature, and extracted with phenol–chloroform–isoamyl alcohol followed by centrifugation at 10,000*g* for 20 min, and the supernatant was collected.

Scintigraphy. Preparations of poly(A)·poly(U) (material used for clinical application) containing 120 to 160 μCi of ^{51}Cr label (in physiological saline) were injected intravenously into the ear vein of rabbits, using injection of Nembutal for anesthesia. Distribution of the ^{51}Cr-labeled poly(A)·poly(U) after injection into the animal was followed with an Angar (Nuclear Enterprises) scintillation camera (useful diameter, 26 cm) equipped with a specially made pinhole-type collimator. This type of collimator allows enlargement or reduction of the resultant image depending on the distance from the subject. The effective field and sensitivity are inverse functions of the enlargement which is taken into account for counting. The scintillation camera is coupled to an informatic system (Scinti 16, Informatek) composed of a computer (31 K bits, T 1600 Télémécanique), two memory storage magnetic disks (2 × 5 M each, Control Data 9427) for treatment of the data, and a graphic display terminal (Tektronix 4012 screen and 4631 dry photocopier) for visual presentation of the output. The numeric treatment of scintigraphic data provides results in the form of analogic images, as curves of total activity in a given organ with time, isocount contours, activity in a given defined zone, or as rati s of activity between two defined volumes. These data can be obtained at given time intervals or in a continuous fashion.

Results. Scintigraph studies were performed in rabbits injected with ^{51}Cr-labeled poly(A)·poly(U) or with the same amount of free $^{51}Cr^{3+}$. Representative printout images at different times after intravenous injection are shown in Figs. 1–3. It can be seen (Fig.

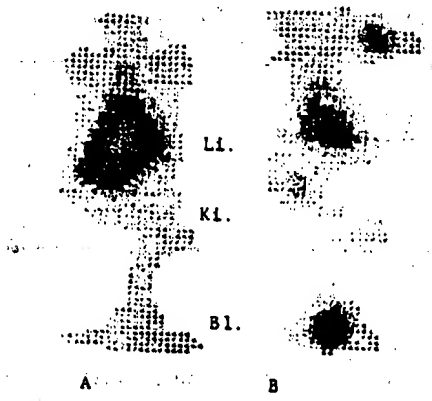

FIG. 1. (A) Localization of ^{51}Cr-labeled poly(A)·poly(U) 15 min after injection. (B) As for A but after injection of the same amount of free $^{51}Cr^{3+}$. Li, liver; Ki, kidney; Bl, bladder.

1A) that after 15 min the highest concentration occurs in the liver in rabbits injected with ^{51}Cr-labeled poly(A)·poly(U). In contrast, maximal concentration appears in the urinary bladder area in rabbits injected with free ^{51}Cr, although the liver and the kidneys are clearly visible (Fig. 1B). One hour after injection of labeled poly(A)·poly(U) the highest concentration is still in the liver. However, a part of the activity is released and concentrated in the bladder (Fig. 2A). With free ^{51}Cr, concentration in the liver is decreased and maximum concentration is in the bladder (Fig. 2B). Twenty-four hours after injection the major concentration of poly(A)·poly(U) is still in the liver; the urinary bladder concentrations are no longer visible (Fig. 3A). In contrast, with free ^{51}Cr the highest concentration is still in the bladder (Fig. 3B). Calculated decay times to 50 and 25% of maximum radioactivity in the liver were 4 and 9 days, respectively, for poly(A)·poly(U). The results are representative of four rabbits which showed identical behavior within the limitations of the technique.

A second series of rabbits was injected intravenously with about 3×10^7 cpm of 16–18 S ^{51}Cr-labeled poly(A)·poly(U) mixed with approximately 1500 μg of unlabeled poly(A)·poly(U) and the radioactivity of aliquots from liver and spleen was determined at different times. As shown in Table I the major part of the labeled poly(A)·poly(U) was incorporated into the liver within 90 min. Although only a minor portion of the complex was located in the spleen, the amounts incorporated were proportionally about nine times higher in the spleen than in the liver, when expressed per gram of tissue.

Nuclei and cytoplasm of spleen cells were prepared, and as shown in Table II the polynucleotide complex was almost equally distributed between the cytoplasmic and nuclear fractions. The sucrose gradient sedimentation profiles (Figs. 4–7) indicate that in spleen cells the complex of size 16–18 S remained undegraded during the first 90 min following inoculation compared to the control. Shorter fragments appear after 24 hr and increased in the course of time. However, even after 7 days a significant proportion

FIG. 2 (A, B). As for Fig. 1 but 1 hr after injection.

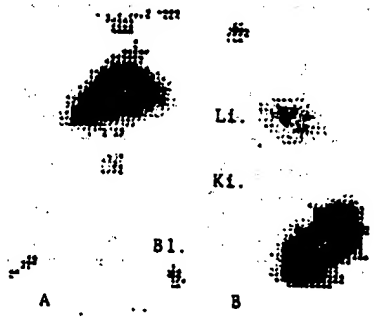

FIG. 3 (A, B). As for Fig. 1 but 24 hr after injection.

	Weigh
	Organ (g)
Liver	
1	180
2	191
Spleen	
1	1.12
2	1.14

Note. cpm injected (I) 1.1 ×

(Table II) still sedimer
coefficient as the inta
Uptake in the spleen
macrophages or other
given the lack of specific
poly(A)·poly(U) for cel
troduction) this seems u

The ^{51}Cr-labeled poly(
lose or exchange the labe
conditions of pH and te
label is not liberated in th
followed by reincorpora
mers is shown by (a) c
^{51}Cr; (b) retention of th
S fraction in sedimenta
with slow production of
lower molecular weight
Cr-labeled monomers o
be substrates (and rath
for various polymerase
could not be reincor
acids.

Discussion. The c
poly(U) to inhibit the

TABLE II. DISTRI

Time after injection	% of input radioactivity in spleen
90 min	3.82 ± 0.1
24 hr	3.15 ± 0.03
76 hr	2.30 ± 0.1
7 days	0.62 ± 0.05

TABLE I

	Weight of total radioactivity			
	Organ (g)	Incorporated (cpm)	% of the input radioactivity	Radioactivity per g of tissue
Liver				
1	180	6,800,000	61.8	37.800
2	191	6,200,000	59.6	32.400
Spleen				
1	1.12	388.000	3.5	346.500
2	1.14	398.400	3.83	349.500

Note. cpm injected (1) 1.1×10^7; (2) 1.04×10^7.

(Table II) still sedimented with the same coefficient as the intact poly(A)·poly(U). Uptake in the spleen may be confined to macrophages or other adherent cells, but given the lack of specificity of attachment of poly(A)·poly(U) for cells in culture (see introduction) this seems unlikely.

The ^{51}Cr-labeled poly(A)·poly(U) does not lose or exchange the label under physiological conditions of pH and temperature. That the label is not liberated in the *in vivo* experiments followed by reincorporation into other polymers is shown by (a) comparison with free ^{51}Cr; (b) retention of the label with a 16–18 S fraction in sedimentation for up to a week, with slow production of labeled molecules of lower molecular weight; (c) if degradation to Cr-labeled monomers occurs these would not be substrates (and rather act as inhibitors) for various polymerase systems and hence could not be reincorporated into nucleic acids.

Discussion. The capacity of poly(A)·poly(U) to inhibit the growth of some types of neoplasia in rodents is well established (1–5). The beneficial effect on tumor inhibition in breast cancer in humans (6, 7) and the absence of any toxic effects confer a special interest to pharmacological studies of this complex.

Scintigraphic examination of organs of rabbits injected with ^{51}Cr-labeled poly(A)·poly(U) showed an unexpected metabolic stability of the double-helical polynucleotide. Maximal amounts are in the liver and the decay times to 50 and 25% of maximum radioactivity were 4 and 9 days, respectively. In contrast the elimination of free ^{51}Cr was relatively rapid and 24 hr after the injection the majority of activity was concentrated in the bladder (Fig. 3B). Direct determination of the radioactivity in the liver and in the spleen 90 min after injection of ^{51}Cr-labeled poly(A)·poly(U) showed that 61.8% of the input radioactivity was incorporated into the liver. Although only 8.5% of the total radioactivity was located in the spleen, the amount incorporated per gram of tissue was about

TABLE II. DISTRIBUTION OF POLY(A)·POLY(U) IN CYTOPLASMIC AND NUCLEAR FRACTIONS OF SPLEEN CELLS AS A FUNCTION OF TIME

Time after injection	% of input radioactivity in spleen	% Radioactivity in nuclei	% Radioactivity in 12–18 S fraction of nuclei	% Radioactivity in cytoplasm	% Radioactivity in 12–18 S fraction of cytoplasm
90 min	3.82 ± 0.1	47.0 ± 1.4	90.0 ± 0.9	53.0 ± 1.4	93.0 ± 1.4
24 hr	3.15 ± 0.03	48.4 ± 0.6	45.7 ± 1.2	51.6 ± 0.7	47.9 ± 1.5
76 hr	2.30 ± 0.1	45.9 ± 0.9	29.6 ± 1.2	54.1 ± 0.9	36.3 ± 1.9
7 days	0.62 ± 0.05	44.6 ± 0.8	21.1 ± 1.5	55.4 ± 0.9	33.2 ± 2

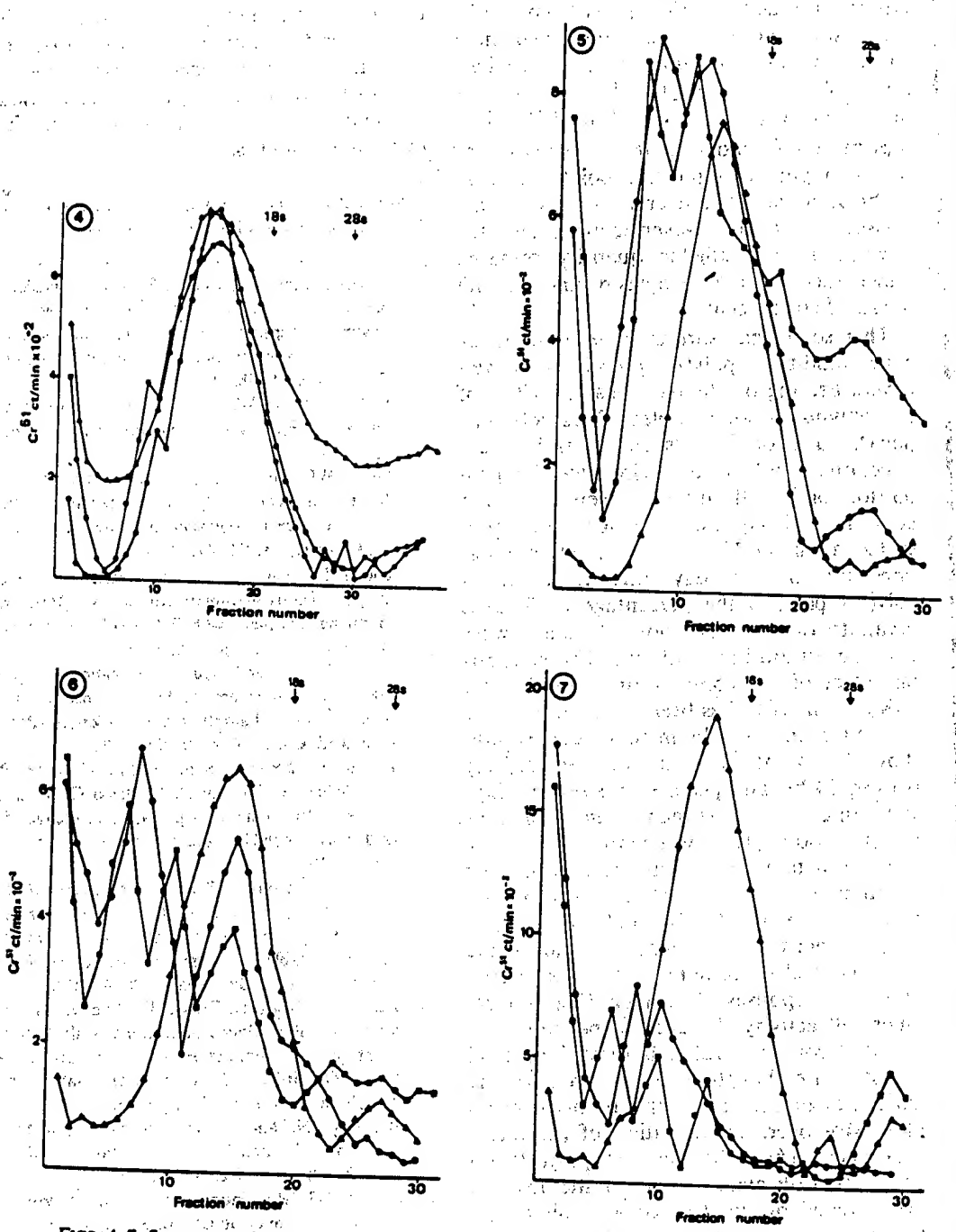

FIGS. 4–7. Sucrose gradient centrifugation of ^{51}Cr-labeled poly(A)·poly(U) of nuclear and cytoplasmic spleen extracts. Rabbits received an intravenous injection of about 3,500,000 cpm/kg and were sacrificed 90 min (Fig. 4), 24 hr (Fig. 5), 72 hr (Fig. 6), and 7 days (Fig. 7) later. Aliquots of the cytoplasmic and nuclear spleen extracts were layered onto 5–20% sucrose and centrifuged at 20,000 rpm for 20 hr at 17°C in a SW 27 rotor of a Beckman ultracentrifuge. Fractions were collected and processed for acid precipitation and counting. The vertical arrows indicate the 18 and 28 S rRNA peaks in the cytoplasmic extracts as determined by measuring the absorption at 260 nm of the corresponding fractions. Control poly(A)·poly(U), ▲; cytoplasmic extracts, ; nuclear extracts, ■.

nine times higher than
gradient sedimentation
during this time the c
degraded in spleen c
profile of intact 16–1
This result is not altog
an *in vitro* study in tu
earlier shown that po
mains intact for at l
present study conduct
shorter fragments of p
24 hr after inoculatio
creases over 7 days. N
1 week a nonnegligi
undegraded in the c
nuclei of spleen cells.

This somewhat su
bolic stability of poly
have a bearing on the
this polynucleotide co
poly(U) acts on T c
injection of 300 μg i
portion of T cells in
peak the 3rd day aft
sented about 80% of
tion. By the 4th d
poly(A)·poly(U) the
began to decrease bu
not reached until the
ing effect of the con
(NK) cell activity has
(5) and men (16). I
showed that the ef
(within 24 hr) and pe
after injection. Tre
poly(U) also leads to
5 A synthetase, an e
production and actio
man and rodents (16
seems to act to vario
cells involved in hun
immune responses
killer cell activity (5
of interferon (11, 1
activities are though
antitumor mechanis
plex. Moreover, an
suppressive effects
neoplastic cells evide
the cyclic adenosine
tem has been report
recently observed tha
produce interferon in

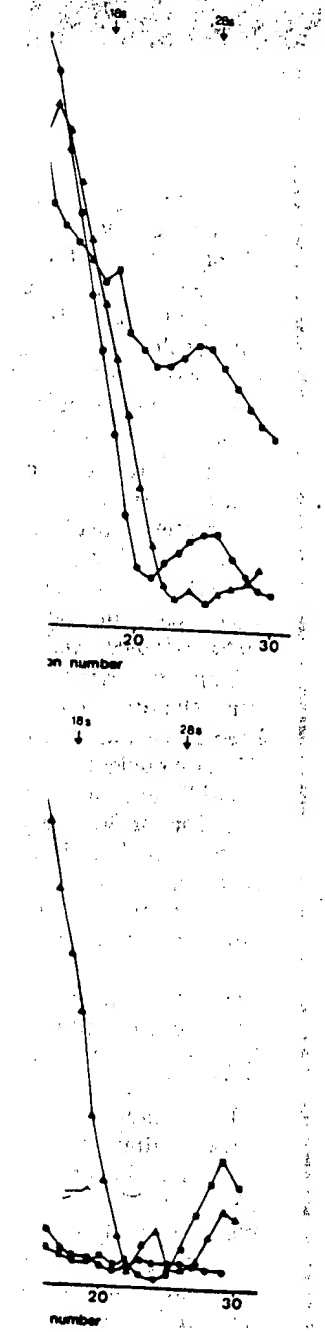

lear and cytoplasmic
3 and were sacrificed
the cytoplasmic and
m for 20 hr at 17°C
processed for acid
s in the cytoplasmic
g fractions. Control

nine times higher than in the liver. Sucrose gradient sedimentation profiles indicate that during this time the complex remained undegraded in spleen cells compared to the profile of intact 16–18 S poly(A)·poly(U). This result is not altogether unexpected since an *in vitro* study in tumor lymphocytes had earlier shown that poly(A)·[^{3}H]poly(U) remains intact for at least $2\frac{1}{2}$ hr (14). The present study conducted *in vivo* shows that shorter fragments of poly(A)·poly(U) appear 24 hr after inoculation and the amount increases over 7 days. Nevertheless, even after 1 week a nonnegligible quantity remains undegraded in the cytoplasm and in the nuclei of spleen cells.

This somewhat surprising *in vivo* metabolic stability of poly(A)·poly(U) may well have a bearing on the biological activities of this polynucleotide complex. Thus poly(A)·poly(U) acts on T cells and after a single injection of 300 μg in A/Sn mice the proportion of T cells in the spleen rose to a peak the 3rd day after injection and represented about 80% of the total cell population. By the 4th day after injection of poly(A)·poly(U) the percentage of T cells began to decrease but normal values were not reached until the 15th day (17). A boosting effect of the complex on natural killer (NK) cell activity has been observed in mice (5) and men (16). In mice kinetic studies showed that the effects occurred rapidly (within 24 hr) and persisted for several days after injection. Treatment with poly(A)·poly(U) also leads to an enhancement of 2–5 A synthetase, an enzyme marker for the production and action of interferon in both man and rodents (16, 18). Poly(A)·poly(U) seems to act to various extents on all of the cells involved in humoral and cell-mediated immune responses (10), including natural killer cell activity (5), and in the induction of interferon (11, 12). All these biological activities are thought to play a role in the antitumor mechanism of this nontoxic complex. Moreover, an indication of the direct suppressive effects of poly(A)·poly(U) on neoplastic cells evidenced as an alteration in the cyclic adenosine 3′5-monophosphate system has been reported (2), and it has been recently observed that tumor cells themselves produce interferon in response to intravenous injection of poly(A)·poly(U) in mice (19). However, the relevance of the long-lasting persistence of undegraded poly(A)·poly(U) in the liver and the spleen to antitumor effects observed both in experimental animal models and in humans remains to be determined. From a practical viewpoint the findings justify (a posteriori) the clinical schedule (injection once a week) used for the treatment of human patients.

We thank B. Perdereau and C. Barbaroux, Institut Curie, for assistance with the scintigraphic work.

1. Lacour F, Spira A, Lacour J, Prade M. Polyadenylic–polyuridylic acid as an adjuvant to surgery in the treatment of spontaneous mammary tumors in C_3H/He mice and transplantable melanoma in hamsters. Cancer Res 32:648, 1972.
2. Webb D, Braun W, Plescia OJ. Antitumor effects of polynucleotides and theophylline. Cancer Res 32: 1814, 1972.
3. Drake WP, Cimino EF, Mardiney MR, Sutherland JC. Prophylactic therapy of spontaneous leukemia in AKR mice by polyadenylic–polyuridylic acid. J Natl Cancer Inst 52:941, 1974.
4. Lacour F, Delage G, Chianale C. Reduced incidence of spontaneous mammary tumors in C_3H/He mice following treatment with Poly(A)·Poly(U). Science (Washington, DC) 187:256, 1975.
5. Youn JK, Lacour F, Hue G. Inhibition of C_3H/He mammary tumor growth by combined treatment with cyclophosphamide and Polyadenylic–Polyuridylic acid. Cancer Res 42:4706, 1982.
6. Lacour J, Lacour F, Spira A, Michelson M, Petit JY, Delage G, Sarrazin D, Contesso G, Viguier J. Adjuvant treatment with polyadenylic·polyuridylic acid (PolyA·polyU) in operable breast cancer. Lancet 2:161, 1980.
7. Lacour J, Lacour F, Spira A, Michelson M, Petit JY, Delage G, Sarrazin D, Contesso G, Viguier J. Adjuvant treatment with polyadenylic·polyuridylic acid in operable breast cancer: Updated results of a randomized trial. Brit Med J 288:589, 1984.
8. Lacour F, Delage G, Fenster E, Harel J. Inhibitory action of PolyA·PolyU on tumor growth: Enhancement of host immune response? In: Gotlieb AA, Plescia OJ, Bishop HL, eds. Fundamental aspects of Neoplasia. New York, Springer-Verlag, p123, 1975.
9. Braun W, Nakano M. Antibody formation: Stimulation by poly-adenylic and polycytidylic acids. Science (Washington, DC) 157:819, 1967.
10. Johson AG. Modulation of the immune system by synthetic polynucleotides. In: Springer Seminar in Immunopathology. New York, Springer-Verlag, Vol 2:p149, 1979.
11. Field AK, Tytell AA, Lampson GP, Hilleman MR.

Inducers of interferon and host resistance. II. Multistranded synthetic polynucleotides complexes. Proc Natl Acad Sci USA 58:1004, 1967.
12. Hovanessian AC, Riviere J, Montagnier L, Michelson M, Lacour J, Lacour F. Enhancement of interferon mediated protein kinase on mouse and human plasma in response to treatment with polyadenylic-polyuridylic acid (PolyA·PolyU) 2:209, 1982.
13. Schell PL. Uptake of polynucleotides by intact mammalian cells. VIII. Synthetic homoribopolynucleotides. Biochim Biophys Acta 240:472, 1971.
14. Fenster ED, Lacour F, Harel J. Nuclear penetration and stimulation of nucleic acids synthesis by poly(A)·poly(U) in mammalian cells. Exp Cell Res 94:315, 1975.
15. Mutchnich J, Han JH, Johnson AG. Mouse thymocytes membrane uptake of polyadenylic–polyuridylic acid complexes. Proc Soc Exp Biol Med 154: 264, 1977.
16. Hovanessian AG, Youn JK, Buffet-Janvresse C, Riviere Y, Michelson M, Lacour J, Lacour F. Activity and 2–5 A synthetase in operable breast cancer patients treated with poly(A)·poly(U). Cancer 55, 1985, in press.
17. Donner M, Vallier D, Lacour F. Changes in lymphocytes subpopulation in mice receiving a single injection of polyA-polyU. Ann Immunol Inst Pasteur 128:1039, 1977.
18. Youn JK, Hovanessian AG, Riviere Y, Hue G, Lacour F. Enhancement of natural killer cell and activity and 2–5 A synthetase in mice pretreated with polyadenylic–polyuryidylic acid. Cell Immunol 72:389, 1983.
19. Riviere Y, Hovanessian AG. Direct action of interferon and inducer of interferon on tumor cells in athemic nude mice. Cancer Res 43:4596, 1983.

Received November 14, 1984. P.S.E.B.M. 1985, Vol. 179.
Accepted February 5, 1985.

Effect of

JAI

Pennsylvania College of

Abstract. The ef
mitochondrial and
Mitochondrial and
vitro peroxidation,
using diene conjug
zinc-deficient anim
all three groups re
peroxidation poten
which may be rela
Biology and Medicine.

Zinc deficiency has
several parameters of
corporation of [^{14}C]ac
triglycerides as well as p
in animals on a zinc-
addition, changes in th
unsaturated fatty acids
A zinc-deficient diet h
crease the levels of 22:
microsomes (2); to inc
tion activity and to dec
activity. Huang *et al.* (
several of the manifesta
are attributable in par
sion of 18:2w6 to 18
accumulation of 18:2v
from O'Dell's labora
chicks fed a diet adequ
fatty acids but low
concentration of ara
skin compared with tl

Zinc deficiency ha
affect lipid peroxidati
have demonstrated i
peroxidation *in vitro*
from rats fed a zinc-de
was of interest for se
have demonstrated in
growth of the plasm
BALB/c mice is inhit
diet (6). Second, repc
eotti (7) have indic
and microsomes isol

rated $(NH_4)_2SO_4$ and stirred 2.5 hours at room temperature. The precipitate was collected by centrifugation (12,000*g* for 30 min) and dissolved in 5 ml of TE buffer. After 30 min at room temperature, the solution was clarified by centrifugation (10,000*g* for 10 min) and filtered through a Millipore filter (0.45 μm). The solution was dialyzed against 0.5 liters of TE buffer overnight at 4°C. The hPRL (85% pure) was finally purified to homogeneity (>95%) by fast-performance liquid chromatography (FPLC) and DEAE fast-flow matrix essentially as described for the purification of hGH (7). After reduction, the purified hPRL shows a pronounced retardation in mobility by SDS-PAGE (as seen for hGH) suggesting that disulfide bonds have formed [S. Pollit and H. Zalkin, *J. Bacteriol.* 153, 27 (1983)]. The concentrations of hPRL and hPRL mutants were determined by measuring absorbance at 280 nm and by using a calculated extinction coefficient of $\epsilon_{280}^{0.1\%} = 0.9$ [D. B. Wetlaufer, *Adv. Protein Chem.* 17, 303 (1962)], which was adjusted accordingly when variants contained mutations in aromatic residues. Concentration values determined by absorbance agreed to within 10% of those determined by laser densitometry of proteins subjected to SDS-PAGE and stained with Coomassie blue for hGH (7, 8).

18. T. A. Bewley, *Recent Prog. Horm. Res.* 35, 155 (1979).
19. B. C. Cunningham, P. Jardieu, J. A. Wells, unpublished data.
20. T. Tanaka *et al.*, *J. Clin. Endocrinol. Metab.* 51, 1058 (1980).
21. K. C. Olson *et al.*, *Nature* 293, 408 (1981).
22. B. C. Cunningham and J. A. Wells, unpublished data.
23. For site-specific mutagenesis [M. J. Zoller and M. Smith, *Nucleic Acids Res.* 10, 6487 (1982)], a synthetic hGH gene template was used that contained multiple unique restriction sites (7). Enrichment for mutant clones was obtained with the use of a mismatch repair-deficient strain of *E. coli*, *mut L* [B. Kramer, W. Kramer, H. J. Fritz, *Cell* 38, 879 (1984)] and by designing mutagenic oligonucleotides to either introduce or eliminate a nearby unique restriction site so that restriction-purification or restriction-selection [J. A. Wells, B. C. Cunningham, T. P. Graycar, D. A. Estell, *Philos. Trans. R. Soc. London Ser. A* 317, 415 (1986)], respectively, could be applied to the first pool of plasmid DNA obtained after transformation of the in vitro–generated heteroduplex. All oligonucleotides were designed to have 12 and 10 bp of exact match at their 5′ and 3′ ends, respectively. Variants of hGH were secreted into the periplasmic space of *E. coli* [C. N. Chang, M. Rey, B. Bochner, H. Heynecker, G. Grav, *Gene* 55, 189 (1987)] and purified as described (7, 8).

24. We thank J. Heinrich for technical assistance in cloning hPRL; E. Chen for sequencing the hPRL cDNA clone; M. Mulkerrin for providing CD spectra; P. Carter and T. Kossiakoff for helpful comments on the manuscript; P. Jardieu for Nb2 cell assays; G. Fuh for providing purified hGH-binding protein; P. Ng, P. Jhurani, and M. Vasser for synthetic oligonucleotides; and W. Henzel for NH_2-terminal protein sequencing.

30 November 1989; accepted 29 January 1990

Direct Gene Transfer into Mouse Muscle in Vivo

JON A. WOLFF,* ROBERT W. MALONE, PHILLIP WILLIAMS, WANG CHONG, GYULA ACSADI, AGNES JANI, PHILIP L. FELGNER

RNA and DNA expression vectors containing genes for chloramphenicol acetyltransferase, luciferase, and β-galactosidase were separately injected into mouse skeletal muscle in vivo. Protein expression was readily detected in all cases, and no special delivery system was required for these effects. The extent of expression from both the RNA and DNA constructs was comparable to that obtained from fibroblasts transfected in vitro under optimal conditions. In situ cytochemical staining for β-galactosidase activity was localized to muscle cells following injection of the β-galactosidase DNA vector. After injection of the DNA luciferase expression vector, luciferase activity was present in the muscle for at least 2 months.

MOST EFFORTS TOWARD POSTNATAL gene therapy have relied on indirect means of introducing new genetic information into tissues: target cells are removed from the body, infected with viral vectors carrying the new genetic information, and then reimplanted into the body (*1*). For some applications, direct introduction of genes into tissues in vivo, without the use of viral vectors, would be useful. Direct in vivo gene transfer into postnatal animals has been achieved with formulations of DNA encapsulated in liposomes, DNA entrapped in proteoliposomes containing viral envelope receptor proteins (*2*), calcium phosphate–coprecipitated DNA (*3*), and DNA coupled to a polylysine-glycoprotein carrier complex (*4*). In vivo infectivity of cloned viral DNA sequences after direct intrahepatic injection with or without formation of calcium phosphate coprecipitates has also been described (*5*). With the use of cationic lipid vesicles (*6*), mRNA sequences containing elements that enhance stability can be efficiently translated in tissue culture cells (*7*) and in *Xenopus laevis* embryos (*8*). We now show that injection of pure RNA or DNA directly into mouse skeletal muscle results in significant expression of reporter genes within the muscle cells.

The quadricep muscles of mice were injected (*9*) with either 100 μg of pRSVCAT DNA plasmid (*10*) or 100 μg of βgCATβ-gA_n RNA (*7*, *11*, *12*). The RNA consists of the chloramphenicol acetyl transferase (CAT) coding sequences flanked by β-globin 5′ and 3′ untranslated sequences and a 3′ polyadenylate tract. CAT activity was readily detected in all four RNA injection sites 18 hours after injection and in all six DNA injection sites 48 hours after injection (Fig. 1). Extracts from two of the four RNA injection sites (Fig. 1, lanes 6 and 8) and from two of the six DNA injection sites (Fig. 1, lanes 11 and 20) contained amounts of CAT activity comparable to those obtained from fibroblasts transiently transfected with the corresponding constructs in vitro under optimal conditions (Fig. 1, lanes 9 and 10 and 21 to 24, respectively). The average total amount of CAT activity expressed in muscle was 960 pg for the RNA injections and 116 pg for the DNA injections. The variability in CAT activity recovered from different muscle sites probably represents variability inherent in the injection and extraction technique, because significant variability was observed when pure CAT protein or pRSVCAT-transfected fibroblasts were injected into the muscle sites and immediately excised for measurement of CAT activity. CAT activity was also recovered from abdominal muscle injected with the RNA or DNA CAT vectors (*13*), indicating that other muscles can take up and express polynucleotides.

The site of gene expression was determined for the pRSV*lac-Z* DNA vector (*14*) expressing the *Escherichia coli* β-galactosidase gene (Fig. 2). Seven days after a single injection of 100 μg of pRSV*lac-Z* DNA into individual quadricep muscles, the entire muscles were removed, and every fifth 15-μm cross section was histochemically stained for β-galactosidase activity. Approximately 60 (1.5%) of the ~4000 muscle cells that comprise the entire quadriceps and ~10 to 30% of the cells within the injection area were stained blue (Fig. 2, A and B). Positive β-galactosidase staining within some individual muscle cells was at least 1.2 mm deep on serial cross sections (Fig. 2, D to F), which may be the result of either transfection into multiple nuclei or the ability of cytoplasmic proteins expressed from one nucleus to be distributed widely within the muscle cell (*15*). Longitudinal sectioning also revealed β-galactosidase staining within muscle cells for at least 400 μm (Fig. 2C). Fainter blue staining often appeared in the bordering areas of cells adjacent to intensely stained cells. This most likely represents an artifact of the histochemical β-galactosidase

J. A. Wolff, P. Williams, W. Chong, G. Acsadi, A. Jani, Departments of Pediatrics and Genetics, Waisman Center, University of Wisconsin, Madison, WI 53706.
R. W. Malone and P. L. Felgner, Vical Inc., San Diego, CA 92121.

*To whom correspondence should be addressed.

stain, in which the reacted product diffuses before precipitating. An alternative hypothesis is that β-galactosidase can be transported from a transfected cell to an adjacent, untransfected cell.

A dose-response effect was observed when quadricep muscles were injected with various amounts of RNA (βgLucβgA$_n$) or DNA (pRSVL) constructs containing the firefly luciferase reporter gene (Fig. 3A). The injection of ten times more DNA resulted in luciferase activity increasing approximately tenfold from 33 pg of luciferase after the injection of 10 μg of DNA to 320 pg of luciferase after the injection of 100 μg of DNA. The injection of ten times more RNA also yielded approximately tenfold more luciferase. On the basis of the amount of DNA delivered, the efficiency of expression from the DNA vectors was similar in both transfected fibroblasts and injected muscles. Twenty micrograms of pRSVL DNA transfected into fibroblasts yielded a total of 120 pg of luciferase (6.0 pg of luciferase per microgram of DNA) (*16*), whereas 25 μg injected into muscle yielded an average of 116 pg of luciferase (4.6 pg of luciferase per microgram of DNA) (Fig. 3A). The expression from the RNA vectors was approximately sevenfold more efficient in transfected fibroblasts than in injected muscles. Twenty micrograms of βgLucβgA$_n$ RNA transfected into fibroblasts yielded a total of 450 pg of luciferase (*7*, *16*), whereas 25 μg injected into muscle yielded 74 pg of luciferase (Fig. 3, A and B).

The time course of expression was also investigated (Fig. 3, B and C). Luciferase activity was assayed at various times after 100 μg of βgLucβgA$_n$ RNA (*7*) or 100 μg of pRSVL DNA (*17*) were injected. After RNA injection, the average luciferase activity reached a maximum of 74 pg at 18 hours and then decreased to 2 pg at 60 hours. In transfected fibroblasts, the luciferase activity was maximal at 8 hours. After DNA injection into muscle, substantial amounts of luciferase were present for at least 60 days.

The luciferase protein and the in vitro RNA transcript appear to have a half-life of less than 24 hours in muscle (Fig. 3B). Therefore, the persistence of luciferase activity for 60 days in muscle after pRSVL DNA injection is not likely to be due to the stability of luciferase protein or the stability of the in vivo RNA transcript. Southern (DNA) blot analysis of muscle DNA indicates that the foreign pRSVL DNA is present within the muscle tissue for at least 30 days (Fig. 4, lanes 6 to 9) and that the amount present at this time is similar to the amount of DNA present in muscle 2 and 15 days after injection (*13*). In muscle DNA digested with Bam HI (which cuts pRSVL once) (Fig. 4, lanes 6 to 9), the presence of a 5.6-kb band that corresponds to linearized pRSVL (Fig. 4, lane 2) suggests that the DNA is present either in a circular, extrachromosomal form or in large tandem repeats of the plasmid integrated into chromosome. In muscle DNA digested with Bgl II (which does not cut pRSVL), the presence of a band smaller than 10 kb (Fig. 4, lanes 12 and 13) and of the same size as the open circular form of the plasmid pRSVL (Fig. 4, lane 1) implies that the DNA is present extrachromosomally in a circular form (*18*). Extrachromosomal DNA of muscle extracts was prepared by the method of Hirt, modified by Pauza and Galindo (*19*). The appear-

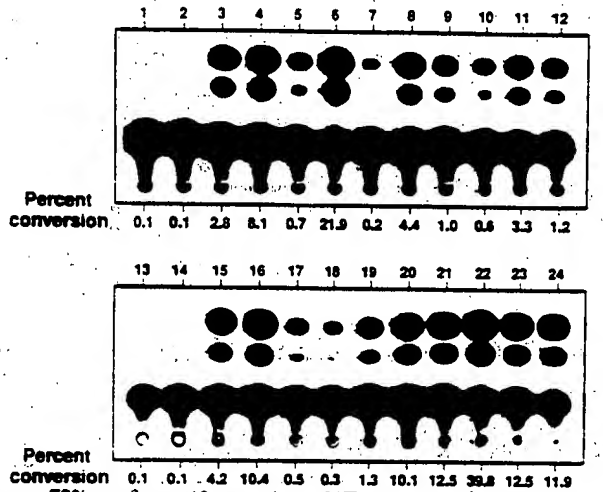

Fig. 1. Autoradiograms from two separate experiments showing CAT activity in extracts from quadricep muscles injected with pRSVCAT DNA or βgCATβgA$_n$ RNA. Lane numbers are above and percent chloramphenicol conversions are below each autoradiogram. Lanes 1 and 13, control fibroblasts; lanes 2 and 14, muscle injected with 5% sucrose solution; lanes 3 and 15, 0.005 unit of noninjected, purified CAT standard (Sigma); lanes 4 and 16, 0.05 unit of noninjected, purified CAT; lanes 5 to 8, muscle injected with 100 μg of βgCATβgA$_n$ RNA in 5% sucrose; lanes 9 and 10, 20 μg of βgCATβgA$_n$ RNA transfected with 60 μg of lipofectin reagent (*6*) into a 70% confluent 60-mm plate of 3T3 cells (~10^6 cells) (*7*, *8*); lanes 11, 12, and 17 to 20, muscle injected with 100 μg of pRSVCAT DNA in 5% sucrose; lanes 21 and 22, 20 μg of pRSVCAT DNA transfected with 60 μg of lipofectin reagent into a 50% confluent 60-mm plate of 3T3 cells (~0.8×10^6 cells); lanes 23 and 24, 20 μg of pRSVCAT DNA transfected with calcium phosphate into a 50% confluent 60-mm plate of 3T3 cells as previously described (*25*). CAT activity was assayed 18 hours after all in vivo and in vitro RNA transfections and 48 hours after all DNA transfections. RNA and DNA polynucleotides were prepared as described (*26*) and muscle extracts were analyzed for CAT activity (*27*, *28*). Similar results have been obtained in five separate experiments.

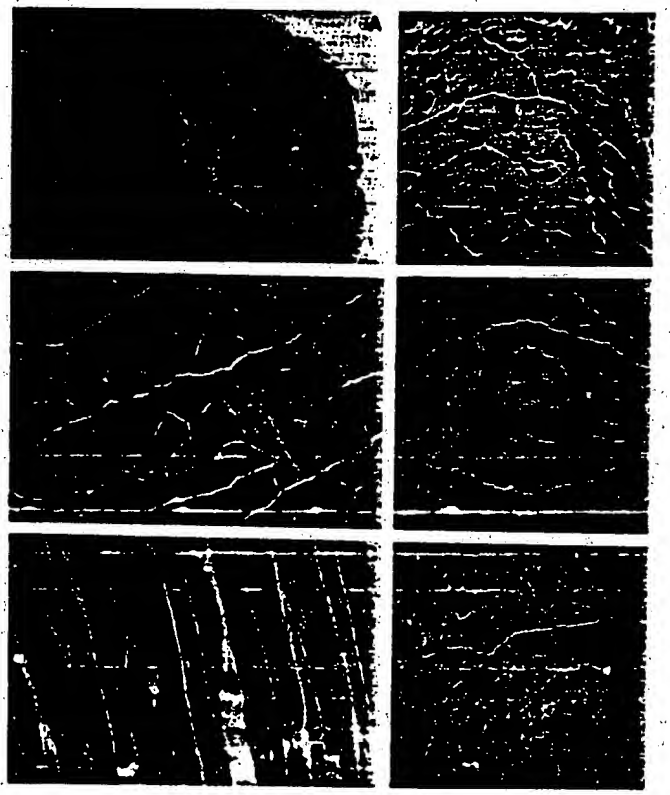

Fig. 2. In situ cytochemical staining of muscle cells for *E. coli* β-galactosidase activity. (**A** and **B**) Cross sections of a muscle injected with pRSV*lacZ* at ×25 and ×160 optical magnification, respectively. (**C**) A longitudinal section of another muscle injected with pRSV*lacZ*, ×160. (**D** to **F**) Serial cross sections of the same muscle that are 0.6 mm apart. Quadriceps muscles were injected once with 100 μg of pRSV*lacZ* DNA (*14*) in 20% sucrose, and the entire quadriceps were removed 7 days after the first injection. The muscle was frozen in liquid isopentane cooled with liquid N_2. Serial sections (15 μm) were sliced with a cryostat and placed immediately on gelatinized slides. The slices were fixed in 1.5% glutaraldehyde in phosphate-buffered saline for 10 min and stained 4 hours for β-galactosidase activity as described (*29*). The muscle was counterstained with eosin. Similar results have been obtained in 16 individual injection sites. Control muscle had no stained muscle cells. Scale bar: (A), 620 μm; (B and C), 100 μm; and (D to F), 260 μm.

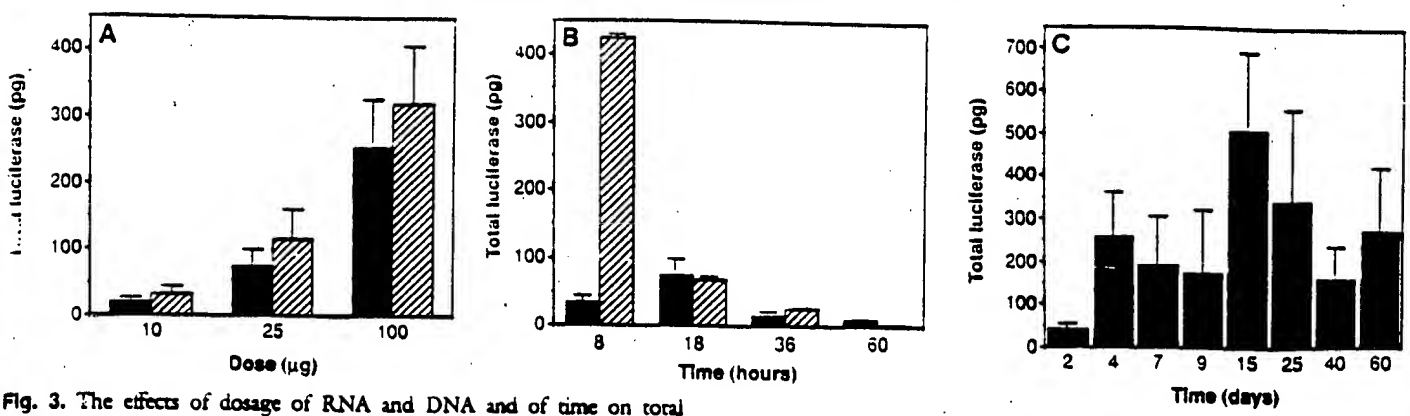

Fig. 3. The effects of dosage of RNA and DNA and of time on total luciferase extracted. Values indicate the average total luciferase activity ± SEM of muscle extracts from four to ten separate quadriceps that were injected or of fibroblast extracts from two to four separate lipofections. (A) Luciferase activity was measured 18 hours after the injection of varying amounts of βgLucβgA$_m$ RNA in 20% sucrose (solid bars) and 4 days after the injection of various amounts of pRSVL in 20% sucrose (striped bars). (B) Luciferase activity was assayed at various times after 20 μg of βgLucβgA$_m$ RNA were lipofected into 10^6 3T3 fibroblasts (striped bars) as previously described (*6, 7*), and after 100 μg of βgLucβgA$_m$ RNA in 20% sucrose was injected into quadriceps (solid bars). (C) Luciferase activity was assayed at various times after 100 μg of pRSVL DNA in 20% sucrose was injected intramuscularly. The RNA and DNA vectors were prepared as in Fig. 1, except that the lysis buffer was 100 m*M* potassium phosphate (*p*H 7.8), 1 m*M* DL-dithiothreitol, and 0.1% Triton X-100. An 87.5-μl portion of the 200-μl extract was analyzed for luciferase activity as described (*17*) with an LKB 1251 luminometer. Light units were converted to picograms of luciferase with a standard curve established by measuring the light units produced by purified firefly luciferase (Analytical Luminescence Laboratory) in control muscle extract. The RNA or DNA preparations did not contain any contaminating luciferase activity before injection. Control muscle injected with 20% sucrose had no detectable luciferase activity. Experiments were performed two or three times; the time points greater than 40 days were performed three times.

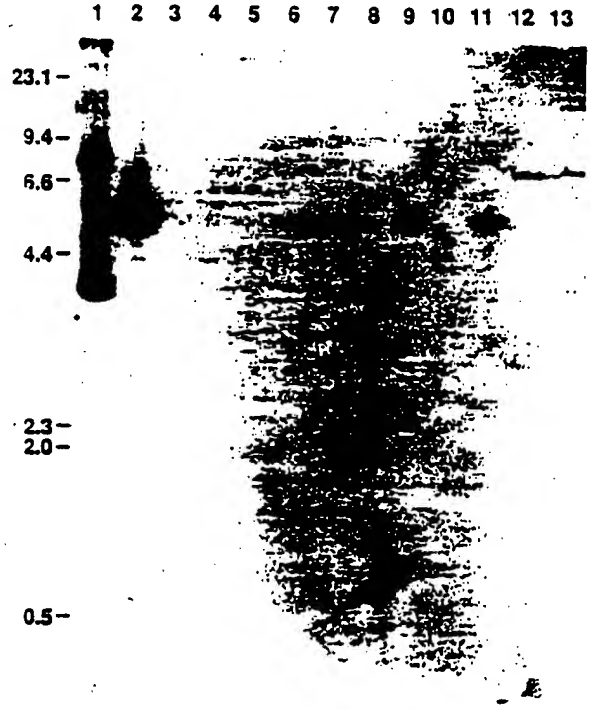

Fig. 4. Southern blot analysis of DNA from muscle injected 30 days previously with pRSVL. Lane 1, 5 ng of undigested pRSVL plasmid; lane 2, 0.05 ng of Bam HI–digested pRSVL; lane 3, empty; lane 4, Bam HI digest of Hirt supernatant from control muscle; lane 5, Bam HI digest of cellular DNA from control, uninjected muscle; lanes 6 and 7, Bam HI digest of Hirt supernatant from two different pools of pRSVL-injected muscles; lanes 8 and 9, Bam HI digest of cellular DNA from two different pools of pRSVL-injected muscle; lane 10, cellular DNA (as in lane 9) digested with Bam HI and Dpn I; lane 11, cellular DNA (as in lane 9) digested with Bam HI and Mbo I; lane 12, cellular DNA digested with Bgl II; and lane 13, Hirt supernatant digested with Bgl II. Preparations of muscle DNA were obtained from control, uninjected quadriceps or from quadriceps 30 days after injection with 100 μg of pRSVL in 20% sucrose. Two entire quadriceps muscles from the same animal were pooled, minced into liquid N_2, and ground with a mortar and pestle. Total cellular DNA and Hirt supernatants were prepared as previously described (*21, 25*). Fifteen micrograms of the total cellular DNA or 10 μl of the 100-μl Hirt supernatant were digested, subjected to electrophoresis on a 1.0% agarose gel, transferred to Nytran (Scheicher & Schnell) with a vacublot apparatus (LKB), and hybridized with multiprimed ^{32}P-labeled luciferase probe (the Hind III–Bam HI fragment of pRSVL). After overnight hybridization, the final wash of the membrane was with 0.2× standard sodium citrate containing 0.5% SDS at 68°C. Kodak XAR5 film was exposed to the membrane for 45 hours at −70°C. Size markers (λ/Hind III) are shown on the left in kilobases.

presence of the pRSVL DNA in Hirt supernatants (Fig. 4, lanes 5, 7, and 13) and in bacteria rendered ampicillin-resistant after transformation with Hirt supernatants (*13*) also suggests that the DNA is present unintegrated. Although the majority of the exogenous DNA appears to be extrachromosomal, low levels of chromosomal integration cannot be definitively excluded. Overexposure of the blots has not revealed smears of hybridizing DNA that would represent plasmid DNA integrated at random sites. The sensitivity of the pRSVL DNA in muscle to Dpn I digestion (Fig. 4, lane 10) and its resistance to Mbo I digestion (Fig. 4, lane 11) suggests, as previously explained (*20*), that the DNA has not replicated within the muscle cells. Thus, the relatively stable expression of luciferase in muscle injected with pRSVL DNA is probably due to the persistence of injected DNA. Most of the DNA exists as a nonintegrated, circular form that does not replicate.

The mechanism of entry of these polynucleotides into the muscle cells is unknown. Polynucleotide expression has been obtained when the composition and volume of the injection fluid and the rate of injection were modified from the described protocol (*21*). Although we have detected low amounts of reporter enzyme in other tissues (liver, spleen, skin, lung, brain, and blood) injected with the RNA and DNA vectors, the levels in muscle were substantially greater. Muscle may be particularly suited to take up and express polynucleotides because of its structural features, such as its multinucleated cells, sarcoplasmic reticulum, and transverse tubule system, which contains extracellular fluid and penetrates deep into the muscle cell (*22, 23*). It is also possible that the polynucleotides enter damaged muscle cells, which then recover.

If direct transfer of genes into human muscle in situ also occurs, it may have several potential clinical applications. The effects of genetic diseases of muscle might be ameliorated by expression of the normal

gene within muscle cells (24). Muscle might also be a suitable tissue for the heterologous expression of a transgene that would modify disease states in which muscle is not primarily involved. The intracellular expression of genes encoding antigens may provide alternative approaches to vaccine development. The use of RNA and a tissue that can be repetitively accessed might be useful for a reversible type of gene transfer, administered much like conventional pharmaceutical treatments.

REFERENCES AND NOTES

1. F. D. Ledley, *J. Pediatrics* **110**, 1 (1987); M. Eglitis and W. F. Anderson, *Biotechniques* **6**, 608 (1988); T. Friedmann, *Science* **244**, 1275 (1989).
2. C. Nicolau *et al.*, *Proc. Natl. Acad. Sci. U.S.A.* **80**, 1068 (1983); Y. Kaneda, K. Iwai, T. Uchida, *Science* **243**, 375 (1989); R. J. Mannino and S. Gould-Fogerite, *Biotechniques* **6**, 682 (1988).
3. N. Benvenisty and L. Reshef, *Proc. Natl. Acad. Sci. U.S.A.* **83**, 9551 (1986).
4. G. Y. Wu and C. H. Wu, *J. Biol. Chem.* **263**, 14621 (1988).
5. C. Seeger, D. Ganem, H. E. Varmus, *Proc. Natl. Acad. Sci. U.S.A.* **81**, 5849 (1984); T. W. Dubensky, B. A. Campbell, L. P. Villareal, *ibid.*, p. 7529.
6. P. L. Felgner and G. M. Ringold, *Nature* **337**, 461 (1989); T. R. Reid, P. L. Felgner, G. M. Ringold, *J. Biol. Chem.*, in press; P. Felgner *et al.*, *Proc. Natl. Acad. Sci. U.S.A.* **84**, 7413 (1987); P. L. Felgner and M. Holm, *Focus* **11**, 21 (1989).
7. R. W. Malone, P. L. Felgner, I. M. Verma, *Proc. Natl. Acad. Sci. U.S.A.* **86**, 6077 (1989).
8. R. W. Malone, *Focus* **11**, 61 (1989).
9. Female and male BALB/c mice (5 to 6 weeks old) were anesthetized by intraperitoneal injection with 0.3 ml of 2.5% Avertin (2.5% tribromoethyl alcohol and 2.5% tert-amyl alcohol in water). A 1.5-cm incision was made on the anterior thigh, and the quadriceps muscle was exposed. Solution (0.1 ml) was injected in a 1-ml syringe through a 27-gauge needle over 1 min, ~0.5 cm from the distal insertion point of the muscle into the knee and ~0.2 cm deep. The skin was closed with stainless steel clips (MikRon).
10. C. M. Gorman *et al.*, *Proc. Natl. Acad. Sci. U.S.A.* **79**, 6777 (1982).
11. P. A. Krieg and D. A. Melton, *Nucleic Acids Res.* **12**, 7057 (1984).
12. A Hind III–Bam HI fragment of the CAT gene from pSV2CAT was inserted into the Bgl II site of the pSP64T plasmid (*11*). The SP6 promoter was replaced with the T7 promoter from pIBI31 (International Biotechnologies) for in vitro transcription by T7 polymerase.
13. G. Acsadi, P. Williams, J. Wolff, unpublished data.
14. P. A. Norton and J. M. Coffin, *Mol. Cell. Biol.* **5**, 281 (1985).
15. E. Ralston and Z. W. Hall, *Science* **244**, 1066 (1989).
16. One million 3T3 mouse fibroblasts in a 60-mm dish were transfected as previously described (*6*, *7*) with 20 μg of DNA or RNA complexed with 60 μg of Lipofectin (BRL) in 5 ml of a modified minimal essential medium (Opti-MEM; Gibco).
17. J. R. de Wet, K. V. Wood, M. DeLuca, D. R. Helinski, S. Subramani, *Mol. Cell. Biol.* **7**, 725 (1987).
18. Because there is some conversion of the closed, circular form to the open, circular form during the extraction, digestion, and electrophoresis steps, the presence of plasmid in the closed, circular form cannot be excluded. G. K. Finn *et al.* [*Mol. Cell. Biol.* **9**, 4009 (1989)] have found plasmid DNA transiently transfected into fibroblasts at the same size as open, circular DNA.
19. B. Hirt, *J. Mol. Biol.* **26**, 365 (1967); C. D. Pauza and J. Galindo, *J. Virol.* **63**, 3700 (1989).
20. M. Lavitrano *et al.*, *Cell* **57**, 717 (1989).
21. Luciferase activity has been observed with 10 to 100 μl of hypotonic, isotonic, and hypertonic sucrose solutions. Opti-MEM, or sucrose solutions containing 2 m*M* $CaCl_2$. Luciferase activity was also observed when the 10- or 100-μl injections were performed over 20 min with a pump instead of within 1 min.
22. R. Rubio and N. Sperelakis, *Z. Zellforsch Mikrosk. Anat.* **124**, 57 (1972); C. Franzini-Armstrong, in *Myology*, A. G. Engel and B. Q. Banker, Eds. (McGraw-Hill, New York, 1986), pp. 125–154.
23. Polynucleotides may enter the sarcoplasmic reticulum just as under certain in vitro conditions extracellular horseradish peroxidase can enter the sarcoplasmic reticulum via the transverse tubular system (*22*). The influx of positively charged calcium ions, which are in high concentration within the sarcoplasmic reticulum, into the cytoplasm during muscle contraction may mediate the entry of the negatively charged polynucleotides into the cytoplasm from the sarcoplasmic reticulum. However, current opinion is that under normal conditions there is no direct conduit between T tubules and sarcoplasmic reticulum.
24. Similar levels of luciferase expression have been detected in *mdx* mice as compared to wild-type mice.
25. F. M. Ausbel *et al.*, Eds., *Current Protocols in Molecular Biology* (Wiley, New York, 1989).
26. Capped βgCATβgA, RNA was prepared in vitro with T7 polymerase (*7*) from the pβgCATβgA, plasmid (*12*). pRSVCAT (*10*) was prepared by alkaline lysis, two purifications on CsCl gradients, dialysis against 1 m*M* tris-HCl (*p*H 7.4) and 0.1 m*M* EDTA, ethanol precipitation, and solvation into water (*25*).
27. Muscle extracts were prepared by excising the entire quadriceps, mincing the muscle into a 1.5-ml microtube containing 200 μl of a lysis solution [20 m*M* tris-HCl (*p*H 7.4), 2 m*M* $MgCl_2$, and 0.1% Triton X-100], and grinding the muscle with a plastic pestle (Kontes) for 1 min. To ensure complete disruption of the muscle cells, we then placed the muscle tissue under 600 psi of N_2 in a bomb (Parr) at 4°C for 30 min before releasing the pressure. Fibroblasts were processed similarly after they were removed from the plates by treatment with trypsin, taken up into media with serum, washed twice with phosphate-buffered saline, and then the final cell pellet was suspended into 200 μl of lysis solution. Portions (75 μl) of the muscle and fibroblast extracts were assayed for CAT activity by incubating the reaction mixtures for 2 hours (*28*). The autoradiograms were made by exposing the thin-layer chromatography (TLC) plates, after spraying them with NEN Enhance, to Kodak XAR5 film for 54 hours at −70°C. Percent conversions were determined by measuring the radioactivity in the scraped TLC spots. Percent conversions were converted to picograms of CAT with the use of a standard log-log curve established by measuring the percent conversion produced by purified CAT (Sigma) and the conversion factor of 100,000 units of protein per milligram (Sigma).
28. C. Gorman *et al.*, *Mol. Cell. Biol.* **2**, 1044 (1982).
29. S. Shimohama *et al.*, *Mol. Brain Res.*, in press; Price, D. Turner, C. Cepko, *Proc. Natl. Acad. Sci. U.S.A.* **84**, 156 (1987).

30. Supported in part by the NIH (grant numbers HD00669-05 and HD03352) and the Lynn F. Talvor Memorial Fund. We thank B. Hansen and P. Walter for providing us with a pSP64T construct containing the CAT gene; E. Langer for technical assistance; S. Kornguth, R. Suffit, and A. Messing for advice on the histologic techniques; M. Rasmussen for help in preparing the manuscript; S. Hunsaker for photographic services; R. Kumar for synthesis of lipofectin reagents and discussions; K. Hostetler, D. Carson, R. Gregg, and L. Barness for discussions; and J. Ross, J. Dahlberg, R. Pauli, E. Spritz, and H. Temin for critical reading of the manuscript.

16 June 1989; accepted 20 December 1989

Is Soot Composed Predominantly of Carbon Clusters?

LAWRENCE B. EBERT

Soot generated from diesel fuel in a combustion tube is characterized by microanalysis, x-ray diffraction, chemical reactivity, and nuclear magnetic resonance to address the recent proposal of the significance of carbon clusters in soot. The data support a traditional model of soot as polynuclear aromatic compounds rather than as clusters of carbon atoms with minimal edge site density. The amounts of noncarbon atoms in the soot (hydrogen, oxygen, nitrogen, and sulfur) are commensurate with the edge density of the crystallites (2 by 2 nanometers) inferred from diffraction. The chemistry of soot, in being reduced by potassium metal and alkylated by alkyl iodides, is that known for aromatic compounds and not that anticipated for materials such as graphite, with a small fraction of carbon atoms on edges.

RECENTLY, IT WAS PROPOSED THAT the C_{60} carbon cluster might shed "a totally new and revealing light on several important aspects of carbon's chemical and physical properties that were quite unsuspected" [(*1*), p. 1139]. One of the outgrowths of this work was the prediction that "C_{60} should be a by-product of combustion and a key to the soot formation process" [(*1*), p. 1145]. Although there was no claim that the closed polyhedron C_{60} was a major component of soot, the idea was advanced that the known spherical morphology of soot could be interpreted as arising from open, spiraling, carbon clusters. Each spherical particle of soot would be a molecule.

There is no doubt that the proposal of carbon clusters is exciting and that the idea has captured the imagination of many. In the laser pyrolysis of carbonaceous substrates, however, two separate groups have failed to find C_{60} to be a dominant species (*2*, *3*), and there is some disagreement over the interpretation of the experiment linking

Exxon Corporate Research Laboratory, Annandale, NJ 08801.

Brief Rapid Communication

Expression of Recombinant Genes in Myocardium In Vivo After Direct Injection of DNA

Hua Lin, MD, Michael S. Parmacek, MD, Gerald Morle, BS, Steven Bolling, MD, and Jeffrey M. Leiden, MD, PhD

The ability to program recombinant gene expression in cardiac myocytes in vivo holds promise for the treatment of many inherited and acquired cardiovascular diseases. In this report, we demonstrate that a recombinant β-galactosidase gene under the control of the Rous sarcoma virus promoter can be introduced into and expressed in adult rat cardiac myocytes in vivo by the injection of purified plasmid DNA directly into the left ventricular wall. Cardiac myocytes expressing recombinant β-galactosidase were detected histochemically in rat hearts for at least 4 weeks after injection of the β-galactosidase gene. These results demonstrate the potential of this method of somatic gene therapy for the treatment of cardiovascular disease. (*Circulation* 1990;82:2217–2221)

Somatic gene therapy, the expression of recombinant genes in non–germ-line tissues of the adult organism, holds great promise for the treatment of many inherited and acquired human diseases (reviewed in Reference 1). The biological requirements for this type of gene therapy include the ability to introduce recombinant genes efficiently into the appropriate cells and tissues and to program the high-level and, in many cases, stable expression of these recombinant genes in vivo. In addition, it is necessary that the process of gene therapy itself not be harmful to the recipient organism, in particular, that the techniques used to introduce the recombinant genes do not result in persistent infection of the host or in deleterious mutations of the recipient cells. Two general approaches have proven useful in animal models of somatic gene therapy. In the first, recombinant genes have been introduced into cultured cells in vitro, and cells expressing the recombinant gene product have then been transplanted into the appropriate tissue of a recipient animal.[2–4] In the second, recombinant genes have been introduced directly into somatic cells in vivo.[5]

From the Howard Hughes Medical Institute (G.M., J.M.L.) and Departments of Internal Medicine (M.S.P., J.M.L.) and Surgery (H.L., S.B.), University of Michigan Medical Center, and the Ann Arbor Veterans Administration Medical Center (M.S.P.), Ann Arbor, Mich.

Supported in part by National Institutes f Health grant DK-42718.

Address for correspondence: Jeffrey M. Leiden, MD, PhD, Howard Hughes Medical Institute, 1150 W. Medical Center Drive, MSRB I, Room 4510, Ann Arbor, MI 48109-0650.

The ability to program recombinant gene expression in adult myocardium in vivo requires both an expression vector with high-level activity in cardiac myocytes and a method for introducing such a vector into myocardial cells in the adult animal. A previous study demonstrated that murine skeletal myocytes display a rather unique ability to take up and express DNA after direct injection in vivo.[6] In the studies described in this report, we show that an expression vector using the Rous sarcoma virus (RSV) long terminal repeat (LTR) programs high-level recombinant gene expression in rat cardiac myocytes in vitro and demonstrate that recombinant genes cloned into this vector can be introduced into and expressed in adult rat cardiac myocytes for at least 4 weeks after direct injection of plasmid DNA into the left ventricular wall.

Methods

Cell Culture and Transient Transfections

Neonatal rat cardiac myocytes were isolated from 1–2-day-old Sprague-Dawley rats (Charles River Laboratories, Wilmington, Mass.) by collagenase digestion as previously described.[7] This method results in the isolation of more than 90% cardiac myocytes.[7] Twenty-four hours after isolation, 1×10^6 freshly isolated myocytes in a 60-mm collagen-coated dish (Collaborative Research Inc., Waltham, Mass.) were transfected with 15 μg of cesium chloride gradient–purified chloramphenicol acetyl transferase (CAT) reporter plasmid DNA plus 5 μg of pMSVβgal reference plasmid DNA as follows: 20 μg of plasmid DNA was resuspended in 1.5 ml of Opti-MEM (GIBCO, Grand Island, N.Y.)

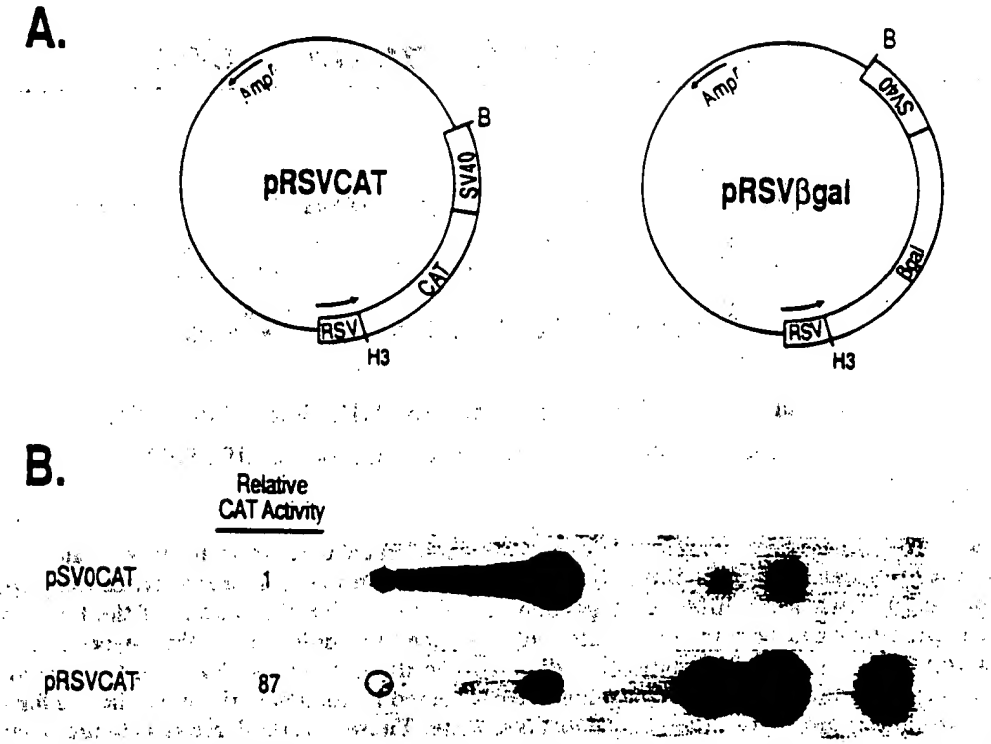

FIGURE 1. *Transcriptional activity of the Rous sarcoma virus (RSV) long terminal repeat (LTR) in rat neonatal cardiocytes in vitro.* Panel A: *A schematic representation of the pRSVCAT and pRSVβgal plasmids. βgal, β-galactosidase gene; CAT, chloramphenicol acetyl transferase gene.* HindIII *(H3) and* BamHI *(B) restriction endonuclease sites are shown.* Panel B: *Transcriptional activity of the RSV LTR in rat neonatal cardiocytes in vitro. Rat neonatal cardiocytes were transfected with 15 μg of the promoterless pSVOCAT control plasmid or the pRSVCAT plasmid (see panel A) and cell extracts prepared 48 hours after transfection were normalized for protein content and assayed for CAT activity as previously described.*[9] *To control for differences in transfection efficiencies, all transfections also contained 5 μg of the pMSVβgal reference plasmid. Data are shown as CAT activity relative to that produced by the pSVOCAT plasmid (which produced 1.7% acetylation) after correction for differences in transfection efficiency.*

and added to 1.5 ml of Opti-MEM containing 50 μl of lipofectin reagent (BRL, Gaithersburg, Md.). The resulting mixture was added to one 60-mm plate of cardiac myocytes. After 5 hours at 37° C in 5% CO_2, 3 ml of Medium 199 plus 5% fetal bovine serum (FCS) (GIBCO) was added to the cells, and the mixture was incubated at 37° C for 48 hours. Cell extracts were prepared and normalized for protein content using a commercially available kit (Biorad, Richmond, Calif.). CAT and β-galactosidase assays were performed as previously described.[9]

Plasmids

The promoterless pSVOCAT plasmid[10] and the pRSVCAT[11] plasmid in which transcription of the bacterial CAT gene is under the control of the RSV promoter have been described previously. The pRSVβgal plasmid was constructed by cloning the 4.0-kb β-galactosidase gene from pMSVβgal[12] into *Hin*dIII/*Bam*HI-digested pRSVCAT (see Figure 1A).

Injection of Recombinant DNA In Vivo

Six- to 11-week-old 250-g Sprague-Dawley rats were h used and cared for according to National Institutes of Health guidelines in the ULAM facility of the University of Michigan Medical Center. Rats were anesthetized with 20 mg/kg pentobarbitol i.p. and 60 mg/kg ketamine i.m., intubated, and ventilated with Harvard (Harvard Apparatus, South Natick, Mass.) respirator. A left lateral thoracotomy was performed to expose the beating heart, and 100 μg of plasmid DNA in 100 μl of phosphate-buffered saline (PBS) containing 5% sucrose (PBS/sucrose) was injected into the apical portion of the beating left ventricle using a 30-g needle. Control animals were injected with 100 μl of PBS/sucrose alone. The animals were killed 3–5 or 21–30 days after injection by pentobarbitol euthanasia; hearts were removed via a medi.. sternotomy, rinsed in ice-cold PBS, and processed for β-galactosidase activity.

Histochemical Analysis

Three-millimeter cross sections of the left ventricle were fixed for 5 minutes at room temperature with 1.25% glutaraldehyde in PBS, washed three times at room temperature in PBS, and stained for β-galactosidase activity with X-gal (Biorad) for 4–16 hours a described by Nabel et al.[2] The 3-mm sections we embedded with glycomethocrylate, and 4–7-μm sections were cut and counterstained with hematoxylin and eosin as described previously.[2] Photomicroscopy was performed using Kodak Ektachrome 200 film and Leitz Laborlux D and Wild M8 microscopes.

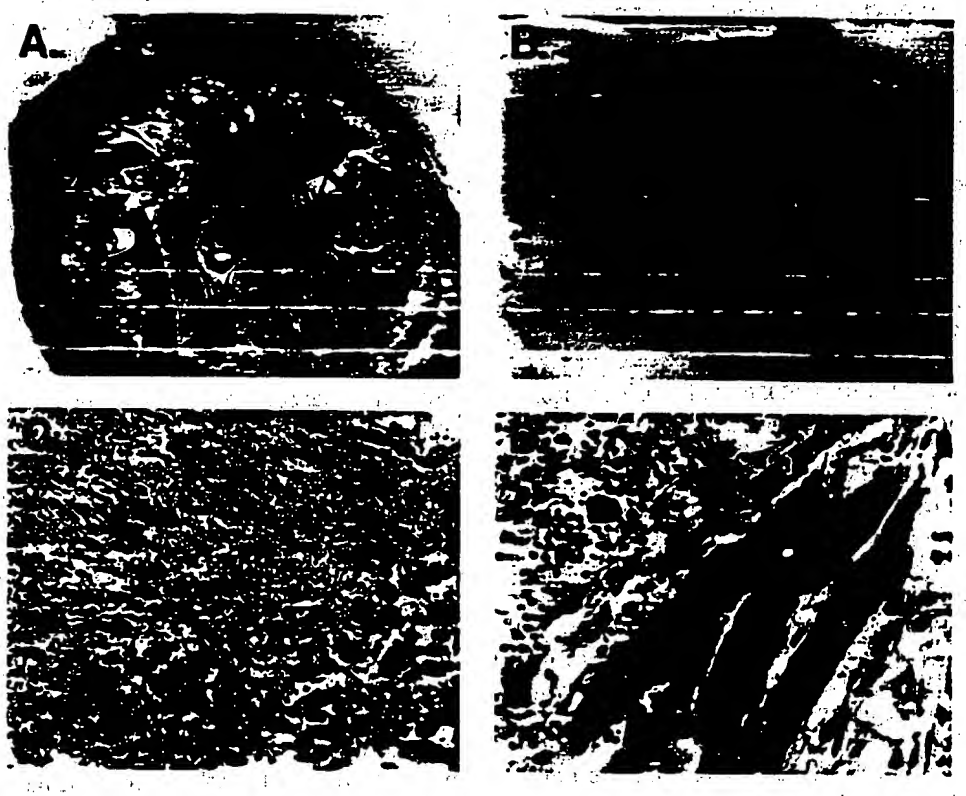

FIGURE 2. *Expression of a recombinant β-galactosidase gene in cardiac myocytes in vivo after direct injection of pRSVβgal DNA into the left ventricular wall. One hundred micrograms of pRSVβgal DNA was injected into the beating apical wall of the left ventricle of Sprague-Dawley rats using a 30-g needle as described in "Methods." Hearts were harvested 3–5 days or 3–4 weeks after injection and stained for β-galactosidase activity.* Panel A: *10× view of a 3-mm section of a heart 3 days after pRSVβgal injection.* Panel B: *18× view of a 3-mm section from a heart 27 days after pRSVβgal injection.* Panels C *and* D: *125× and 250× views, respectively, of 4-μM sections from a heart 3 days after pRSVβgal injection. β-Galactosidase activity (dark-blue staining) is seen only within cardiac myocytes that can be identified by their myofibrillar architecture.*

Results

RSV LTR Promotes High-Level Gene Expression in Rat Neonatal Cardiocytes In Vitro

Although the RSV LTR displays high-level transcriptional promoter activity in a wide variety of immortalized cell types,[11] previous transgenic studies have suggested that this promoter is preferentially active in skeletal and cardiac myocytes in vivo.[13,14] To test directly the transcriptional activity of the RSV LTR in rodent cardiac myocytes, the pRSVCAT vector[11] in which expression of the bacterial CAT gene is under the control of the RSV LTR was transfected into primary neonatal rat cardiac myocytes using lipofectin. Two days after transfection, the cultures were harvested and assayed for CAT activity as previously described.[9] All transfections also contained 5 μg of the pMSVβgal plasmid[12] to correct for differences in transfection efficiencies. As shown in Figure 1, the RSV LTR was able to increase transcription of the CAT gene 17-fold compared with the promoterless pSVOCAT control plasmid. The pRSVCAT-transfected cardiac myocyte extracts produced 95% acetylation in a standard thin-layer chromatography assay.[9] By comparison, identically prepared extracts of 3T3 or HeLa cells transfected with this same vector produced 22% and 35% acetylation, respectively (data not shown). Because the activities of cotransfected pMSVβgal reference plasmids were almost identical in all three transfections, these results demonstrated that the RSV LTR programs high-level transcription in primary cardiac myocytes in vitro.

The ability to unambiguously identify the cell types that are expressing recombinant gene products is an important requirement of all animal models of gene therapy. Because the bacterial β-galactosidase reporter gene (but not the bacterial CAT gene) allows direct histological visualization of recombinant gene expression, we constructed a pRSVβgal vector in which bacterial β-galactosidase gene expression is regulated by the RSV LTR promoter for further studies of recombinant gene expression in vivo (Figure 1B).

Expression of β-Galactosidase Gene in Rat Cardiac Myocytes After Injection of pRSVβgal DNA Into the Left Ventricular Wall In Vivo

In an attempt to program recombinant β-galactosidase gene expression in rat cardiac myocytes in

vivo, we took advantage of a previously described technique for producing recombinant gene expression in murine skeletal myocytes in vivo.[6] Briefly, 100 μg of pRSVβgal DNA was resuspended in 100 μl of PBS containing 5% sucrose (PBS/sucrose) and injected via a 30-g needl directly into the beating left ventricular wall of 6–11-week-old Sprague-Dawley rat hearts. Control rats received injections of 100 μl of PBS/sucrose without DNA. Rats were killed either 3–5 days or 3–4 weeks after injection, and hearts were fixed and stained for β-galactosidase activity. β-Galactosidase activity as manifested by dark-blue staining was readily apparent to the naked eye in sections of three of four of the pRSVβgal-injected hearts at 3–5 days and four of five of the pRSVβgal-injected hearts at 3–4 weeks after DNA injections (Figures 2A and 2B). This staining, which was focal and patchy, occurred only in a single area of each heart injected with pRSVβgal DNA and was not seen in five control hearts injected with PBS/saline alone (data not shown). Failure to observe staining in two of nine of the pRSVβgal-injected hearts may have been due to the lack of DNA uptake or expression in these hearts or, more likely, to technical difficulties in successfully centering and anchoring the needle in the relatively thin beating left ventricular wall during the injection process.

Because the normal ventricular wall contains both myocytes and fibroblasts and because the injection of DNA might be expected to cause a localized inflammatory response, it was important to determine which cell types were expressing the recombinant β-galactosidase gene. Histochemical analysis of sections from hearts injected with the pRSVβgal DNA clearly demonstrated β-galactosidase activity within cardiac myocytes that were easily identified by their myofibrillar architecture (Figures 2C and 2D). Between one and 10 positively staining myocytes were seen per high-power field, and these were often noncontiguous, suggesting that the uptake of DNA and/or its expression is a relatively low-frequency event. Because it was difficult to accurately identify the extent of DNA injection and because the positively staining areas were quite focal and patchy, it was impossible to accurately quantitate either the percentage or the total number of cells expressing recombinant β-galactosidase activity in a given heart. However, it is clear that only a small fraction of cardiac myocytes expressed the recombinant protein. In addition, it is worth noting that sections from the 3–5-day postinjection hearts often showed evidence of an acute inflammatory response along the track of the needle (Figure 2C) and that in several cases fibrosis along the needle track was observed in sections from the 3–4-week postinjection hearts (data not shown).

Discussi n

The studies presented hav demonstrated that it is possible to program recombinant gene expression in cardiac myocytes after direct injection of DNA into the left ventricular wall. Functi nal recombinant protein expression in myocytes was demonstrated directly using an enzymatic assay for β-galactosidase. Recombinant gene expression was observed in myocytes from seven of nine of the injected hearts at both 3–5 days and 3–4 weeks after injection. Expression was patchy and was observed only in direct contiguity with the site of injection. These findings have several implications regarding both the use of this method for somatic gene therapy in the heart and the biology of recombinant DNA uptake and expression in muscle cells.

A previous study suggested that murine skeletal muscle cells possess a unique ability to take up and express injected recombinant DNA.[6] Our results have extended this observation to cardiac muscle cells in a second rodent species. It has previously been thought that successful DNA transfection and expression may require recipient cell division and, more specifically, breakdown of the recipient cell nuclear membrane to allow DNA entry. Because skeletal myocytes have a limited potential for mitosis,[15] it remained possible that the previously reported successful transfection of skeletal myocytes was dependent on their mitotic potential. In contrast to skeletal myocytes, adult cardiac muscle cells are unable to divide.[16] Thus, our results demonstrate that mitosis is not necessary for successful transfection of cells with DNA. The mechanisms that allow preferential uptake of DNA into cardiac and skeletal myocytes remain unclear. However, our data suggest that they must be dependent on structural or functional properties that are shared by skeletal and cardiac muscle. Current hypotheses include the possibility of specialized muscle cell transport systems or the unique ability to physically disrupt the cell membranes of muscle cells in a reversible fashion during the recombinant DNA injections.

The technique of somatic gene therapy using direct DNA injection into myocardium, as described in this report, has several advantages compared with other previously described methods of gene therapy. First, infectious viral vectors are not required, eliminating the possibility of persistent infection of the host. Second, a previous study[6] has suggested that recombinant DNA taken up and expressed in skeletal myocytes persists as an episome and therefore does not have the same potential for host cell mutagenesis as do retroviral vectors that integrate into the host chromosome. Finally, this method does not require the growth of recipient cells in vitro, a requirement that would render transfection of nondividing cardiac myocytes particularly difficult.

Direct injection of recombinant DNA into the myocardium holds promise for the treatment of many acquired and inherited cardiovascular diseases. We are particularly interested in the possibility of stimulating collateral circulation in areas of chronic myocardial ischemia by expressing recombinant angiogenesis factors locally in the ventricular wall. Although the method described in this report is a first step toward such gene therapy approaches, many questions and problems remain to be addressed

before this type of gene therapy can become a reality. First, it must be demonstrated that human myocytes, like their rodent counterparts, are able to take up and express recombinant DNA. The longevity of recombinant gene expression must be more fully examined, and the possibility that some of the recombinant DNA is integrated into the host genome with the concomitant potential for mutagenesis must be ruled out. Modifications of the current transfection protocol must be developed to increase the frequency of recombinant gene expression in cardiac myocytes. Of equal importance, the inflammatory response to the injected DNA must be controlled to prevent the formation of arrhythmogenic foci. Finally, it will of interest to determine whether high-level recombinant gene expression can be programmed in vivo by the injection of expression vectors containing cardiac-specific transcriptional regulatory elements. Ongoing studies in our laboratory are designed to address these problems. Nevertheless, the initial studies described in this report suggest that somatic gene therapy in the heart may eventually become a useful therapeutic modality.

Acknowledgments

The authors would like to thank Dr. James Wilson for critical review of the manuscript, Mrs. Jeanelle Pickett for expert secretarial assistance, and Ms. Beverly Burck for the preparation of the illustrations. We would also like to thank Kaye Brabec, Lorita Dudus, and Dr. Kent Christensen for help with histochemical staining.

References

1. Swain JL: Gene therapy: A new approach to the treatment of cardiovascular disease. *Circulation* 1989;80:1495–1496
2. Nabel EG, Plautz G, Boyce FM, Stanley JC, Nabel GJ: Recombinant gene expression *in vivo* within endothelial cells of the arterial wall. *Science* 1989;244:1342–1344
3. Wilson JM, Birinyi LK, Salomon RN, Libby P, Callow AD, Mulligan RC: Implantation of vascular grafts lined with genetically modified endothelial cells. *Science* 1989;244:1344–1346
4. Dichek DA, Neville RF, Zwiebel JA, Freeman SM, Leon MB, Anderson WF: Seeding of intravascular stents with genetically engineered endothelial cells. *Circulation* 1989;80:1347–1353
5. Nabel EG, Plautz G, Nabel GJ: Site-specific gene expression in vivo by direct gene transfer into the arterial wall. *Science* 1990 (in press)
6. Wolff JA, Malone RW, Williams P, Chong W, Acsadi G, Jani A, Felgner PL: Direct gene transfer into mouse muscle in vivo. *Science* 1990;247:1465–1468
7. Engelmann GL, Gerrity RG: Biochemical characterization of neonatal cardiomyocyte development in normotensive and hypertensive rats. *J Mol Cell Cardiol* 1988;20:169–177
8. Curran T, Miller AD, Zokas L, Verma IM: Viral and cellular fos proteins: A comparative analysis. *Cell* 1984;36:259–268
9. Parmacek MS, Bengur AR, Vora AJ, Leiden JM: Structure and regulation of expression of the murine fast skeletal troponin C gene: Identification of a developmentally-regulated, muscle-specific transcriptional enhancer. *J Biol Chem* 1990 (in press)
10. Gorman CM, Moffat LF, Howard BH: Recombinant genomes which express chloramphenicol acetyl-transferase in mammalian cells. *Mol Cell Biol* 1982;77:1432–1436
11. Gorman C, Padmanabhan R, Howard BH: High efficiency DNA-mediated transformation of primate cells. *Science* 1983; 221:551–553
12. Donoghue M, Ernst H, Wentworth B, Nadal-Ginard B, Rosenthal N: A muscle-specific enhancer is located at the 3' end of the myosin light-chain 1/3 gene locus. *Genes Dev* 1988;2:1779–1790
13. Overbeek PA, Lai S-P, Van Quill KR, Westphal H: Tissue-specific expression in transgenic mice of a fused gene containing RSV terminal sequences. *Science* 1986;231:1574–1577
14. Swain JL, Stewart TA, Leder P: Parental legacy determines methylation and expression of an autosomal transgene: A molecular mechanism for parental imprinting. *Cell* 1987;50: 719–727
15. Zak R: Development and proliferation capacity of cardiac muscle cells. *Circ Res* 1974;34-35(suppl II):II-17–II-26
16. Korecky B, Rakusan K: Normal and hypertrophic growth of the rat heart: Changes in cell dimensions and numbers. *Am J Physiol* 1978;234:H123–H128

KEY WORDS • gene therapy • DNA

© 1992 Oxford University Press

Human Molecular Genetics, Vol. 1, No. 6 363–369

Long-term persistence of plasmid DNA and foreign gene expression in mouse muscle

Jon A.Wolff*, James J.Ludtke, Gyula Acsadi+, Phillip Williams and Agnes Jani

Department of Pediatrics and Medical Genetics, Waisman Center, University of Wisconsin, Madison, WI 53705, USA

Received July 13, 1992; Revised and Accepted August 7, 1992

ABSTRACT

Plasmid pRSVL persisted and expressed luciferase for at least 19 months in mouse skeletal muscle after intramuscular injection. Other injected plasmids also stably expressed long-term suggesting that any plasmid DNA could stably persist and express in muscle. Plasmid DNA was demonstrated by quantitative PCR in some of the muscle DNA samples for at least 19 months after injection. The methylation pattern of the plasmid DNA remained in its bacterial form indicating that the foreign DNA did not replicate in the muscle cells. The electroporation of total cellular DNA from injected muscle into bacteria indicated that the plasmid DNA was extrachromosomal. Chromosomal integration of plasmid DNA was searched for by electroporating the injected muscle DNA into bacteria after restriction enzyme digestion and ligation. No plasmids containing plasmid/chromosome junctions were observed in over 1800 colonies examined. Lack of integration increases the theoretical safety of this gene transfer technique. Long-term stability of plasmid DNA in muscle indicates that muscle is an attractive target tissue for the introduction of extrachromosomal plasmid or viral DNA for the purpose of gene therapy.

INTRODUCTION

Previous studies demonstrated the ability of intramuscularly injected plasmid DNA to express exogenous genes in both skeletal (1) and cardiac muscle (2, 3, 4). Expression of the plasmid genes was localized to the skeletal myofibers or the cardiac muscle cells (1). The mechanism of plasmid uptake by the muscle cells is not yet certain but may be due to an active uptake process by the differentiated muscle cells that is not dependent on injury to the myofibers (2, 5, J.Wolff, in preparation). It appeared that expression was stable in mouse skeletal muscle for at least two months (1). It was not clear from the previous study whether expression would continue for longer periods. The present study examined whether expression in mouse skeletal muscle continued for the remaining lifetime of the mouse, approximately one and a half years.

The persistence of plasmid expression in skeletal muscle for at least two months was unexpected. Plasmid expression is transient after transfection into cultured fibroblasts (6). The persistent expression in muscle was most likely due to persistence of the plasmid DNA. Expression was unstable when artificial mRNA was injected into muscle, suggesting that stable expression after plasmid injection was not due to persistence of the *in vivo* transcript or protein. Southern blot analysis indicated that plasmid DNA in the muscle, one month after injection, was in an unintegrated, circular form that had not replicated (1). In the present study, the amount of injected plasmid DNA in muscle and its methylation pattern were determined over longer time periods using the more sensitive technique of quantitative PCR.

A small percentage of the DNA could have integrated without being detected on the Southern blots (1), given the small amount of plasmid DNA in the muscles. In the present study a more sensitive approach was employed to detect integration of the injected plasmid into the muscle chromosomes, which involved the bacterial cloning of plasmid DNA extracted from injected muscle. Integration of plasmid DNA into muscle chromosomal DNA was searched for because it could cause deleterious effects.

RESULTS

Reporter gene expression in muscle over time

One hundred μg of undigested, covalently closed circular (CCC), pRSVL plasmid DNA (7) were injected into quadricep (rectus femoris) muscles of six to ten week old mice. Luciferase activity was measured in six to twelve muscles at varying times until the study was stopped at one and a half years after injection when some of the older mice began to die (Figure 1A). Substantial levels of luciferase were still present for at least one and a half years after injection. The differences between the mean values at the various time-points greater than 60 days were not statistically significant. These results indicate that luciferase expression persisted essentially for the lifetime of the mice.

Stability of expression was followed after injection of linear pRSVL (Figure 1B). CCC pRSVL was made linear by digestion with BamHI which cuts it once 3′ to the SV40 polyA addition signal (7). After transfection of the BamHI-digested pRSVL into 3T3 cells using Lipofectin (BRL), luciferase activity was one half of the level obtained after transfection using CCC pRSVL (data not shown). However, after injection of 100 μg of linear pRSVL into mouse quadriceps, the mean luciferase levels were approximately ten to twenty times less than the luciferase levels after injection of CCC PRSVL (Figure 1B). Nonetheless, luciferase activity still persisted for at least 120 days.

The pRSVCat plasmid (9), which expresses chloramphenicol acetyltransferase (CAT) from the RSV promoter, was used to determine if stable expression also occurs with another reporter

* To whom correspondence should be addressed

+ Present address: Montreal Neurological Hospital, McGill University, 3801 University Street, Montreal, Quebec H3A 2B4, Canada

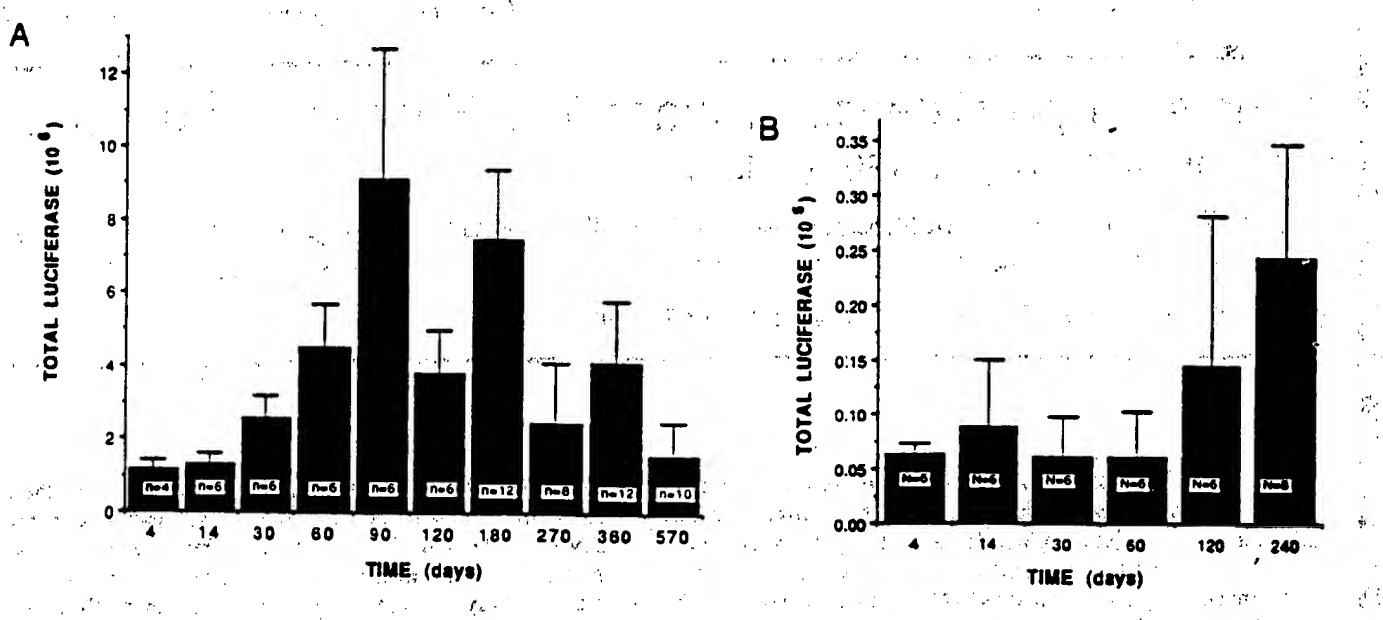

Figure 1. Total mean luciferase activity (L.U.) in quadriceps at varying times after injection of 100 μg of undigested, CCC pRSVL (A) or BamHI-digested pRSVL (B). 'n' indicates the number of muscles analyzed. T bars indicate standard errors.

gene. Substantial levels of CAT activity were present in most of the muscles for at least four months, indicating that stable expression can occur with another reporter gene (Figure 2).

The pCMVLux plasmid was used for stability studies because it has several differences from the pRSVL plasmid such as the π suppressor gene for bacterial selection and the immediate early cytomegalovirus (CMV) promoter (10). After intramuscular injection of 100 μg of pCMVLux, total mean luciferase activity was 0.47×10^6 L.U. ($\pm$ 0.22×10^6, n = 6) at 105 days and 1.04×10^6 ($\pm$ 0.37×10^6, n = 8) at 180 days. These results indicate that luciferase expression persisted after injection of pCMVLux.

Stability of luciferase expression in dividing and non-dividing fibroblasts

In order to determine whether the rate of cell division affects the stability of expression from plasmid DNA, pRSVL was transfected into Rat1 fibroblasts (Figure 3). After transfection, the fibroblasts were split into one fraction that continued to divide as they were continually passed prior to confluency. The other cell fraction was significantly less mitotic since fibroblasts reached confluency and were treated with dexamethasone (11). In both the dividing and confluent cells, luciferase was maximal at seven days post-transfection. Substantial luciferase activity was still present in the confluent cells for at least 28 days post-transfection, but decreased to background levels by 21 days in the cells that were passed. After seven days post-transfection, the percent decrease in total luciferase activity per day was approximately five percent in the unpassed cells and approximately forty percent in the passed cells. These results indicate that the stability of expression after transient transfection was affected by the mitotic rate of the cells.

Persistence of muscle plasmid DNA

Total muscle DNA was prepared from muscles that were also assayed for luciferase. Quantitative PCR was used to determine the amount of pRSVL DNA that was present in the muscles at varying times after injection (Figure 4). Southern blot analysis was not sensitive enough to detect the pRSVL DNA at the longer time points. At 14 days after injection, all of the six muscles contained more than 1 pg of pRSVL DNA/μg total DNA. Occasionally, uninjected muscle yielded a very faint band as shown in a control sample (Figure 4, lane 7). At 60 days after injection, four of the six muscles contained pRSVL levels above background (Figure 4, lanes 8, 10, 11 and 12) while only one of the muscles had more than 0.5 pg of pRSVL DNA/μg total DNA (Figure 4, lane 12). At 5.5 months and one year after injection, two of the six muscles for each time period contained concentrations of pRSVL DNA above background (Figure 4, lanes 17, 20, 24, and 26). For any of the times after injection, there was no correlation between the amount of luciferase and pRSVL DNA in each muscle. These results demonstrate that plasmid DNA can persist in muscle long-term.

Methylation status of muscle plasmid DNA

In order to determine whether the plasmid DNA replicated or was repaired while in the muscle long-term, the muscle DNA preparations were digested with BamHI and then DpnI, MboI or Sau3A prior to performing the quantitative PCR analysis (Figure 5). Plasmid DNA from bacteria contain a methylated adenosine within the GATC recognition site for DpnI, MboI, or SauIIIA. MboI cleaves the site less efficiently if the A is methylated; DpnI cleaves the site less efficiently if the A is not methylated; and SauIIIA cleaves it efficiently regardless of methylation. If the plasmid DNA replicates in mammalian cells, then the bacterial methylation pattern is lost. All DNA samples were digested with BamHI because PCR amplification with linear plasmid yielded more product than circular, undigested plasmid (data not shown). The procedure was first evaluated using uninjected, muscle DNA spiked with 0.5 pg of plasmid pRSVL DNA/μg total DNA as a control for non-replication of the injected plasmid DNA. As expected, an amplified fragment only appeared in the samples digested with BamHI alone or with MboI (Figure 5, unint. pRSVL). No amplified fragments were evident

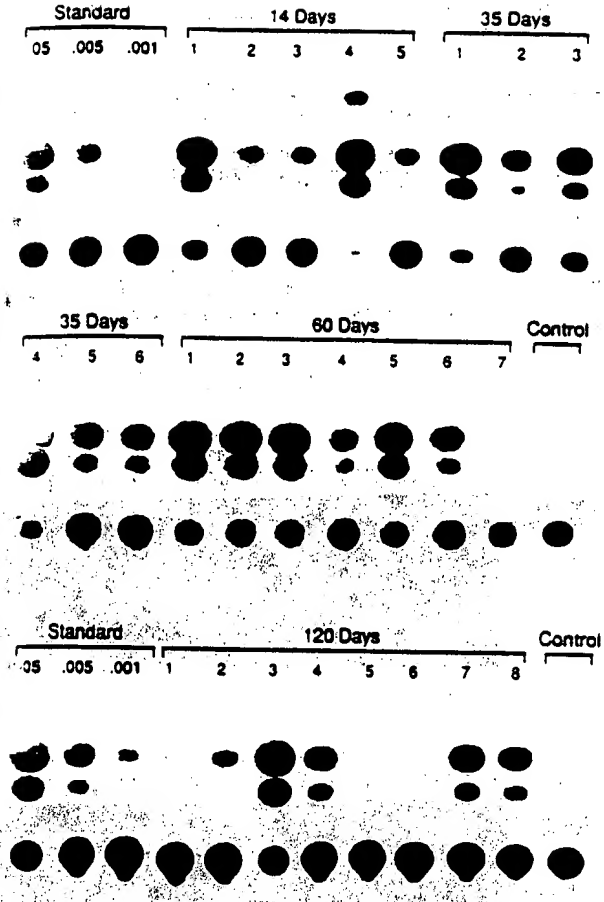

Figure 2. Autoradiogram demonstrating CAT activity in quadriceps at varying times after injection of 100 μg of undigested, CCC pRSVCAT. Controls were injected muscles.

If the samples were digested with DpnI or Sau3IIIA prior to PCR, since there are four GATC restriction sites between the primers. DNA from fibroblasts containing stably integrated pRSVL served as a control for pRSVL DNA that had replicated in mammalian cells (Figure 5, int. pRSVL). Amplified fragments were present in samples digested with DpnI but not in those digested with MboI. These results with the control DNA samples confirm the ability for this procedure to detect pRSVL DNA replication in mammalian cells.

Four samples of total muscle DNA obtained 12 or 19 months after injection were subjected to the above procedure (Figure 5). In all four muscle DNA samples, pRSVL DNA was amplified after DpnI digestion but not after MboI digestion. Both the control and experimental samples sometimes contained less intact pRSVL DNA when digested with BamHI and MboI than when digested with BamHI alone because GATC sequences with the A methylated (bacterial pattern) are only partially resistant to MboI digestion. These results indicate that the bacterial methylation pattern of the injected pRSVL DNA did not change after it was maintained in muscle for at least 19 months.

Electroporation of undigested muscle DNA

Electroporation was used to clone the plasmid DNA in muscle to determine its integration state. Electroporation of control DNA samples was performed to determine whether this approach could

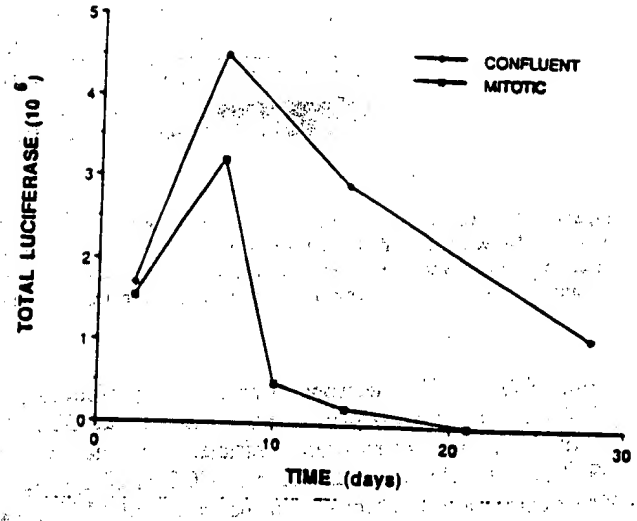

Figure 3. Total, mean luciferase activity (L.U.) in pRSVL-transfected Rat1 fibroblasts confluent or mitotic. The total mean luciferase values represent the mean of total activities in four plates. Standard errors were less than 30%.

be used for this purpose (Table IA). Electroporation efficiencies of 10^8 to 10^9 colonies per μg of pure CCC plasmid DNA were obtained 80% of the time. When pRSVL plasmid DNA was electroporated with 1.0 μg of total muscle or fibroblast DNA, similar electroporation efficiencies were obtained (Table IA), indicating that the genomic DNA did not affect the plasmid electroporation efficiency. Total cellular DNA from a 3T3 fibroblast clone stably transfected with pRSVL served as a control for plasmid integration. The clone contained approximately 40 pg of pRSVL DNA/μg genomic DNA as determined by quantitative PCR. Essentially no ampicillin-resistant colonies were obtained when 1.0 μg of this total cellular DNA containing integrated pRSVL was electroporated into DH10B bacteria (Table IA). Similarly, DNA from G-418-resistant clones containing only pSV2Neo did not yield any ampicillin-resistant bacterial colonies after electroporation. These results indicate that integrated plasmid DNA cannot directly transform bacteria.

Total cellular DNA from muscles injected two weeks, five months, or one year previously with pRSVL were directly electroporated into DH10B bacteria (Table IB). In the two week DNA samples, up to 200 ampicillin resistant colonies/μg genomic DNA were obtained. In the five month and one year DNA samples, 50 and 10 ampicillin resistant colonies/μg genomic DNA, respectively, were obtained. Digestion of the plasmids from the ampicillin-resistant colonies with several different restriction enzymes indicated that these colonies contained the pRSVL plasmid. Less than two ampicillin resistant colonies/μg genomic DNA were obtained with DNA from uninjected, control muscle. The ability of cellular DNA from pRSVL-injected muscle to transform bacteria with pRSVL suggested that the pRSVL was maintained extrachromosomally for at least one year.

Additional electroporations were performed to explore why approximately ten times fewer colonies were obtained after electroporation of the pRSVL-injected muscle samples than expected from the quantitative PCR results (Table I). The presence of genomic DNA could not explain this discrepancy because the electroporation efficiency of control, muscle DNA spiked with pRSVL was the same as the efficiency of pRSVL

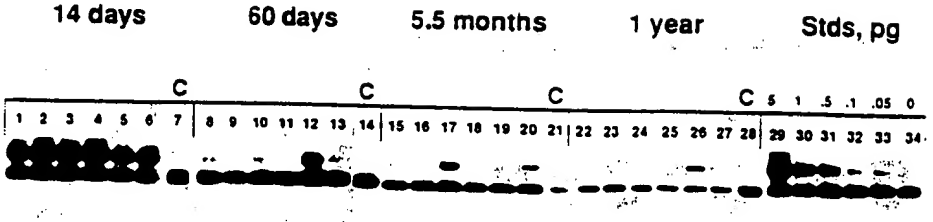

Figure 4. Quantitative PCR determination of the amount of pRSVL DNA in muscles at varying times after injection of 100 μg of pRSVL. After one μg of total muscle DNA was amplified, the PCR product was detected by Southern blot analysis using a luciferase cDNA probe. Upper band represents the experimental amount of pRSVL DNA, while the lower band represents the internal standard. 'C' indicates the amplification of cellular DNA from uninjected muscles. 'Stds' indicates the amplification of varying amounts of pRSVL DNA in 1 μg of control, muscle DNA.

alone (Table I). The electroporation efficiency of linear pRSVL DNA alone was approximately 100-times less than CCC pRSVL (Table IA). The electroporation efficiency of relaxed, circular pRSVL DNA alone was the same as CCC pRSVL (Table IA). The electroporation efficiency of nicked plasmid DNA was not determined.

Electroporation of digested and ligated muscle DNA

Further studies using bacterial electroporation were performed to determine if any of the injected plasmid DNA had integrated. Total cellular DNA from fibroblasts stably transfected with pSV2Neo served as a positive control for these experiments. When this cellular DNA was digested with BglII (which cleaves pSV2Neo once within the neomycin-resistance gene), ligated, and electroporated, ampicillin-resistant colonies were obtained. Most of the bacterial clones contained pSV2Neo unaltered in size when cut with BglII (Figure 6, lane 3). In the remaining one half to one fifth of the bacterial clones (depending on the specific G-418-resistant fibroblast clone), the BglII-digested plasmid DNA was not of the same size as BglII-digested pSV2Neo (Figure 6, lanes 4 and 5). Transfected plasmid DNA typically integrates as tandem repeats. The plasmids unaltered in size from pSV2Neo, were most likely derived from plasmids within tandem repeats. The plasmids altered in size from pSV2Neo, were probably derived from pSV2Neo at the junction between plasmid and chromosomal DNA.

For the experimental studies with intramuscularly injected plasmids, the plasmid pUC19 was used for these studies to allow for β-galactosidase screening in the electroporated bacteria. Loss of β-galactosidase expression would indicate disruption of the Lac-Z coding region and a possible integration event. Total cellular DNA from two muscles injected one month previously with pUC19 were used for these electroporation studies. When these muscle DNA's were electroporated without prior digestion, approximately 5% of the colonies were white. The muscle DNA was then digested with either PstI or BamHI restriction enzymes that cut pUC19 once within the Lac-Z gene. After ligation and electroporation, approximately 5% of 1800 ampicillin-resistant colonies were white. Plasmid DNA was prepared from 78 white colonies obtained from electroporation of the muscle DNA's either electroporated straight or digested and ligated. Restriction enzyme analysis and sequencing indicate that some of the plasmids from the white colonies contained an insert within the PstI or BamHI site of pUC19, which probably arose during the ligation step and does not represent an integration event (data not shown). Other plasmids from the white colonies were contaminating plasmids that were present in the laboratory. None

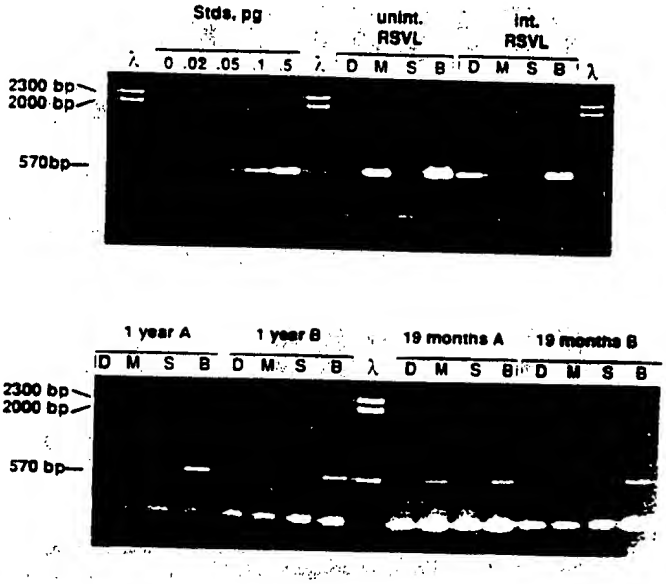

Figure 5. Methylation status of pRSVL DNA in muscle at one year and 19 months after injection. Agarose gel electrophoresis after PCR amplification of 1.0 μg of cellular DNA digested with BamHI and DpnI (D), BamHI and MboI (M), BamHI and SauIIIA (S), or BamHI alone (B). 'Unint. pRSVL' indicates PCR amplification of 1.0 μg of cellular DNA from control, untransfected 3T3 fibroblasts spiked with 0.5 pg of pRSVL, while 'int. pRSVL' indicates PCR amplification of 1.0 μg of cellular DNA from pRSVL-stably transfected 3T3 fibroblasts. λ indicates 0.7 μg of HindIII-digested λ DNA. Stds indicates the amplification of varying amounts of pRSVL DNA in 1 μg of control, muscle DNA.

of the plasmids were altered in size as were the recloned plasmids that were obtained from fibroblasts stably transfected with pSV2Neo (Figure 6). The inability to find any plasmids containing chromosomal/plasmid junctions indicates that it is highly unlikely that the plasmid DNA in the muscle for one month had integrated.

DISCUSSION

These results demonstrate that expression from plasmid DNA can persist in mouse muscle for at least 19 months. An increase in luciferase expression has been observed often from four to 30 days after injection and may be due to either the slow entry of the plasmids into the nucleus or the delayed expression of intranuclear plasmid DNA. It is not known whether the increase in luciferase expression after 30 days is reproducible and it may just reflect the variable levels of expression. Long-term, stable

Table 1. Number of bacterial colonies obtained after electroporation of muscle or fibroblast DNA

A. Electroporation of control DNA samples

Sample	# Colonies[a]
μg uninjected control muscle	<2
pg CCC pRSVL alone	<2
.5 pg pRSVL +1 μg uninjected control muscle	1040
0 pg pRSVL +1 μg uninjected control muscle	525
0 pg pRSVL +1 μg uninjected control muscle	940
μg DNA from pRSVL-integrated 3T3 cells	2700
pg linear pRSVL alone	<2
pg relaxed, circular pRSVL alone	3
	1328

B. Electroporation of total cellular DNA from muscles injected with pRSVL

injection	# Colonies/μg DNA[b]	pg pRSVL/μg DNA per quantitative PCR[c]
weeks	150	1.0–5.0
months	50	0.5
year	10	0.05–0.1

[a] This represents the total number of colonies obtained when electroporation efficiency was ~ 10^9 colonies/μg plasmid DNA using pRSVL alone.
[b] This represents the total number of colonies obtained per μg of total cellular DNA normalized for an electroporation efficiency of 10^9 colonies/μg plasmid DNA using pRSVL alone.
[c] 2 week, 5 month, and 1 year samples correspond to lanes 3, 17, and 26, respectively in Figure 4. These experiments were repeated three times.

Figure 6. Agarose gel electrophoresis of plasmids obtained after electroporation of plasmid DNA from fibroblast clones stably-transfected with pSV2Neo. Lane 1, 5 μg of HindIII-digested I DNA. Lane 2, BglII-digested, control pSV2Neo. Lanes 3 to 5, BglII-digested plasmids isolated after electroporation of DNA obtained from fibroblasts stably-transfected with pSV2Neo. The fibroblast DNA was digested with BglII and re-ligated prior to electroporation.

expression was also possible with the CAT reporter gene, suggesting that the stable expression of other proteins should be possible. Nonetheless, immunologic factors could prevent stable myofiber expression of some foreign proteins, as occurs in cardiac tissue (10, 12).

The presence of plasmid DNA was demonstrated by quantitative PCR in some of the muscle DNA samples for at least 19 months after injection. In each sample, there was no correlation between the amount of luciferase activity and the amount of pRSVL plasmid DNA. The lack of correlation was probably due to variability of DNA extraction. Variable extraction of luciferase from muscle is less likely based on our previous data (5). In addition, a variable percentage of the intramuscular plasmid DNA may be extranuclear or intranuclear but transcriptionally inactive. This may also explain why the amount of plasmid DNA decreased over time while luciferase expression did not. Perhaps, the extranuclear or transcriptionally inactive plasmids were lost over time, whereas the intranuclear and transcriptionally active plasmids were maintained.

The methylation status of the injected plasmid DNA was assessed by DpnI and MboI digestion and PCR amplification. The bacterial methylation pattern of the injected DNA was preserved for at least 19 months indicating that the plasmid DNA did not replicate in muscle. These results are in agreement with the previous Southern blot analysis using DpnI and MboI digestion (1), which also suggested that the injected plasmid DNA does not replicate in the muscle *in vivo*.

It is unlikely that specific plasmid sequences are required for persistence of plasmid DNA. The pCMVLux and pUC19 are substantially different from pRSVL, suggesting that any plasmid DNA could stably persist and express in muscle. None of the plasmids studied to date have a known chromosomal origin of replication. Although they may have occult origins of replication, plasmids containing known mammalian chromosomal origins of replication have all required transacting proteins and/or selection conditions to be stably maintained extrachromosomally (13, 14). Once in the nucleus, it is possible that plasmid DNA is treated by the non-dividing cell as chromosomal DNA. In addition, it is unlikely that the nuclear DNases are specific for plasmid DNA or are sequence specific. Extrachromosomal DNA's exist naturally in several types of mammalian cells and tissues (15). The lower expression of injected, linear plasmid pRSVL was most likely due to exonuclease digestion prior to its nuclear entry. Once within the nucleus, stable expression may have occurred either because the DNA circularized or the linear DNA was not accessible to nuclear exonuclease activity. Another possibility is that the minimal expression from injected, linear plasmid was due to residual CCC plasmid DNA.

Expression of plasmid DNA was unstable after transfection into replicating fibroblasts. The loss of expression in the fibroblasts was presumably due to loss of plasmid DNA either through degradation of the transfected plasmid by DNases and/or loss of the plasmid DNA when the cell divides. When the nuclear membrane dissolves during mitosis, the plasmid DNA distributes throughout the cell and is partitioned when the nuclear membrane re-forms after mitosis. The greater stability of expression in slowly-dividing, confluent fibroblasts suggests that a decreased mitotic rate increases the stability and expression of plasmid DNA. Correlating these fibroblast findings to the muscle results, the post-mitotic state of the myofiber nuclei may enable persistence of the injected, plasmid DNA.

The stable expression of plasmids in muscle suggests that plasmids should stably express in other post-mitotic or slowly mitotic tissues such as brain and liver. However, when fetal, rat brain cells were transfected *in vitro* with pRSVL plasmid DNA and transplanted back into adult rat brains, luciferase expression persisted *in vivo* less than two months (16). In contrast, when muscle cells were transfected *in vitro* with pRSVL and transplanted back into adult rat brains, luciferase expression persisted *in vivo* for at least two months (17). Plasmids transfected into non-hepatectomized liver via polylysine conjugates expressed for less than a few days (18). Most likely, loss of expression

in the liver and brain cells was due to loss of the plasmid DNA. Although other factors may be causing the loss of the plasmid DNA in brain and liver tissue, plasmid DNA may persist in muscle cells not only because it is very slowly mitotic, but because the multinucleated nature of myofibers is conducive to plasmid stability. In summary, the unique, long-term expression of plasmid DNA in skeletal muscle may be due to muscle's post-mitotic state as well as other tissue-specific features.

High efficiency transformation of bacteria by electroporation was used to determine the integration state of the injected, plasmid DNA. The ability to obtain ampicillin-resistant colonies, after the electroporation of total cellular DNA from pRSVL-injected muscle, indicate that some of the plasmid DNA remained unintegrated for at least one year (Table I). In contrast, ampicillin-resistant colonies were not obtained after the electroporation of stably-integrated plasmids. In the injected muscle DNA, it is unclear why ten-fold fewer colonies were obtained than expected from the amount of pRSVL DNA present per quantitative PCR. This was evident even in cellular DNA from muscle injected two weeks previously with pRSVL. On Southern blot analysis the majority of the pRSVL DNA in the muscle two weeks after injection was in a relaxed, circular form (data not shown). Non-nicked, relaxed, circular pRSVL prepared by topoisomerase I reaction had the same electroporation efficiency as CCC pRSVL. Possibly, the plasmid DNA in the muscle was present not only relaxed and circular, but nicked also. Nicked, plasmid DNA may be electroporated less efficiently than CCC, plasmid DNA. Attempts to determine whether the muscle, plasmid DNA was nicked were inconclusive. One such approach involved PCR amplification preceded by treatment with exonuclease III which digests nicked DNA and exonuclease I which does not. In summary, the ability to obtain ampicillin-resistant colonies from muscles injected with plasmid DNA provided evidence in addition to the previous Southern blot analysis (1) that the injected, plasmid DNA persisted in an unintegrated form.

Junctions between chromosomal and plasmid DNA that would indicate integration were searched for by electroporating injected, muscle DNA that was cut and re-ligated. Over 1800 plasmids derived from the muscle DNA were screened for loss of β-galactosidase activity which would indicate a possible integration event. Approximately five percent of the plasmids were either contaminating plasmids that were present in the laboratory or pUC19 with a genomic DNA insert. None of the plasmids in white colonies represented integration events as was observed in plasmids derived from fibroblasts stably-integrated with pSV2Neo. Another approach involving the PCR amplification of high molecular DNA was also used to search for integration events (data not shown). However, the frequent contamination of the high molecular DNA with unintegrated plasmid DNA prevented a definitive conclusion from being reached. The electroporation results suggest that integration of plasmid is unlikely. Plasmid DNA may not be able to integrate into chromosomal DNA in post-mitotic myofibers just as retroviral, adenoviral, or herpes DNA does not efficiently integrate into chromosomal DNA of post-mitotic cells (19, 20). The lack of any integration increases the safety of plasmid gene transfer into human muscle by avoiding any potential deleterious effects of chromosomal integration.

Stable *in vivo* expression of ex genous genes has also been observed long-term after the transplantation of retrovirally infected fibroblasts (21), hepatocytes (22) and bone marrow derived cells (23). However, other studies indicate unstable expression of retrovirally-transduced genes in cultured fibroblasts (24), transplanted fibroblasts (11), transplanted hepatocytes (25, 26) and transplanted bone marrow derived cells (27). Most likely the unstable expression of some retroviral vectors is due to an interaction between the specific regulatory sequences in the vector and the specific cellular milieu. In addition, flanking chromosomal sequences may contribute to the unstable expression of the integrated, retrovirally transduced genes. If so, then the expression of non-integrated plasmid DNA may be less susceptible to suppression.

The unprecedented ability of plasmid DNA to stably express foreign genes in muscle for the lifetime of a mouse has important implications for gene therapy. Intramuscularly injected plasmid DNA was also stably expressed in non-human primate muscle for at least four months (28). Modifications of the naked plasmid DNA approach and other methods of gene transfer are under investigation because the levels of expression achieved to date with the naked plasmid DNA approach may not be sufficient for human gene therapy (28). The stable expression of circular and linear, plasmid DNA suggests that foreign DNA introduced into myofibers by other means such as by particle-acceleration (29, 30) or by viral transduction should also be stably maintained and expressed. The very long-term stability of plasmid DNA in muscle indicates that muscle is an attractive target tissue for the introduction of extrachromosomal plasmid or viral DNA for the purpose of gene therapy. Muscle is an important target tissue not only for intrinsic muscle diseases such as Duchenne muscular dystrophy (10) but also for the heterologous expression of proteins that can immunize, be secreted in the blood, or clear a circulating toxic metabolite.

MATERIALS AND METHODS

Muscle studies

Covalently closed, circular (CCC), plasmid DNA was prepared by standard methods involving alkaline lysis and two cesium chloride gradients (28). Injections of the plasmid DNA into mouse quadricep muscle were done as previously reported (5). At varying times after injections, the entire quadricep muscles were excised and ground under liquid N_2. Approximately 10% of the ground muscle, was transferred into a tared 1.5-ml tube that was then weighed. Two hundred μl of lysis solution [100 mM potassium phosphate (pH 7.8), 1 mM DL-dithiothreitol, and 0.1% TritionX-100] were added to the tubes and 20 μl of the supernatant were assayed for luciferase as previously reported using a Monolight 2010 instrument (ALL) (1). Luciferase activity was presented as the total relative light units in each muscle. In the muscles injected with 100 μg of pRSVCAT, 20 μl of the total 200 μl muscle extract were assayed for chloramphenicol acetyltransferase (CAT). CAT activities were assayed using a one hour reaction time at 37°C (6). Purified CAT enzyme (Sigma) was used as a standard.

Total cellular DNA was prepared from the remaining ground muscle fraction (31). The amount of pRSVL DNA was determined by quantitative PCR as previously reported (10). The luciferase gene served as a template. Prior to PCR, 0.1 pg of an altered luciferase template, containing a deleted sequence between the primers, was added. This altered template generated a 317-bp fragment that served as an internal standard.

Fibroblast studies

Three million rat1 fibroblasts (19) were transfected with 15 μg of pRSVL DNA using 45 μg of Lipofectin (BRL) in a 100 mm dish (32). After overnight incubation, the transfected cells in thirteen plates were pooled together and then plated in twenty-six 100 mm dishes, in duplicate. In one set of the twenty-six dishes, two cultures became confluent and were treated with 10^{-5} M dexamethasone to reduce cell division (19). At 2, 7, 14, and 28 days post-transfection, four of the twenty confluent plates were analyzed for luciferase activity at each of these times. In the other set of twenty-six dishes, six dishes were passed and three plates were analyzed for luciferase activity at 2, 7, 10, 14, and 21 days (1, 8). Total luciferase activities in relative light units were calculated for these passed cultures by taking into account the dilutional effect of splitting the cultures. The luciferase activities

...n the passed cultures were multiplied by the number of plates that would have ...een generated if no cells were discarded when the cultures were passed.

Mouse 3T3 fibroblasts stably integrated with various plasmids served as controls ... the PCR and electroporation studies. Fibroblast clones containing pRSVL ...tained by transfecting 18.8 μg of pRSVL and 0.2 μg of pSV2Neo with Lipofectin into one million 3T3 cells. After selection in 400 mg/ml of ...tin, clones were screened for luciferase activity, and the amount of pRSVL DNA per μg of cellular DNA was determined by PCR amplification of the luciferase gene. Fibroblast clones containing only pSV2Neo stably integrated were similarly obtained.

Bacterial electroporation studies

DH10B bacteria (BRL) were prepared for electroporation as previously described with two washing steps (8). DH10B bacteria were used because they lack methyl-dependent restriction systems and can be efficiently transformed with DNA ...taining a mammalian methylation pattern (33). They can also be efficiently ...med with prokaryotic DNA. One μg of cellular DNA was added to 20 ...acteria and electroporated using 2400 V and pulse time of ~5 msec. ...se conditions allowed efficiencies of 10^8 to 10^9 colonies per μg with pure ...CC plasmid depending on the particular batch of bacteria prepared. Relaxed, circular plasmid was prepared by treatment with topoisomerase I (BRL) per manufacturer's instructions. As previously described for the cloning of flanking chromosomal sequences in transgenic mice (33), total cellular DNA was digested at a single site outside of the sequences required for replication in bacteria, re-ligated, and then electroporated into DH10B bacteria. Three μg of total cellular DNA from pUC19-injected muscles were digested with 10 to 20 units of PstI or BamHI in 50 μl for 6 hrs at 37°C. After digestion, the enzyme was heat inactivated at 65°C for 10 min. The 50 μl solution containing 3.0 μg of digested DNA was brought up to 700 μl containing 1400 units of T4 DNA ligase (NEB), ... Tris–HCl (pH 7.5), 10 mM $MgCl_2$, 10 mM DTT, 1 mM ATP and ... BSA/ml. After ligation overnight at 16°C, the DNA was precipitated in isopropanol and potassium acetate as previously described (8). The DNA pellet was taken up into 3.0 μl of water and 1.0 μl was electroporated into DH10B cells.

ACKNOWLEDGEMENTS

We thank S.Hunsaker for photography, Amy Kolbeck for DNA sequencing, and R.Gregg and members of J.Wolff's laboratory for helpful suggestions. Supported by the NIH (DK42709 and HD03352).

REFERENCES

1. Wolff,J.A., Malone,R.W., Williams,P., Chong,W., Acsadi,G., Jani,A. and Felgner,P.L. (1990) *Science* **247**, 1465–1468.
2. Acsadi,G., Jiao,S.S., Jani,A., Duke,D., Williams,P., Chong,W. and Wolff,J. (1991) *The New Biologists*, 71–81.
3. Lin,H., Parmacek,M.S., Morle,G., Boning,S. and Leiden,J.M. (1990) *Circulation* **82**, 2217–2221.
4. Kitsis,R.N, Buttrick,P.M., McNally,E.M., Kaplan,M.L. and Leinwand,L.A. (1991) *Proc. Natl. Acad. Sci. USA* **88**, 4138–4142.
5. Wolff,J.A., Williams,P., Acsadi,G., Jiao,S., Jani,A. and Chong,W. (1991) *BioTechniques* **11**, 474–485.
6. Sambrook,J.E., Fritsch,F. and Maniatis,T. (1989) *Molecular Cloning: A Laboratory Manual*, 2nd edn. Cold Spring Harbor Laboratory Press, Cold Spring Harbor, NY.
7. de Wet,J.R., Wood,K.V., DeLuca,M., Helinski,D.R. and Subramani,S. (1987) *Mol. Cell. Biol.* **7**, 725–737.
8. Zabarovsky,E.R., and Winberg,G. (1990) *Nucleic Acids Res.* **18**, 5912.
9. Gorman,C.M., Merlino,G.T., Willingham,M.C., Pastan,I. and Howard,B.H. (1982) *Proc. Natl. Acad. Sci. USA* **79**, 6777–6781.
10. Acsadi,G., Dickson,G., Love,D.R., Jani,A., Walsh,F.S., Gurusinghe,A., Wolff,J.A. and Davies,K.E. (1991) *Nature* **352**, 815–818.
11. Palmer,T., Rosman,G., Osborne,W. and Miller,A. (1991) *Proc. Natl. Acad. Sci. USA* **88**, 1330–1334.
12. Wang,J., Jiao,S.S., Wolff,J.A. and Knechtle,S.J. (1992) *Transplantation* **53**, 703–705.
13. Hecsas,J. and Sugden,B. (1987) *Annu. Rev. Cell Biol.* **3**, 87–108.
14. Burhans,W.C., Vasilev,L.T., Caddle,M.S., Heintz,N.H. and DePamphilis,M.L. (1990) *Cell* **62**, 955–965.
15. Rush,M.G. and Misra,R. (1985) *Plasmid* **14**, 177–191.
16. Jiao,S., Acsadi,G., Jani,A., Felgner,P. and Wolff,J.A. (1992) *Exp. Neurol.* **115**, 400–413.
17. Jiao,S., Schultz,E. and Wolff,J.A. (1992) *Brain Res.* in press.
18. Wu,C., Wilson,J. and Wu,G.Y. (1989) *J. Biol. Chem.* **264**, 16985–16987.
19. Miller,D.G., Adam,M.A. and Miller,A.D. (1990) *Mol. Cell. Biol.* **10**, 4239–4242.
20. Mellerick,D.M. and Fraser,N.W. (1987) *Virology* **158**, 265–275.
21. Scharfmann,R., Axelrod,J.H. and Verma,I.M. (1991) *Proc. Natl. Acad. Sci. USA* **88**, 4626–4630.
22. Chowdhury,J.R., Grossman,M., Gupta,S., Chowdhury,N.R., Baker,J.R. and Wilson,J.M. (1991) *Science* **254**, 1802–1805.
23. Fletcher,F.A., Moore,K.A., Ashkenazi,M., De Vries,P., Overbeek,P.A., Williams,D.E. and Belmont,J.W. (1991) *J. Exp. Med.* **174**, 837–845.
24. Xu,L., Yee,J.-K., Wolff,J.A. and Friedmann,T. (1989) *Virology* **171**, 331–341.
25. Kay,M.A., Baley,P., Rothenberg,S., Leland,F., Fleming,L., Ponder,K.P., Liu,T.-J., Finegold,M., Darlington,G., Pokorny,W. and Woo,S.L.C. (1992) *Proc. Natl. Acad. Sci. USA* **89**, 89–93.
26. Miyanohara,A., Elam,R.L., Witzum,J.L. and Friedmann,T. (1992) *New Biologist* **4**, 261–267.
27. Friedmann,T. (1989) *Science* **244**, 1275–1281.
28. Jiao,S., Williams,P., Berg,R.K., Hodgeman,B.A., Liu,L., Repetto,G. and Wolff,J.A. (1992) *Hum. Gene Therapy* **3**, 21–33.
29. Yang,N.-S., Burkholder,J., Roberts,B., Martinell,B. and McCabe,D. (1990) *Proc. Natl. Acad. Sci. USA* **87**, 9568–9572.
30. Williams,S.R., Johnston,S.A., Riedy,M., DeVit,M.J., McElligot,S.G. and Sanford,J.C. (1991) *Proc. Natl. Acad. Sci. USA* **88**, 2726–2730.
31. Ausbel,F.M., Brent,R., Kingston,R.E., Moore,D.D., Seidman,J.G., Smith,J.A. and Struhl,K. (eds), (1989) *Current Protocols in Molecular Biology*. Wiley, New York.
32. Felgner,P.L., Gadek,T.R., Holm,M., Roman,R., Chan,H.W., Wenz,M., Northrop,J.P., Ringold,G.M. and Danielsen,M. (1987) *Proc. Natl. Acad. Sci. USA* **84**, 7413–7417.
33. Grant,S.G.N., Jessee,J., Bloom,F.R. and Hanahan,D. (1990) *Proc. Natl. Acad. Sci. USA* **87**, 4645–4649.

Kidney International, Vol. 46 (1994), pp. 1554–1556

Antisense inhibition of hypertension: A new strategy for renin-angiotensin candidate genes

M. IAN PHILLIPS, DONNA WIELBO, and ROBERT GYURKO

Department of Physiology, College of Medicine, University of Florida, Gainesville, Florida, USA

Antisense inhibition of hypertension: A new strategy for renin-angiotensin candidate genes. There are several ways of experimentally studying the influence of candidate genes on hypertension. The approach proposed here is antisense inhibition with antisense oligodeoxynucleotides (AS-ODNs) constructed to the 5′ region of known sequences of angiotensinogen mRNA and angiotensin II type-1 receptor mRNA. The AS-ODNs were applied *in vivo* and *in vitro*. *In vivo*, direct injection of 50 μg of AS-ODN into the lateral ventricles of SHR reduced hypertension significantly ($P < 0.01$). There was no effect of AS-ODN i.c.v. in normotensive WKY rats. The phosphorothiated AS-ODN to the AT_1 receptor mRNA also produced a long-lasting decrease in blood pressure in SHR (7 days). After AS-ODN treatment AT_1 receptors were reduced in the PVN and anterior third ventricle area and Ang II levels were reduced in the brainstem. The results show the *in vivo* feasibility of using antisense inhibition of renin-angiotensin mRNA to reduce hypertension.

The renin-angiotensin system has components that appear to be candidate genes for hypertension [1]. There are several ways of experimentally tackling the problem of genetic control of hypertension. These include: breeding, studies with backcross breeding to show gene linkage between hypertension and candidate genes, transgenic techniques with the insertion of a candidate gene, and gene knockout. These techniques are currently being used and have advantages and disadvantages in isolating linkage to hypertension. For example, Kimura et al [2] have shown that the angiotensinogen gene inserted in transgenic mice is associated with hypertension, particularly with the expression of the gene in brain tissue. Previous work indicated that brain angiotensin is an important factor in the hypertension of the genetic strain of spontaneously hypertensive rats (SHR) [3–6]. Cost and lack of experience have prevented us from undertaking genetic breeding studies to breed out hypertension and measures of brain RAS components. A more cost effective approach is to inhibit proteins with antisense oligonucleotides to specific gene expression [7]. Recently we have begun applying this approach to inhibit the mRNA expression of angiotensinogen and AT_1 receptors by antisense inhibition. The antisense approach is based on observations that bacteria can regulate gene replication and transcription by producing small complementary antisense RNA molecules. Many reports have followed describing the down-regulation of translation *in vitro* of various oncogenes by both DNA and RNA antisense techniques [7]. Antisense has the advantage of being as specific as a genetic approach, and yet as available as a pharmacological approach. We have recently demonstrated that *in vivo* delivery of antisense oligodeoxynucleotides (AS-ODN) to components of the renin-angiotensin system in the brain can significantly reduce high blood pressure in the SHR [8].

Antisense ODNs are constructed to the base sequence of the 5′ coding region of the known sequence of candidate gene molecules. The initial constructs were phosphodiester linked ODNs. These were effective even though they were unmodified. Phosphorothioated ODNs were also produced as they are considered to be more stable because of the modified phosphate groups in the backbone of the molecule and have longer-lasting effects than the unmodified antisense.

Methods

Adult male SHR and WKY rats (250 to 300 g) supplied by Harlan, Inc. were cannulated in the right brain ventricle with a 23 gauge stainless steel cannula. Five days after surgery the rats were catheterized in the left common carotid artery. All experimental procedures were approved by the University of Florida Animal Welfare Committee.

Antisense and scrambled ODNs were constructed to target the angiotensinogen gene [9] (antisense: 5′-CCGTGGGAGTCATCACGG-3′, sense: 5′-CCGTGATGACTCCCACGG-3′, scrambled: 5′-CAGGGATCTCTGGCGGAC-3′.) The AS sequence targeted to the AT_1 receptor mRNA [10] was: 5′-TAACTGTGGCTGCAA-3′. The sense sequence was: 5′-TGGCAGGCACAGTTA-3′.

Groups of six rats received three i.c.v. injections at 12 hour intervals with 50 μg of angiotensinogen AS, S, or SC ODN or a vehicle of 5 μl isotonic saline. Systolic blood pressure was measured either via the catheter or in longer term experiments by tailcuff blood pressure measurement.

Northern blots of angiotensinogen mRNA were analyzed in SHR and WKY after ODN treatment. Tissue RNA was extracted by the method of Chomczynsky and Sacchi [11]. Tissue samples from chronically treated rats were taken two hours after final treatment.

Kidney and brain tissue and plasma samples were obtained two hours after final ODN injection. The samples were frozen and stored for later extraction and radioimmunoassay procedures [12].

T measure the effect of AS-ODN targeted to the AT_1 receptor mRNA, autoradiography was carried out on frozen sections cut at 20 μm thickness at −20°C. The sections were incubated with 500 pM ^{125}I-Sar-Ile-Ang II for two hours in the presence of absence of 1 μm Ang II. Sections were washed in 10 mM sodium biphosphate

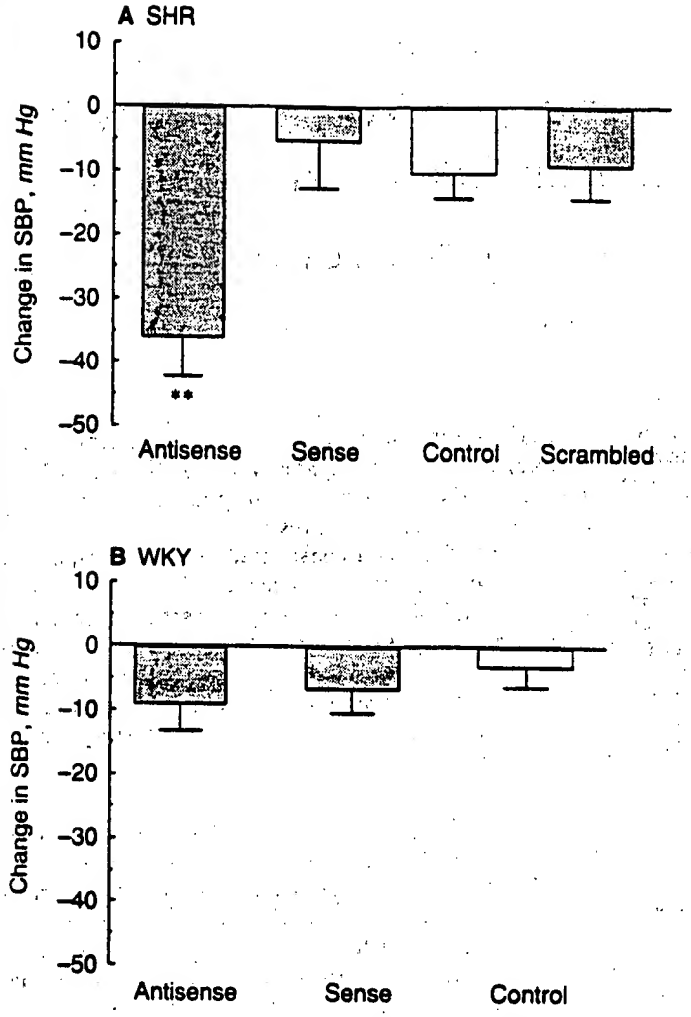

Fig. 1. *Change in systolic blood pressure (SBP) in chronically treated SHR and WKY rats.* Intracerebroventricular administration of three doses of 50 μg (10 μg/μl) angiotensinogen antisense (AS), sense (S), scrambled (Sc) ODN or 5 μl isotonic saline (C). Systolic blood pressure was reduced from baseline levels in SHR's treated with AS-ODN 35.5 ± 6.2 mm Hg, $N = 6$, $^{**}P < 0.01$.

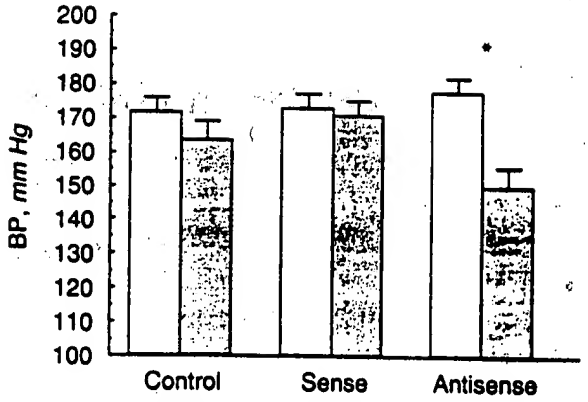

Fig. 2. *Decrease in mean arterial pressure (MAP) in SHR 24 hours after i.c.v. injection of 50 μg antisense ODN to the AT_1 receptor mRNA.* Symbols are: (□) pre-treatment; ( ) 24 hours. For blood pressure measurements, the carotid artery was catheterized. Baseline blood pressure data was recorded one hour before injection. $N = 6$, control; $N = 7$, sense; $N = 7$, antisense; $^{*}P < 0.01$.

buffer and dried. Autoradiograms were generated by apposition of slide mounted tissues with x-ray film (Hyperfilm-^{3}H, Amersham) for three days. Densitometric analysis was carried out with Image Systems (MCID M1 software).

All values were expressed as means ± SEM. Statistical analysis was performed by ANOVA with Duncan multiple range test for individual comparisons.

Results

A highly significant decrease in blood pressure was observed in the chronically treated SHR rats (Fig. 1A). Systolic blood pressure was reduced from baseline levels after AS-ODN treatment by 35.5 ± 6.2 mm Hg ($N = 6$, $P < 0.01$). The controls, sense vehicle and scrambled, produced no significant effect on the blood pressures. In the normotensive rat (WKY), AS, S and vehicle had no effect on the blood pressure (Fig. 1B). The decrease in blood pressure began two hours after the first dose of 50 μg (10 μg/μl) but the maximum effect was seen two hours after the last of the three doses given at 12 hour intervals. The treatment normalized the high blood pressure to levels below 150 mm Hg in SHR.

The effect of the AS-ODN was to reduce Ang II levels in the brainstem, compared to control groups of S, Sc and saline treated SHR (59 ± 6.1 vs. 71 ± 6.4 pg/g tissue, $P < 0.05$, $N = 6$). No change in Ang II was observed in the kidney or in the plasma Ang II levels in SHR after treatment.

The effect of AS inhibition of the AT_1 receptor mRNA was a significant reduction in blood pressure. Rats injected with the receptor AS-ODN (50 μg in 5 μl saline) received one dose. This resulted in a significant fall in mean arterial pressure of 27 ± 8 mm Hg ($P < 0.01$) in SHR (Fig. 2). Neither control nor sense ODN produced a decrease in blood pressure. The reduced blood pressure lasted for seven days. Autoradiography shows a significant decrease in ^{125}I-Sar-Ile Ang II binding in the PVN and in the AV3V region, particularly the organum vasculosum of the lamina terminalis (OVLT). Northern blot analysis of mRNA for Ao showed no change in mRNA levels between AS and control treated groups or between SHR and WKY strains.

Discussion

The experiments illustrate the viability of antisense inhibition *in vivo* for reduction of blood pressure in genetically hypertensive rats. Both antisense to angiotensinogen mRNA and to AT_1 receptor mRNA were successful in reducing blood pressure [8]. Reduction in blood pressure was correlated to an inhibition of Ang II synthesis and AT_1 receptor binding, respectively. Further experiments in our laboratory are being carried out on the effects of AS on angiotensinogen levels in brain, kidney and liver after angiotensinogen mRNA AS-ODN treatment and n receptor binding, *in vitro*. Physiological mechanisms associated with an overactive brain angiotensin, are also inhibited by the AS-ODN. These include: Ang II induced thirst and Ang II induced vasopressin release.

There are several practical issues that have to be considered in order to use AS-ODNs efficiently. These include a method of delivery, the stability of the ODNs in tissue and their ability t be taken up across the plasma membrane and delivered to the

mRNA for binding. The mechanisms by which antisense ODNs inhibit gene expression and the site of action in the nucleus also require further investigation. *In vitro* studies in our laboratory with FITC labeled AS-ODN have demonstrated the uptake of the ODN into hepatoma cells. The intracellular location of the labeled AS-ODN is revealed by confocal mincroscopy. For delivery of AS-DNA to tissues we are constructing a viral vector in a Sendai viral envelope. This method should integrate the AS-DNA into the chromosome and produce long-lasting inhibition of the angiotensinogen gene or AT_1 receptor gene. Our present results do show that sufficient ODN uptake occurs *in vivo* to provide inhibition of blood pressure which appears to be related to the inhibition of angiotensinogen gene or AT_1 receptor gene expression. The fact that AS treatment has no apparent effect on mRNA level is consistent with the proposed mechanism of action of AS molecules being at the translational level. The experiments demonstrate the feasibility of antisense ODN application for treatment of hypertension and we are currently developing methods of vector delivery for long-term inhibition and prevention of hypertension.

Acknowledgment

This work is supported by NIH HL27334.

Reprint requests to M. Ian Phillips, Department of Physiology, Box 100274, College of Medicine, University of Florida, Gainesville, Florida 32610-0274, USA.

References

1. Jeunemaitre X, Soubrier F, Kotelevtsev YV, Lifton RP, Williams CS, Charru A, Hunt SC, Hopkins PN, Williams RR, Lalouel J-M, Corvol P: Molecular basis of human hypertension: Role of angiotensinogen. *Cell* 71:169–180, 1992
2. Kimura S, Mullins J, Bunnemann B, Metzgher R, Hilgenfeldt U, Zimmerman F, Jacob H, Fuxe K, Ganten D, Kaling M: High blood pressure in transgenic mice carrying the rat angiotensinogen gene. *Embo* 11:821–827, 1992
3. Phillips MI, Mann JFE, Haebara H, Hoffman WE, Dietz R, Schelling P, Ganten D: Lowering of hypertension by central saralasin in the absence of plasma renin. *Nature* 270:445–447, 1977
4. Naruse M, Naruse K, McKenzie JC, Schelling P, Inagami T: Regional distribution of renin and angiotensinogen in the brain of normotensive (WKY) and spontaneously hypertensive (SHR) rats. *Brain Res* 333:147–150, 1985
5. Yongue BG, Angulo JA, McEwen BS, Myers MM: Brain and liver angiotensinogen messenger RNA in genetically hypertensive and normotensive rats. *Hypertension* 17:485–491, 1991
6. Gehlert DR, Speth RC, Wamsley JK: Quantitative autoradiography of angiotensin II receptors in the SHR. *Peptides* 7:1021–1027, 1986
7. Neckers L, Whitesell L, Rosolen A, Geselowitz DA: Antisense inhibition of oncogene expression. *Crit Rev Oncogene* 3:175–231, 1992
8. Gyurko R, Wielbo D, Phillips MI: Antisense inhibition of AT_1 receptor mRNA and angiotensinogen mRNA in the brain of spontaneously hypertensive rats reduces hypertension of neurogenic origin. *Reg Pept* 49:167–174, 1993
9. Ohkubo H, Kageyama R, Ujihara M, Hirose T, Inayama S, Nakanishi S: Cloning and sequence analysis of cDNA for rat angiotensinogen. *Proc Natl Acad Sci USA* 80:2196–2200, 1983
10. Murphy TJ, Alexander RW, Griending KK, Runge MS, Bernstein KE: Isolation of a cDNA encoding the vascular type-1 angiotensin II receptor. *Nature* 351:233–235, 1991
11. Chomczynsky P, Sacchi N: Single-step method of RNA isolation by acid guanidinium thiocyanate-phenol-chloroform extraction. *Anal Biochem* 162:156–159, 1987
12. Phillips MI, Kimura B, Raizada MK: Measurements of brain peptides: (vol 6) Angiotensin and ANP in tissue and cell cultures, in *Methods in Neuroscience*, 1991, pp 177–206

Molecular Brain Research, 21 (1994) 55–61

BRESM 70675

Specific inhibition of endogenous neuropeptide Y synthesis in arcuate nucleus by antisense oligonucleotides suppresses feeding behavior and insulin secretion

Akira Akabayashi [a], Claes Wahlestedt [b], Jesline T. Alexander [a] and Sarah F. Leibowitz [a]

[a] *The Rockefeller University, New York, NY 10021 (USA) and* [b] *Division of Neurobiology, Department of Neurology and Neuroscience, Cornell University Medical College, New York, NY 10021 (USA)*

(Accepted 1 June 1993)

Key words: Neuropeptide Y; Antisense oligonucleotide; Arcuate nucleus; Paraventricular nucleus; Feeding behavior

Neuropeptide Y (NPY), which is synthesized in neurons of the arcuate nucleus (ARC) that project to different hypothalamic nuclei, is known to have potent effects on eating behavior and hormone secretion after hypothalamic administration. To test the hypothesis that endogenous NPY is essential for the normal expression of these responses, the present study used two unmodified antisense oligodeoxynucleotides (ODNs) to disrupt the synthesis of NPY in the ARC and to examine the impact of this disturbance on nutrient intake, as well as on circulating levels of insulin and the adrenal steroids, corticosterone and aldosterone. Brain-cannulated rats maintained on macronutrient diets were given daily, bilateral injections, over a 4-day period, of NPY antisense ODNs, sense ODNs or saline into the ARC. The NPY antisense ODNs produced a significant decline (−33% relative to sense ODNs and −40% relative to saline, $P < 0.05$) in NPY levels in this nucleus, without causing any direct neural damage. Peptide levels in other hypothalamic areas, namely, the paraventricular nucleus and medial preoptic nucleus, were not significantly affected. In association with this reduction in ARC NPY, the antisense-treated animals exhibited a significant decrease in feeding behavior measured during the first 90 min of the natural feeding cycle, as well as over the 24-h period. In the 90-min interval, both carbohydrate and fat intake were suppressed by 65–70% ($P < 0.05$, relative to both saline and sense ODNs control scores). In addition, circulating insulin levels, in blood samples taken before the initiation of feeding, were significantly reduced by 50–55% ($P < 0.05$ relative to both saline and sense ODNs groups), while levels of corticosterone, aldosterone or glucose were unaltered. These findings provide the first evidence for physiological disturbances that may result from an inhibition of endogenous NPY production within neurons of the ARC.

INTRODUCTION

Neuropeptide Y (NPY), a member of the pancreatic polypeptide family[40], is highly concentrated within the hypothalamus[6,10]. It is synthesized within neurons of the arcuate nucleus (ARC), which project to several other hypothalamic nuclei, including the paraventricular nucleus (PVN) which is particularly dense with NPY terminals. This peptide exhibits bioactivity in multiple systems, at nanomolar concentrations, and is highly conserved across species[44], reflecting its possible importance as a brain neuromodulator. This is supported by a variety of evidence linking NPY to physiological processes related to feeding behavior, endocrine systems and circadian rhythms[11,22].

The specific role for NPY in these processes has been revealed by central injection studies. These investigations have shown NPY administration into the PVN[37] or into the third ventricle[9] to stimulate food intake, as well as induce the release of the glucoregulatory hormones, corticosterone (CORT)[23,45] and insulin[1]. These phenomena appear to be closely interrelated, as demonstrated by the finding that the feeding stimulatory effect of NPY, characterized by a specific preference for carbohydrate[34], is dependent upon CORT[36], which has a primary function in replenishing carbohydrate stores in the body. Their close relationship is also reflected by measurements of endogenous NPY levels in the ARC and PVN, which rise sharply at the beginning of the natural feeding cycle when there occurs a similar peak in circulating levels of CORT, as well as in appetite for carbohydrate[16,20,33]. These studies, in addition to findings showing increased NPY synthesis to be activated during states of negative energy balance, in-

Correspondence: S.F. Leibowitz, The Rockefeller University, 1230 York Avenue, New York, NY 10021, USA. Fax: (1) (212) 327-7974.

SSDI 0169-328X(93)E0104-8

cluding food deprivation, obesity and diabetes[7,11,31,46], indicate that NPY may contribute significantly to processes involved in maintaining or replenishing energy and nutrient stores, in particular, carbohydrate[22].

A critical step in substantiating this hypothesis is the demonstration that alterations in endogenous NPY or its receptors result in significant changes in feeding behavior and hormone release. Such studies have been precluded by the limited availability of tools that effectively modulate peptide synthesis within the brain. While there are two reports which demonstrated a reduction in food intake or carbohydrate ingestion after central injections of an NPY antiserum[38] and NPY receptor antagonist[24], important studies directly manipulating endogenous NPY synthesis itself have yet to be conducted.

The present investigation attempted this task by injecting antisense oligodeoxynucleotides (ODNs) to preproNPY mRNA directly into the ARC, where the hypothalamic NPY-synthesizing neurons are concentrated[6,10]. Antisense technology has been widely used to inactivate genes in vitro[3,13,27]. However, only very recently has an antisense ODN been demonstrated to be a powerful tool for blocking peptide synthesis in vivo. This has been shown in two publications, which have administered the ODN into either the cerebral ventricles[43] or the forebrain[8]. In the present report, the NPY ODNs injection was made into the ARC, which is believed to provide the major NPY projection involved in food ingestion[17,22]. Blockade of NPY production in this nucleus would be expected to cause a suppression of natural feeding and may also interfere with the secretion of pancreatic and adrenal hormones needed to metabolize the ingested food.

MATERIALS AND METHODS

Animals

Adult, male Sprague–Dawley rats ($n = 22$), obtained from the Charles River laboratory, were used in these studies. The animals, weighing 350–375 g at the start of the experiment, were individually housed in stainless steel cages (43 cm × 22 cm × 19 cm) in a temperature-controlled room (22 ± 2°C) illuminated on a 12:12 h light/dark schedule, with lights off at 15:30 h.

Diets

The animals were maintained on a free-feeding, self-selection paradigm and were provided with separate sources of protein, carbohydrate and fat, to allow them to alter separately intake of each of these nutrients while maintaining proper growth[33]. The protein diet (3.7 kcal/g) consisted of 93% casein (Bioserv) mixed with 4% minerals (USP XIV Salt Mixture Briggs, ICN Pharmaceuticals), 2.97% vitamins (Vitamin Diet Fortification Mixture, I.C.N. Pharmaceuticals), and 0.03% cysteine (L-cysteine-hydrochloride, ICN Pharmaceuticals). The carbohydrate diet (3.7 kcal/g) was composed of 28% dextrin, 28% corn starch (I.C.N. Pharmaceuticals), 37% sucrose (Domino) mixed with 4% minerals and 3% vitamins. The fat diet (7.7 kcal/g) consisted of 86% lard (Armour) mixed with 8% minerals and 6% vitamins. These diets were placed in separate glass jars at the front of the cage, with their placement changed daily to prevent position preferences. Water was available to the animals ad libitum, from a water pipe protruding through an opening at the back of the cage.

Food intake measurements

The animals were maintained on the 3 macronutrient diets prior to ODNs injection. Introduction of fresh diet and jar rotation was scheduled approximately 5 h before the onset of the nocturnal cycle (10:00 and 11:00 h), to ensure minimal disturbance to the animals at the start of their active feeding period. Over the course of the experiment, measurements of 24-h nutrient intake, as well as consumption during the first 90 min of the natural feeding cycle, were taken daily. Body weight measurements were recorded weekly.

Surgery

Animals were allowed to adapt to the macronutrient diets 2 weeks prior to cannulation. Rats were stereotaxically implanted, under Nembutal anesthesia, with chronic 26-gauge guide cannulae bilaterally aimed at the hypothalamic ARC. Stereotaxic coordinates used, with the incisor bar set 3.5 mm below interaural line, were: 6.4 mm anterior to interaural line; 0.2 mm lateral to midline suture; and 8.0 mm ventral to skull surface. The tip of the guide cannula ended approximately 1.5–2.0 mm dorsal to the ARC, to prevent excessive tissue damage to the area around the nucleus. The injector (33 gauge) extended 1.5 mm below the tip of the guide cannulae to reach the dorsal surface of the ARC. An obturator, which was the same length as the guide cannula, was inserted when injections were not being given. One week prior to the onset of the injection period, the animals were adapted to the experimental conditions by daily handling and mock injections.

Microinjection of antisense ODNs

Two 18-base antisense and sense unmodified ODNs to rat preproNPY mRNA[21] were designed and synthesized. The first antisense ODN corresponds to a sequence overlapping the initiation codon (5′-TTT-GTT-ACC-TAG-CAT-CTG-3′) and was microinjected in combination with another ODN, which corresponds to amino acids 18–23 of the mature NPY peptide (5′-AGC-GGA-GTA-GTA-TCT-GGC-3′). The corresponding sense ODNs (5′-AAA-CAA-TGG-ATC-GTA-GAC-3′ and 5′-TCG-CCT-CAT-CAT-AGA-CCG-3′), in addition to saline vehicle, were used as controls.

The antisense ODNs' inhibition of translation (translation arrest) is thought to result from interference with ribosomal activity (blockade of message read-through), ribonuclease H-mediated degradation of mRNA, or both[3,13,27]. The first sequence, designed to overlap the initiating codon, was used to block the message read-through effectively, a method shown to be successful in a recent study[43]. The second antisense ODN's sequence, corresponding to the mature NPY peptide, was utilized to facilitate further possible inhibition mechanisms specific to NPY. We have done a complete homology search for both sequences and have found nothing in the database for rodents (GENBANK) that would hybridize with the antisense sequences described above. To facilitate uptake of ODNs by cells, short lengths of 18 mers were used in this study.

These pairs of ODN probes, either the antisense or sense, were dissolved together in saline at a concentration of 125 ng/0.3 μl/probe, or a total 250 ng for both probes/0.3 μl. Dosage and length of injection period were determined from earlier work[43] and from preliminary experiments conducted in this laboratory using these antisense ODNs. Animals were injected manually over the course of approximately 1 min, with saline vehicle ($n = 6$, 0.3 μl/side), sense ($n = 7$, 250 ng/side, 500 ng/rat/day) or antisense ($n = 9$, 250 ng/side, 500 ng/rat/day) ODNs given bilaterally. Injections, given daily between 9:30 and 11:30 am over a 4-day period, were made using a Hamilton 10 μl syringe attached to a polyethylene tubing connected to the injector. Animals did not receive injections on the day of sacrifice (day 5), to minimize any disturbances prior to sacrifice.

Brain microdissection

On the 5th day, the rats were rapidly sacrificed by decapitation at the onset of the dark cycle (15:30 h), trunk blood was collected, and their brains were quickly removed, frozen on dry ice, and then stored at −80°C. Blood samples were also stored at −80°C until assay. Serial sections of 300 μm were cut, and the location of the injection site and any resulting damage was examined under a dissection microscope. Three hypothalamic areas, namely, the ARC, PVN, and medial preoptic nucleus (POM), were then micropunched, using the technique of Palkovits et al.[29] following the atlas of Paxinos and Watson[30]. In all cases, these 3 areas received minimal damage from the implanted cannulas. The PVN was chosen for investigation because of its known involvement in nutrient intake and hormone secretion[1,23,45], while the POM was selected as a reference site distant from the ODNs injection. Bilateral tissue samples were placed in 200 μl of 0.5 N cold acetic acid, boiled for 20 min and centrifuged, and the supernatant was then lyophilized and stored at −80°C until assayed for NPY. The pellet was dissolved in 1.0 N NaOH, and the protein content was measured according to the method of Lowry[25].

NPY radioimmunoassay

Neuropeptide Y-like immunoreactivity in the microdissected tissues were measured by radioimmunoassay, as described previously[4] with minor modifications. Briefly, the assay buffer was a 0.05 M phosphate buffer pH 7.4, 0.1% sodium azide, 0.25% bovine serum albumin. Porcine NPY (Peninsula, Belmont, CA) was used as standard. Antiserum for NPY was generously supplied by Dr. M.R. Brown, University of California, San Diego. The antiserum (100 μl), at a final dilution of 1/240000, and the standards or reconstituted samples (200 μl in assay buffer) were preincubated for 24 h at 4°C. Then 100 μl of tracer (^{125}I-NPY labeled with Bolton Hunter reagent, NEX222, Dupont Chemicals, Boston MA) was added and incubated for a further 24 h. The free and the antibody-bound NPY was separated by adding 500 μl of charcoal (2.5%) and dextran-70 (0.25%) solution. Bound fraction was measured in a gamma counter. The final dilution of antibody was chosen to achieve a total binding of ^{125}I-NPY of 40–45%. The assay sensitivity was 10 pg/tube, and the decrease of 50% of the bound activity was obtained for 50 pg/tube. The non-specific binding for the assay buffer was less than 9.0%, and intra- and interassay coefficients of variation were 5.0% and 9.4%, respectively.

Hormone radioimmunoassays

Serum CORT and insulin were measured according to the methods of Krey et al.[19] and Herbert et al.[14], respectively. Serum aldosterone (ALDO) levels were assayed using the commercially available KIT (TKAL2, Diagnostic Products Corporation, Los Angeles, CA). Serum glucose levels were analyzed with a Beckman Glucose Analyzer no. 2.

Statistics

The behavioral data reflect an average of measurements recorded for days 2–4 of the 4-day injection sequence. (The scores of 2 rats with highly variable 24-h intake measures were omitted from the average). Statistical analyses of saline vs. antisense/sense data were analyzed via one-way analysis of variance (ANOVA), while post hoc comparisons between individual means were made using Duncan's new multiple range test.

RESULTS

Examination of the bilateral injection sites for the NPY antisense and sense ODNs or saline showed that, in the 22 rats examined in this study, the tip of the injection was located along the dorsolateral border of the ARC, as illustrated by representative animals in Fig. 1, and there was no apparent damage to the

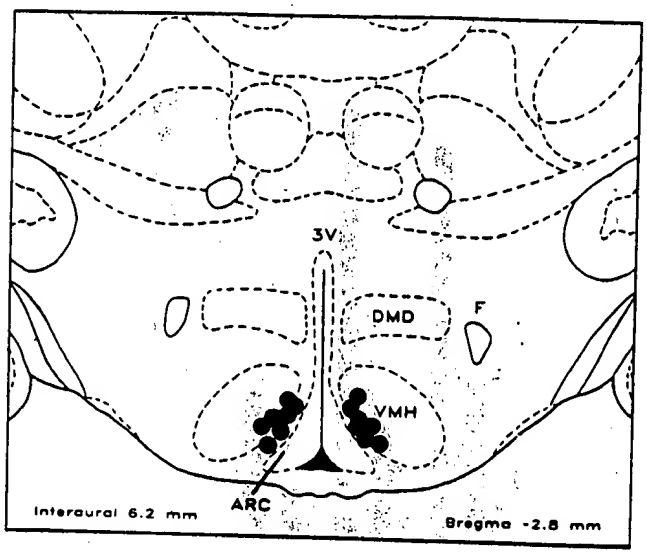

Fig. 1. Representative frontal diagram of the rat brain based on the atlas of Paxinos and Watson[30], illustrating central injection sites. ARC, arcuate nucleus; VMH, ventromedial hypothalamic nucleus; F, fornix; DMD, dorsomedial hypothalamic nucleus; 3V, third ventricle.

nucleus itself. Based on evidence mapping the spread within the hypothalamus of ^{125}I-NPY, administered in a similar volume of 0.3 μl[39], the ODNs would be expected to spread through most of the nucleus, including its most ventral extent which lies < 1.0 mm from the tip of the injector.

The results of the analyses of the NPY levels in the ARC, where the NPY cell bodies are concentrated, and in the PVN and POM, which contain primarily NPY terminals, are presented in Fig. 2. One-way ANOVA showed a significant change in NPY only in

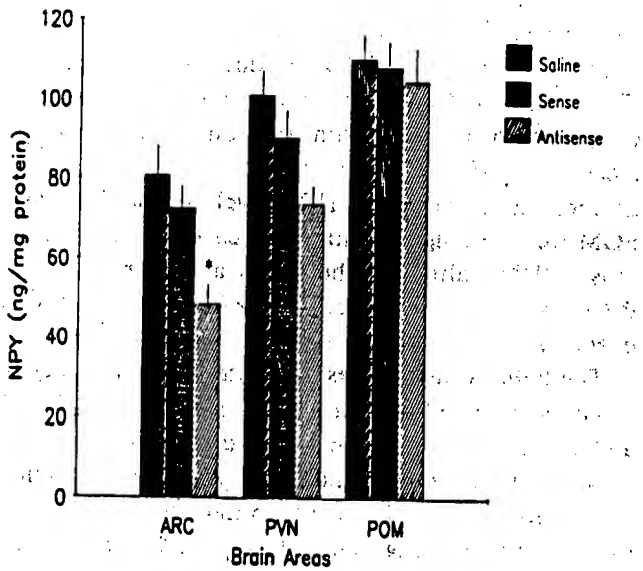

Fig. 2. Levels of NPY (ng/mg protein) in hypothalamic nuclei of rats after saline, sense or antisense oligodeoxynucleotides injections. * $P < 0.05$, relative to saline control and sense control by Duncan's new multiple range test. ARC, arcuate nucleus; PVN, paraventricular nucleus; POM, medial preoptic nucleus.

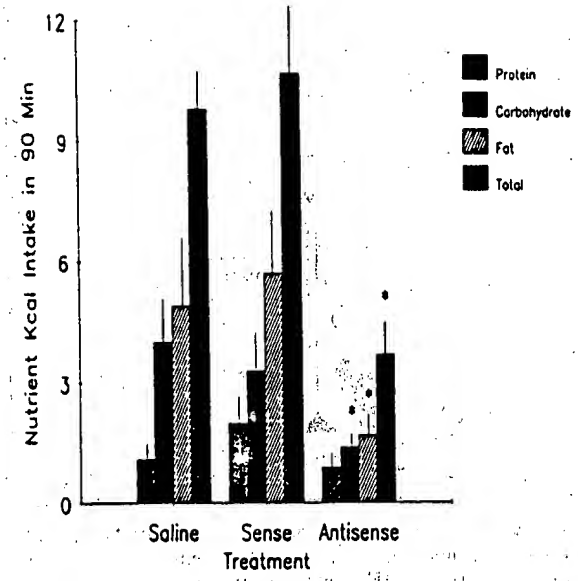

Fig. 3. Effect of saline, sense or antisense oligodeoxynucleotides treatment on 1.5-h macronutrient intake after dark onset. * $P < 0.05$, relative to saline and sense control by Duncan's new multiple range test.

the ARC ($F_{2,19} = 8.87$, $P < 0.01$). Comparisons between individual means showed that the baseline NPY levels of 80 ng/mg protein in this nucleus, detected in these cannulated rats after saline injection, were comparable to those measured in intact rats without brain cannulas[2]. Thus, the cannulation and injection procedures had minimal impact on endogenous NPY production. Comparisons between the sense and saline injections also showed no significant difference, indicating that the sense ODNs had no effect on NPY synthesis (Fig. 2). However, the antisense ODNs were effective in reducing NPY production in the ARC. They caused a 40% reduction ($P < 0.05$) in NPY levels compared to the saline control group and a 33% decrease ($P < 0.05$) compared to the sense ODNs group. In contrast to the ARC, NPY levels in the PVN and POM were not significantly affected by the NPY antisense ODNs, although there was a tendency for the PVN to show a decline (−27%) relative to saline injection.

The behavioral changes associated with this decline of endogenous NPY in the ARC are shown in Fig. 3 and Table I. Animals that received bilateral injections of the antisense ODNs showed a significant reduction in total food intake during the initial, 90-min period of the natural feeding cycle ($F_{2,19} = 9.45$, $P < 0.001$; −65% relative to sense and −62% relative to saline, $P < 0.05$). This decline in total caloric intake after NPY antisense ODNs was associated with a marked decrease in carbohydrate intake ($F_{2,19} = 3.84$, $P < 0.05$) and fat intake ($F_{2,19} = 4.06$, $P < 0.05$), between 65 and

TABLE I

Effect of saline, sense and antisense oligodeoxynucleotides administration on 24 h nutrient intake (kcal)

Values given are means ± S.E.M.

	Saline (n = 6)	*Sense (n = 7)*	*Antisense (n = 9)*
Protein	24.0 ± 3.5	26.1 ± 4.6	20.6 ± 3.5
Carbohydrate	30.5 ± 13.9	23.2 ± 4.6	28.8 ± 7.6
Fat	54.9 ± 13.8	46.9 ± 12.7	28.2 ± 5.2
Total	112.6 ± 3.3	96.3 ± 8.7	77.5 ± 2.9 *

* $P < 0.05$ relative to saline and sense control via Duncan's new multiple range test.

70% ($P < 0.05$) relative to both sense and saline control values. There was no significant change in protein ingestion ($F_{2,19} = 2.04$, $P > 0.10$).

The measurements of 24-h intake are presented in Table I. The antisense ODNs produced a clear decrease in total daily nutrient intake ($F_{2,17} = 5.32$, $P < 0.05$), between 20% and 30% ($P < 0.05$) relative to the sense and saline control values. A similar examination of the data for the individual nutrients, via ANOVA, failed to reveal any significant change, including the 49% decrease in 24-h fat intake ($F_{2,17} = 1.50$, $P > 0.10$). Body weights of the 3 treatment groups were found to be similar, remaining relatively stable over the 5-day experimental period.

The results obtained for the circulating hormones (Table II) demonstrated a significant change only in one hormone, namely, insulin, in association with the decrease in NPY levels of the ARC ($F_{2,19} = 4.74$, $P < 0.05$). While levels of CORT, ALDO and glucose remained stable after the sense or antisense ODNs injections, circulating insulin, at normal levels (65–70 μU/ml) in the two control groups, was significantly reduced (−56%, $P < 0.05$ relative to saline control;

TABLE II

Serum hormone and glucose levels after saline, sense and antisense oligodeoxynucleotide administration

Values given are means ± S.E.M.

	Saline (n = 6)	*Sense (n = 7)*	*Antisense (n = 9)*
Insulin (μU/ml)	70.1 ± 13.0	64.5 ± 11.2	31.0 ± 5.8 *
Corticosterone (μg%)	11.7 ± 1.0	15.5 ± 3.6	15.1 ± 2.5
Aldosterone (pg/ml)	249 ± 107	375 ± 104	321 ± 99
Glucose (mg/dl)	131 ± 5	133 ± 9	125 ± 6

* $P < 0.05$ relative to saline and sense control via Duncan's new multiple range test.

-52%, $P < 0.05$ relative to sense ODNs control groups) in the NPY antisense ODN-injected rats.

DISCUSSION

This study constitutes the first full report to show the effectiveness of antisense ODNs in altering endogenous NPY levels in the brain, as well as in having significant consequences in relation to specific physiological and behavioral processes. One of the first investigations with in vivo injections of an antisense ODN[43] examined an antisense ODN for the NPY Y_1 receptor after injections into the rat cerebral ventricles. This study demonstrated a significant reduction in cortical Y_1, but not Y_2, receptors, which was associated with a behavioral pattern of increased anxiety. Another report, using an antisense phosphorothioate ODN to c-*fos* mRNA, described a decrease in c-*fos* immunoreactivity in the striatum[8], and there are recent preliminary studies which have investigated antisense ODNs to NPY mRNA[15], vasopressin mRNA[12] or to estrogen/progesterone receptors[26,28]. The present report, which examined the antisense ODNs for NPY itself, administered the probes directly into the ARC, which accounts for at least 70% of the NPY innervation within the hypothalamus[6]. The antisense ODNs, after 4 days of injection, were effective in causing a 40% reduction in NPY levels within the ARC, in contrast to the NPY sense ODNs which had no apparent effect on NPY levels relative to saline. This result indicates that the antisense ODNs entered the ARC NPY-synthesizing neurons, presumably via receptor-mediated endocytosis[3,13], and remained sufficiently stable[18] to block NPY synthesis.

The behavioral consequences of this reduction in peptide levels in the ARC provide the first direct evidence that endogenous NPY, originating from neurons in this nucleus, is essential for the control of natural feeding patterns[22]. With this reduction in NPY levels of the ARC, the animals exhibited a profound decrease in their nutrient intake at the beginning of the natural feeding cycle, which was reflected in a smaller decline over the 24-h cycle. Neuropeptide Y is believed to be most active at the onset of the nocturnal feeding cycle, when it is most effective in stimulating carbohydrate intake[41] and when peak levels in the ARC, as well as the PVN, are detected[16]. A strong depression in carbohydrate ingestion (-65%) was seen after ARC injection of the antisense ODNs, consistent with a proposed role for endogenous NPY in the control of carbohydrate intake during the initial meals of the feeding cycle[22]. Fat ingestion was also depressed in these animals. Whereas hypothalamic injections of NPY invariably stimulate carbohydrate intake regardless of baseline preferences, this peptide may also potentiate fat ingestion in fat-preferring animals[35,41]. Together with the present results, this evidence indicates that endogenous NPY may contribute to the ingestion of fat in those animals with strong preferences for this nutrient. Since protein intake remained relatively stable in these animals, at the onset of the dark cycle as well as over the 24-h period, the reduction in carbohydrate and fat intake produced by the antisense ODNs does not appear to reflect a general debilitation.

A variety of evidence has indicated a primary role for the PVN, which is dense in NPY-containing terminals, in the control of nutrient intake. Local injection studies have shown this nucleus to be responsive to the stimulatory actions of NPY on carbohydrate intake[34], while biochemical studies have consistently shown profound changes in NPY levels of the PVN, similar to the ARC, in association with manipulations of nutritional status[31], as well as with natural preferences specifically for carbohydrate[17]. In response to ARC injections of NPY antisense ODNs, the animals of the present study, while exhibiting a clear decrease in NPY levels of ARC, showed a considerably smaller (insignificant) decline in peptide levels of the PVN, to which the ARC projects. This small change may reflect the fact that the PVN receives additional NPY projections from the lower brainstem[32], which would not have been affected by the antisense ODN injection.

In addition to controlling carbohydrate intake, NPY innervation to the PVN has also been implicated in the secretion of insulin from the pancreas[1]. Consistent with the evidence that PVN injection of NPY stimulates circulating levels of this hormone, the results of the present study revealed a dramatic decrease in insulin levels of animals with reduced NPY levels in the ARC after the antisense ODNs. Since the animals were sacrificed prior to the onset of their natural feeding and as much as 12 h since their last meal, this reduction in insulin appears to be a direct consequence of the reduced NPY production, rather than to any change in their feeding pattern. This control of insulin secretion by NPY may occur predominantly at the beginning of the natural feeding cycle, when peak hormone levels are detected[5] particularly in response to carbohydrate ingestion[42], and also when NPY levels in the ARC and PVN are highest[16].

A similar role for NPY in stimulating CORT secretion from the adrenal glands has also been proposed[23,45]. The antisense ODNs, however, failed to alter circulating levels of CORT, in contrast to insulin. Levels of ALDO and glucose were also unaltered.

Since the cell bodies synthesizing corticotropin-releasing factor in the PVN are very likely the site of NPY's endocrine action, the failure to reveal any change in CORT or ALDO release may be attributed to the fact that NPY innervation to the PVN was only partially affected by ARC antisense ODN injections and may, in part, be controlled by brainstem projections.

In summary, this report provides exciting new evidence for a method that can be used to modulate endogenous neuropeptide synthesis within the brain, as well as to test the physiological actions of the neuropeptides. The results obtained with the use of these antisense probes argue strongly for a role of hypothalamic NPY, originating from neurons in the ARC, in controlling nutrient intake during the initial periods of the natural feeding cycle, as well as the secretion of insulin in response to this nutrient ingestion.

Acknowledgements. This research was supported by USPHS Grant MH 43422 (S.F.L.), DA 06805 (C.W.), and a fellowship from The Naito Foundation (A.A.). The authors would like to thank Wai Cheung and Ivan Silva of Rockefeller University for their excellent technical assistance and Ms. Yim Dam of St-Luke's-Roosevelt Hospital Obesity Core Center for assistance with the insulin and glucose determinations.

REFERENCES

1 Abe, M., Saito, M. and Shimazu, T., Neuropeptide Y and norepinephrine injected into the paraventricular nucleus of the hypothalamus activate endocrine pancreas, *Biomed. Res.*, 10 (1989) 431–436.
2 Akabayashi, A., Zaia, C.T.B.V., Silva,I., Chae, H.J. and Leibowitz, S.F., Neuropeptide Y in the arcuate nucleus is modulated by alterations in glucose utilization, *Brain Res.*, in press.
3 Akhtar, S. and Juliano, R.L., Cellular uptake and intracellular fate of antisense oligonucleotides, *Trends Cell Biol.*, 2 (1992) 139–144.
4 Allen, R., Boublik, J., Hauger, R.L., Scott, N., Rivier, J. and Brown, M.R., Neuropeptide Y radio-immunoassay: Characterization and application, *Clin. Exp. Pharmacol. Physiol.*, 18 (1991) 825–833.
5 Armstrong, S., A chronometric approach to the study of feeding behavior, *Neurosci. Biobehav. Rev.*, 4 (1980) 27–53.
6 Bai, F.L., Yamano, M., Shiotani, Y., Emson, P.C., Smith, A.D., Powell, J.F. and Tohyama, M., An arcuato-paraventricular and -dorsomedial hypothalamic neuropeptide Y-containing system which lacks noradrenaline in the rat, *Brain Res.*, 331 (1985) 172–175.
7 Beck, B., Burlet, A., Nicolas, J.-P. and Burlet, C., Hypothalamic neuropeptide Y (NPY) in obese zucker rats: Implications in feeding and sexual behaviors, *Physiol. Behav.*, 47 (1990) 449–453.
8 Chiasson, B.J., Hooper, M.L., Murphy, P.R. and Robertson, H.A., Antisense ODN eliminates in vivo expression of c-*fos* in mammalian brain, *Eur. J. Pharmacol.*, 227 (1992) 451–453.
9 Clark, J.T., Kalra, P.S., Crowley, W.R. and Kalra, S.P., Neuropeptide Y and human pancreatic polypeptide stimulate feeding but inhibits sexual behavior in rat, *Endocrinology*, 155 (1984) 427–429.
10 DeQuidt, M.E. and Emson, P.C., Distribution of neuropeptide-Y like immunoreactivity in the rat central nervous system — II. Immunohistochemical analysis, *Neuroscience*, 18 (1986) 545–618.
11 Dumont, Y., Martel, J.C., Fournier, A., St-Pierre, S. and Quirion, R., Neuropeptide Y and neuropeptide Y receptor subtypes in brain and peripheral tissues, *Prog. Neurobiol.*, 38 (1992) 125–167.
12 Flanagan, L.M., McCarthy, M.M., Brooks, P.J., Pfaff, D.W. and McEwen, B.S., Arginine vasopressin (AVP) levels after daily infusions of antisense ODNs into the supraoptic nucleus (SON), *Soc. Neurosci. Abstr.*, 18 (1992) 481.
13 Helene, C. and Toulme, J.-J., Specific regulation of gene expression by antisense, sense and antigene nucleic acids, *Biochim. Biophys. Acta*, 1049 (1990) 99–125.
14 Herbert, V., Lau, K.S., Gottlieb, C.W. and Bleicher, S.J. Coated charcoal immunoassay of insulin, *J. Clin. Endocrinol. Metab.*, 25 (1965) 1375–1384.
15 Hulsey, M.G., Pless, C.M. and Martin, R.J., Effect of icv-administered anti-neuropeptide-Y antisense oligonucleotide on body weight and food intake in rats, *FASEB Abstr.*, 7 (1993) A88.
16 Jhanwar-Uniyal, M., Beck, B., Burlet, C. and Leibowitz, S.F., Diurnal rhythm of neuropeptide Y-like immunoreactivity in the suprachiasmatic, arcuate and paraventricular nuclei and other hypothalamic sites, *Brain Res.*, 536 (1990) 331–334.
17 Jhanwar-Uniyal, M., Beck, B., Jhanwar, Y.S., Burlet, C. and Leibowitz, S.F., Neuropeptide Y projection from arcuate nucleus to parvocellular division of paraventricular nucleus: Specific relation to the ingestion of carbohydrate, *Brain Res.*, in press.
18 Jirikowski, G.F., Sanna, P.P., Maciejewski-Lenoir, D. and Bloom F.E., Reversal of diabetes insipidus in brattleboro rats: intrahypothalamic injection of vasopressin mRNA, *Science*, 255 (1992) 996–998.
19 Krey, L., Lu, K.H., Hotchkiss, W., Piva, J. and Knobil, E. Surgical disconnection of the medial basal hypothalamus and pituitary function in the rhesus monkey. II. GH and cortisol secretion, *Endocrinology*, 96 (1975) 1088–1094.
20 Krieger, D.T., Rhythms in CRF, ACTH and corticosteroids. In D.T. Krieger (Ed.), *Endocrine Rhythms*, Raven, New York, 1979, pp. 123–142.
21 Larhammar, D., Ericsson, A. and Persson, H., Structure and expression of the rat neuropeptide Y gene, *Proc. Natl. Acad. Sci. USA*, 84 (1987) 2068–2072.
22 Leibowitz, S.F., Brain neuropeptide Y: An integrator of endocrine, metabolic, and behavioral processes, *Brain Res. Bull.*, 27 (1991) 333–337.
23 Leibowitz, S.F., Sladek, C., Spencer, L. and Tempel, D.L., Neuropeptide Y, epinephrine and norepinephrine in the paraventricular nucleus: Stimulation of feeding and the release of corticosterone, vasopressin and glucose, *Brain Res. Bull.*, 21 (1988) 905–912.
24 Leibowitz, S.F., Xuereb, M. and Kim, T., Blockade of natural and neuropeptide Y-induced carbohydrate feeding by a receptor antagonist PYX-2, *NeuroReport*, 3 (1992) 1023–1026.
25 Lowry, O.H., Rosebrough, N.J., Farr, A.L. and Randall, R.J., Protein measurement with the folin phenol reagent, *J. Biol. Chem.*, 193 (1951) 265–271.
26 McCarthy, M.M., Schlenker, E. and Pfaff, D.W., Neonatal intracerebral infusion of antisense DNA to estrogen receptor mRNA alters estrogen-dependent parameters in adult rats, *Soc. Neurosci. Abstr.*, 18 (1992) 893.
27 Murray, J.A.H. and Crockett, N., Antisense techniques: overview. In J.A.H. Murray (Ed.), *Antisense RNA and DNA*, Wiley, New York, 1992, pp. 1–50.
28 Ogawa, S., Olazabal, U.E. and Pfaff, D.W., Effects of hypothalamic administration of antisense DNA for progesterone receptor mRNA on lordosis behavior and progesterone receptor immunoreactivity, *Soc. Neurosci. Abstr.*, 18 (1992) 893.
29 Palkovits, M., Isolated removal of hypothalamic or other brain nuclei of the rat, *Brain Res.*, 59 (1973) 449–450.
30 Paxinos, G. and Watson, C., *The Rat Brain in Stereotaxic Coordinates*, 2nd ed., Academic Press, Orlando, FL, 1986.
31 Sahu, A., Kalra, P.S. and Kalra, S.P., Food deprivati n and ingestion induce reciprocal changes in neuropeptide Y concentrati ns in the paraventricular nucleus, *Peptides*, 9 (1988) 83–86.
32 Sawchenk , P.E., Swanson, L.W., Grzanna, R., Howe, P.R.C., Bloom, S.R. and Polak, J.M., Colocalization of neuropeptide Y immunoreactivity in brainstem catecholaminergic neurons that project to the paraventricular nucleus of the hypothalamus, *J. Comp. Neurol.*, 241 (1985) 138–153.

33 Shor-Posner, G., Ian, C., Brennan, G., Cohn, T., Moy, H., Ning, A. and Leibowitz, S.F., Self-selecting albino rats exhibit differential preferences for pure macronutrient diets: Characterization of three subpopulations, *Physiol. Behav.*, 50 (1991) 1187–1195.
34 Stanley, B.G., Daniel, D.R., Chin, A.S. and Leibowitz, S.F., Paraventricular nucleus injections of peptide YY and neuropeptide Y preferentially enhance carbohydrate ingestion, *Peptides*, 6 (1985) 1205–1211.
35 Stanley, B.G., Anderson, K.C., Grayson, M.H. and Leibowitz, S.F., Repeated hypothalamic stimulation with neuropeptide Y increases daily carbohydrate and fat intake and body weight gain in female rats, *Physiol. Behav.*, 46 (1989) 173–177.
36 Stanley, B.G., Lanthier, D., Chin, A.S. and Leibowitz, S.F., Suppression of neuropeptide Y-elicited eating by adrenalectomy or hypophysectomy: reversal with corticosterone, *Brain Res.*, 501 (1989) 32–36.
37 Stanley, B.G. and Leibowitz, S.F., Neuropeptide Y: Stimulation of feeding and drinking by injection into the paraventricular nucleus, *Life Sci.*, 35 (1984) 2635–2642.
38 Stanley, B.G., Magdalin, W., Seirafi, A., Nguyen, M.M. and Leibowitz, S.F., Evidence for neuropeptide Y mediation of eating produced by food deprivation and for a variant of Y1 receptor mediating this peptide's effect, *Peptides*, 13 (1992) 581–587.
39 Stanley, B.G., Magdalin, W., Seirafi, A., Thomas, W.J. and Leibowitz, S.F The perifornical area: the major focus of (a) patchily distributed hypothalamic neuropeptide Y-sensitive feeding system(s), *Brain Res.*, 604 (1993) 304–317.
40 Tatemoto, K., Carlquist, M. and Mutt, V., Neuropeptide Y – a novel brain peptide with structural similarities to peptide YY and pancreatic polypeptide, *Nature*, 296 (1982) 659–662.
41 Tempel, D.L. and Leibowitz, S.F., Diurnal variations in the feeding responses to norepinephrine, neuropeptide Y and galanin in the PVN, *Brain Res. Bull.*, 25 (1990) 821–825.
42 Unger, R.H. and Dobbs, R.E., Insulin, glucagon, and somatostatin secretion in the regulation of metabolism, *Annu. Rev. Physiol.*, 40 (1978) 307–343.
43 Wahlestedt, C., Merlo Pich, E., Koob, G.F., Yee, F. and Heilig, M., Modulation of anxiety and neuropeptide Y-Y1 receptors by antisense oligodeoxynucleotides, *Science*, 259 (1993) 528–531.
44 Wahlestedt, C. and Ries, D.J., Neuropeptide Y-related peptides and their receptors — are the receptors potential therapeutic drug targets?, *Annu. Rev. Pharmacol. Toxicol.*, 32 (1993) 309–352.
45 Wahlestedt, C., Skagerberg, G., Edman, R., Heilig, M., Sundler, F. and Hakanson, R., Neuropeptide Y (NPY) in the area of the paraventricular nucleus activates the pituitary-adrenocortical axis in the rat, *Brain Res.*, 417 (1987) 33–38.
46 Williams, G., Gill, J.S., Lee, Y.C., Cardoso, H.M., Okpere, B.E. and Bloom, S.R., Increased neuropeptide Y in specific hypothalamic nuclei of the streptozotocin-diabetic rat, *Diabetes*, 38 (1989) 321–327.

Proc. Natl. Acad. Sci. USA
Vol. 91, pp. 4499–4503, May 1994
Medical Sciences

Biologic and therapeutic significance of *MYB* expression in human melanoma

NOBUKO HIJIYA*, JIN ZHANG*, MARIUSZ Z. RATAJCZAK*, JEFFREY A. KANT*, KIM DERIEL†, MEENHARD HERLYN‡, GERALD ZON¶, AND ALAN M. GEWIRTZ*§‖

Departments of *Pathology and §Internal Medicine, University of Pennsylvania School of Medicine, †Temple University School of Medicine, and ‡Wistar Institute for Anatomy and Biology, Philadelphia, PA 19104; and ¶Lynx Therapeutics, Inc., Hayward, CA 94545

Communicated by Peter C. Nowell, November 25, 1993

ABSTRACT We investigated the therapeutic potential of employing antisense oligodeoxynucleotides to target the disruption of *MYB*, a gene which has been postulated to play a pathogenetic role in cutaneous melanoma. We found that *MYB* was expressed at low levels in several human melanoma cell lines. Also, growth of representative lines *in vitro* was inhibited in a dose- and sequence-dependent manner by targeting the *MYB* gene with unmodified or phosphorothioate-modified antisense oligodeoxynucleotides. Inhibition of cell growth correlated with specific decrease of *MYB* mRNA. In SCID mice bearing human melanoma tumors, infusion of *MYB* antisense transiently suppressed *MYB* gene expression but effected long-term growth suppression of transplanted tumor cells. Toxicity of the oligodeoxynucleotides was minimal in mice, even when targeted to the murine *Myb* gene. These results suggest that the *MYB* gene may play an important, though undefined, role in the growth of at least some human melanomas. Inhibition of *MYB* expression might be of use in the treatment of this disease.

Cutane us melanoma is a highly malignant and increasingly comm n neoplasm (1). Because metastatic melanoma remains incurable, new treatment approaches are needed. The ability to selectively disrupt the function of genes involved in malignant cell growth is an increasingly attractive therapeutic strategy. Technologies relevant to this purpose include homologous recombination, which actually destroys the targeted gene (2), and use of reverse complementary (antisense) RNA (3) or DNA (4–6) to interfere with utilization of the target gene's mRNA. The latter may be particularly well suited to therapeutic purposes since antisense oligodeoxynucleotides (ODNs) can be chemically synthesized and introduced directly into cells without the need for viral vectors. Problems attendent to the use and manufacture of viral vectors are thereby avoided. Further, the transient effect of antisense DNA on gene expression, as opposed to permanent alteration of the genome, may be desirable under these circumstances.

We previously reported that phosphorothioate-modified antisense ODNs (antisense [S]ODNs) targeted to the *MYB* protooncogene controlled the growth of a human leukemia in a SCID mouse model (7). *MYB* encodes a transcriptionally active nuclear binding protein, MYB, which plays an important regulatory role in cell proliferation (8) and differentiation (9). *MYB* is located on chromosome 6q22–23 in humans (10), where some human melanomas also have structural aberrations. Altered *MYB* expression has been implicated in the pathogenesis of melanoma (11–14). Accordingly, we targeted the *MYB* gene in human melan ma cells with antisense ODNs to learn more about the biologic importance of its expression in this disease and the therapeutic potential f disrupting its function.

The publication costs of this article were defrayed in part by page charge payment. This article must therefore be hereby marked "*advertisement*" in accordance with 18 U.S.C. §1734 solely to indicate this fact.

MATERIALS AND METHODS

ODNs. Unmodified phosphodiester ODNs and [S]ODNs (Lynx Therapeutics, Hayward, CA) complementary to the *MYB* gene were synthesized as reported (8, 15).

Cell Culture and *in Vitro* ODN Exposure. Melanoma cell lines were obtained from the American Type Culture Collection (Hs294T, A375, C32) or from Dupont Guerry (University of Pennsylvania School of Medicine) (SK-MEL-37, WM39). Cells were cultured in 96-well plates (10^3 cells/200 μl per well) to which ODNs (10–100 μg/ml) were added once or on two or five consecutive days. Effects on cell proliferation were determined by 3-(4,5-dimethylthiazol-2-yl)-2,5-diphenyltetrazolium (MTT) assay (CellTiter 96 nonradioactive cell-proliferation assay, Promega) (16).

Mice. Seven- to 8-week-old female CB-17/ACRTAC/*scid*/SDS mice were obtained from Taconic Farms. Animals with elevated IgM levels, as measured by ELISA (17), were excluded from the study.

Melanoma Transplantation into SCID Mice and Administration of [S]ODNs. Single-cell suspensions of Hs294T human melanoma cells (2×10^6 in 0.2 ml of Dulbecco's modified Eagle's medium) were injected subcutaneously in the right lower dorsal region of mice. [S]ODNs were administered by subcutaneously implanted Alzet constant-infusion pumps (Alza) (7).

Evaluation of Tumor Growth in Mice. Tumor weights *in vivo* were estimated from three separate diagonal measurements (18). Actual tumor weights were obtained at the time of sacrifice. Statistical significance of tumor weight differences was assessed by the Mann–Whitney nonparametric method.

RNA Extraction and Reverse Transcription–Polymerase Chain Reaction (RT–PCR). *MYB* and β-actin mRNA transcripts were detected by RT–PCR as described save that RT was primed with random hexamers (2 ng/μl) (19). The *MYB* amplification primers corresponded to mRNA nt 195–215 (5′ primer) and nt 444–464 (3′ primer) (10). The PCR product was detected with a probe corresponding to nt 355–375. β-Actin expression was detected with 5′ and 3′ primers corresponding to nt 600–621 and 905–885, respectively. The β-actin PCR product was detected with a ^{32}P-labeled probe corresponding to nt 795–815 (20).

Detection of Antisense [S]ODN in Tumor Tissue. Excised tumors were minced and multiply washed. DNA was extracted by standard methods, and 50 μg was electrophoresed in a 4% l w-melting agarose gel (FMC) and then transferred to a nylon membrane (Pall) in 3 M NaCl/0.3 M sodium citrate, pH 7. DNA was probed with a ^{32}P-end-labeled *MYB* sense oligomer complementary t the antisense DNA sequence.

Abbreviati ns: ODN, ligode xynucle tide; [S]ODN, phosphorothioate ODN; RT, reverse transcription.

‖To wh m reprint requests sh uld be addressed at: Room 230–John Morgan Building, University f Pennsylvania School of Medicine, 36th Street and Hamilton Walk, Philadelphia, PA 19104.

RESULTS

***MYB* Expression in Human Melanoma Cell Lines.** Though the integrity of the *MYB* locus on chromosome 6 has been scrutinized (11, 13, 14, 21), data concerning *MYB* expression in melanomas are sparse (22, 23). We therefore screened five human melanoma cell lines (Hs294T, SK-MEL-37, A375, C32, and WM39) for *MYB* mRNA by Northern analysis (19). Total RNA from each cell line (20 μg) was blotted to nitrocellulose and then probed with a ^{32}P-labeled human *MYB* cDNA (24). None of the lines gave a positive signal with this technique. However, when a sensitive RT–PCR was employed, *MYB* mRNA was unambiguously detected in all five cell lines (data not shown). Accordingly, *MYB* is most likely expressed in some melanoma cell lines, albeit at a low level. In accord with this finding, MYB protein levels were below detection limits in Western blot analysis of protein extracted from 7×10^3 SK-MEL-37 and Hs294T cells (data not shown).

Effect of Disrupting *MYB* Expression in Human Melanoma Cells. To determine the biological significance of low-level *MYB* expression in melanoma cells, we targeted the *MYB* message in SK-MEL-37 and Hs294T cells with unmodified or phosphorothioate antisense ODNs. Control DNA sequences were evaluated simultaneously to ensure that any effects observed were sequence specific. In Hs294T cells, for example, exposure to *MYB* sense sequences had no statistically significant effect on cell proliferation in comparison to untreated controls. In contrast, the *MYB* antisense DNA inhibited growth in a dose-responsive manner up to ≈60% ($P < 0.001$) of control cell values (data not shown). Growth inhibition was accompanied by loss of RT–PCR-detectable *MYB* mRNA, but not β-actin mRNA, suggesting that growth inhibition was secondary to pertubation of *MYB* expression.

Visual examination of the cultures revealed some clue regarding the mechanism of inhibition, which appeared to vary with the cell line. For example, after exposure to *MYB* antisense, Hs294T cells appeared to undergo cytolysis, suggesting that *MYB* perturbation could be a lethal event in these cells (Fig. 1*A*), whereas SK-MEL-37 cells appeared to undergo growth arrest with or without what appeared morphologically to represent differentiation toward a more mature phenotype (Fig. 1*B*).

Relationship of ODN Dose, Frequency of Exposure, and Inhibition of Cell Growth. We also examined cell growth inhibition as a function of ODN concentration and frequency of exposure. When SK-MEL-37 cells were exposed to ODNs, the most important factor for achieving growth inhibition was initial exposure to high concentrations of ODN (Fig. 2). For example, no effect on cell growth was observed when the ODNs were added to cultures in divided doses of 20 μg/ml per day for 2 days, or 10 μg/ml per day for 5 days. In contrast, when cells were exposed to a single bolus of 50 μg/ml, cell growth was inhibited ≈25% in comparison to untreated controls. This relationship was even more apparent at higher doses. A single total ODN dose of 100 μg/ml inhibited growth much more significantly than the same total dose delivered in divided doses of 20 μg/ml per day for 5 days (Fig. 2*A*). Even at doses up to 250 μg/ml, 50 μg/ml per day for 5 days was not as effective as a total of 200 μg/ml given as 100 μg/ml per day for 2 days (50% vs. 70% inhibition, respectively).

T determine whether these results were influenced by possible degradation of unmodified ODN, we carried out similar experiments with Hs294T cells exposed to the more stable [S]ODN. A similar but less strict relati nship between extracellular concentration and inhibition of cell growth was again observed (Fig. 2*B*). That is, initial high c ncentrations were more effective than equivalent final concentrations built up by cumulative lower doses. Accordingly, it appears that for either type of comp und, sufficient cellular uptake t

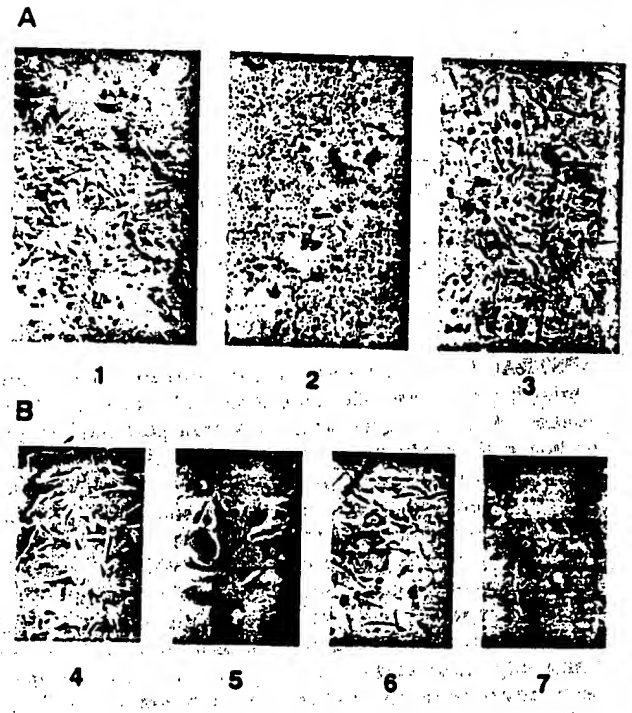

FIG. 1. Photomicrographs of Hs294T and SK-MEL-37 human melanoma cells incubated with *MYB* ODNs (100 μg/ml per day for 5 days). (*A*) Hs294T cells incubated with sense (*1*) or antisense (*2*) [S]ODNs or without ODNs (*3*). (*B*) SK-MEL-37 cells incubated with *MYB* sense (*4*) or antisense (*5*) ODNs without treatment (*6*), r with the differentiation-inducing agent mitomycin C (50 ng/ml per day for 5 days) (*7*). Note the morphologic similarity of cells in *5* and *7*. Under each culture condition cells display a flattened, stellate appearance, multiple dendrites, and increased numbers of pigment granule, all characteristics which suggest that the cells have undergone differentiation (25).

inhibit the target gene is achieved only by initial exposure to some critical "high" concentration of compound. Why cumulative lower doses of a stable compound are less effective is uncertain, but examination of this phenomenon may provide valuable information on oligomer uptake mechanisms, intracellular trafficking, and interactions with target mRNA.

Effect of *MYB* Antisense [S]ODN on Melanoma Tumor Growth *in Vivo*. We examined the effect of the *MYB* antisense

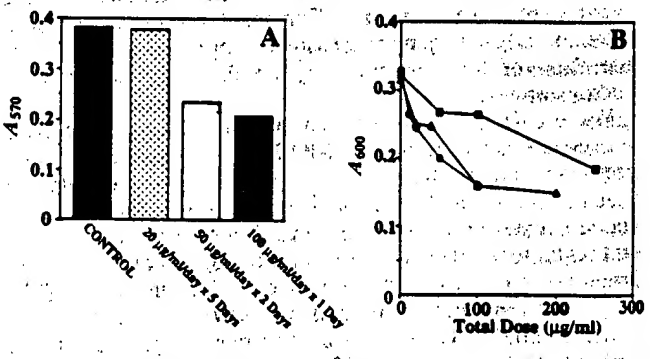

FIG. 2. Effects f c ncentrati n and frequency of ODN exposure on melan ma cell growth. (*A*) Effect f a total ODN dose of 100 μg/ml n SK-MEL-37 cell growth. Cells were exposed to *MYB* antisense ODNs f r five consecutive days (20 μg/ml per day), two consecutive days (50 μg/ml per day), or once (100 μg/ml). Cell growth was quantitated by MTT assay (A_{570} or A_{600}) 10 days after the start f culture. (*B*) A similar experiment carried out with [S]ODNs n Hs294T cells. T tal [S]ODN dose to which the cells were exposed is shown n the abscissa. The total dose was delivered either as a single d se ( ) r in equal divided daily d ses given ver 2 days (▲) or 5 days (■).

DNA on human melanoma cell growth in a SCID mouse model. In the first of three experiments to assess this question, 41 mice were inoculated with Hs294T cells. When tumor nodules became palpable, animals were randomly assigned to receive no treatment (13 animals) or 7-day infusions (500 μg/day; 25 μg/g of body weight) of *MYB* sense (14 animals) or antisense (14 animals) [S]ODN. Animals were examined daily for 40 days to determine the effects of the [S]ODN on survival and tumor growth. The antisense [S]ODN treatment significantly inhibited local tumor growth in comparison to the untreated and sense [S]ODN-treated groups. In fact, until ≈day 35, calculated tumor weights in the antisense group were ≈50% lower than the other groups. After this time, growth in the antisense-treated group recovered and essentially paralleled that seen in the untreated and sense-treated animals. Nevertheless, when the mice were sacrificed on day 40, tumors removed from the antisense-treated animals were significantly smaller ($P < 0.05$), 2.5 ± 0.5 g (mean ± SD), than those from the untreated and sense-treated groups, 3.5 ± 1.7 g and 3.3 ± 1.2 g, respectively.

We then examined the growth-inhibitory effects of the *MYB* antisense [S]ODN against a subclinical tumor burden. In this experiment, mice were subcutaneously inoculated with 2×10^6 Hs294T tumor cells. Three days later animals were randomized to receive no treatment (9 mice) or a 7-day infusion (500 μg/day) of *MYB* sense (8 mice) or antisense (10 mice) [S]ODN. Tumor growth was evaluated over a 65-day period (Fig. 3*A*). While no untreated mice were lost during this period, 3 sense- and 4 antisense-treated mice died of uncertain causes. In the remaining animals, inhibition of tumor growth in the antisense-treated group was again noted throughout the observation period and appeared to be greater than that observed in the first experiment. When the mice were sacrificed at 60 days after the pumps were implanted, mean tumor weights of untreated, sense, and antisense groups were 4.5 ± 1.7 g, 4.0 ± 1.5 g, and 2.1 ± 1.2 g, respectively. The differences between these groups were statistically significant ($P < 0.05$). Fig. 4 illustrates typical tumors observed in these mice.

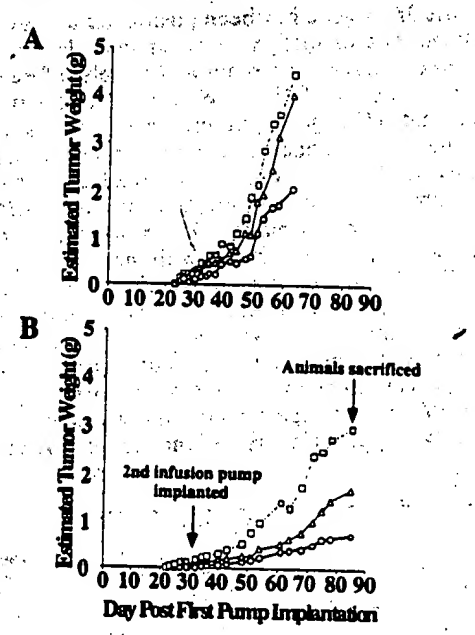

FIG. 3. Effect of *MYB* [S]ODN infusion n human melan ma tumor growth in SCID mice. Doses were 500 μg/day f r 7 days initiated 3 days after melanoma cell inoculation (*A*) r 500 μg/day for 14 days administered 3 days after inoculati n and then again 16 days after the first infusi n ended. ○, Antisense-treated; △, sense-treated; □, untreated.

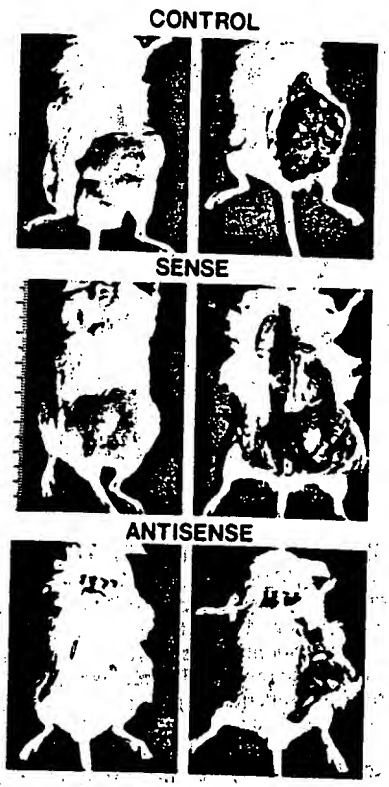

FIG. 4. Representative photomicrographs of melanomas *in situ* in animals which received *MYB* ODN infusions (500 μg/day for 7 days) beginning 3 days after tumor cell inoculation. Infusion pumps can be seen in the sense- and antisense-treated mice.

We lastly examined the effect of a repeat infusion on tum r growth. Mice (10 per group) were again inoculated with 2×10^6 tumor cells. Three days later they were randomized to receive no treatment or an infusion of sense or antisense [S]ODN (500 μg/day for 14 days). Sixteen days after the first infusion ended, a repeat infusion of identical dose and duration was begun. In this experiment, 3 control animals died tumor-related deaths during the observation period. In the antisense-treated animals tumor growth inhibition was more dramatic than in the previous experiments and persisted throughout the observation period (Fig. 3*B*). When animals were sacrificed 85 days after the first pump was implanted, mean tumor weights of control ($n = 7$), sense ($n = 9$), and antisense ($n = 10$) groups were 3.0 ± 2.0 g, 1.7 ± 1.5 g, and 0.7 ± 0.5 g. The difference in tumor weights between the untreated and antisense-treated groups was highly significant ($P < 0.01$), as was the difference between the sense-treated and antisense-treated groups ($P < 0.05$). Though it appeared that tumor sizes differed between the untreated and sense-treated groups, the differences were not of statistical significance ($P > 0.05$).

In contrast to the experiments carried out with a lower total dose of [S]ODN, none of the animals in the high dose, repeat-infusion sense- or antisense-treated groups died before the experiment was terminated. These results suggest that [S]ODN toxicity was n t a cause f animal deaths.

[S]ODN Uptake in Tum r Tissue and Correlation of Growth Inhibition with *MYB* mRNA Levels. To determine the extent of [S]ODN uptake int tumor tissue and to correlate effects on *MYB* expression with tum r growth, five mice with established tumors (≈0.5 g) were infused with *MYB* antisense [S]ODN (500 μg/day) for 7 days. On days 7, 9, and 11 after the infusion was begun, an animal was sacrificed and its tumor was excised to determine *MYB* mRNA levels in the tissue. *MYB* mRNA was measurably decreased (as normal-

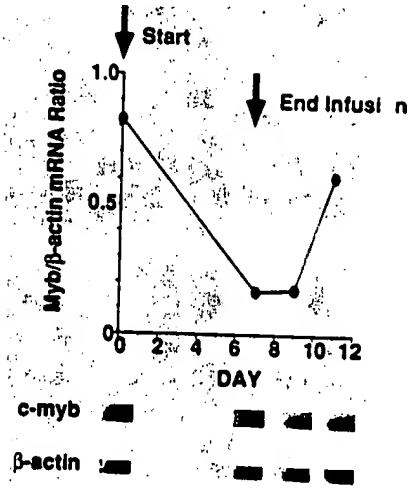

FIG. 5. Effect of *MYB* [S]ODNs on *MYB* mRNA expression in tumor tissue. *MYB* [S]ODNs (500 μg/day for 7 days) were infused into mice with established tumors (≈1.0 g). On days 7, 9, and 11 tumors were excised and total RNA was extracted from approximately equivalent amounts of tissue for RT–PCR detection of *MYB* and β-actin mRNA expression. The relative amount of *MYB* mRNA in each sample was estimated by normalization to the β-actin mRNA detected in the same sample.

ized to β-actin mRNA), but not completely eliminated, in comparison to control expression (Fig. 5). This decrement in *MYB* expression persisted for ≈2 days after the infusion finished but returned toward baseline thereafter.

Normalization of *MYB* expression may have been related to [S]ODN concentration in tissue falling below a critical level. In support of this hypothesis, [S]ODN levels in the tumor tissue decreased rapidly from an estimated 500 ng (per 50 μg of extracted DNA) during the infusion to 10–50 ng (per 50 μg of extracted DNA) on day 8, 1 day after the infusion finished (Fig. 6). Nevertheless, while human *MYB* expression will be selectively suppressed by the antisense DNA, the PCR primers employed for detection will amplify both human *MYB* mRNA and murine Myb mRNA. Since murine blood and stromal elements gradually infiltrate the tumor, some of the *MYB* mRNA detected could be contributed from this source.

T xicity of Murine *MYB* Antisense Oligomers in Mice. Mice receiving human *MYB* ODN behaved and fed normally and l st no weight. In addition, histopathologic examination of tissue fixed at the time of sacrifice revealed no organ damage (data not shown). As mentioned above, however, a small number of animals died of unexplained causes during the infusion studies. Such deaths occurred approximately equally in each treatment group and were therefore unrelated to the ODN sequence infused. Further, since there were no unexplained deaths in the animals that received the highest

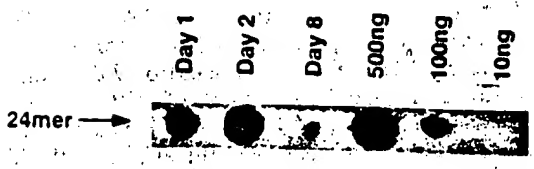

FIG. 6. Detection of *MYB* antisense ODN in tumor tissue. Mice with established tumors were infused with *MYB* antisense ODN (500 μg/day for 7 days). The tumors were excised on days 1, 2, and 8 after start of the infusion. Tumor DNA was extracted, electrophoresed in 4% agarose, and blotted to nylon membranes as noted above. Tumor [S]ODN content was estimated by probing the blotted material with a ^{32}P-end-labeled *MYB* sense oligomer. Relative band intensity was then compared with known DNA standards of 500, 100, and 10 ng (shown in the three lanes at right).

ODN doses (i.e., two infusions), it appears that while [S]ODN toxicity cannot be ruled out as a cause of death in these cases, this explanation seems unlikely.

To model potential toxicity in a human host, mice were also infused with murine *MYB* sense and antisense sequences, up to 1 mg/day for 14 days. No clinically significant untoward effects were observed in these mice (Table 1). The mice behaved normally and their body weights did not change. Of interest, however, mice did manifest thrombocytopenia which appeared to be neither sequence nor dose related. The level of thrombocytopenia was mild to moderate and caused no detectable bleeding abnormality. Animals receiving the highest dose of antisense DNA also manifested splenomegaly. Histopathology of hypertrophied spleens demonstrated lymphoid and myeloid hyperplasia with increased megakaryocytes. We therefore posit that the spleen, an important hematopoietic organ in the mouse, may have been compensating for hematopoietic suppressive effects of the *MYB* antisense [S]ODN.

DISCUSSION

Though the *MYB* gene has been postulated to play a role in the pathogenesis of malignant melanoma, data supporting this hypothesis have been scant and largely inferential (11–14). Using antisense DNA, we now provide some direct evidence that *MYB* gene expression is important for the growth and maintenance of several human melanoma cell lines. Why MYB deprivation causes cytolysis in some cells (Hs294T) and apparent differentiation in others (SK-MEL-37) is unclear. Also enigmatic is the prolonged growth suppression (>2 months) associated with the transient suppression of *MYB*. In the first *in vivo* experiment this might have been more apparent than real, since after an initial delay, growth of the tumor mass in antisense-treated animals appeared to parallel that seen in the control groups. However, this did not seem to be the case in the second (Fig. 4*A*) and third (Fig. 4*B*) *in vivo* experiments, where tumor growth was considerably suppressed. Here one could postulate that

Table 1. Toxicity of murine *MYB* antisense [S]ODNs for BALB/c mice

[S]ODN	Dose, μg/day	Leukocytes, no. × 10⁻³ per mm³			Hematocrit, %			Platelets, n . × 10⁻³ per mm³			Spleen weight, mg
		Day 0	Day 14	Day 21	Day 0	Day 14	Day 21	Day 0	Day 14	Day 21	Day 21
Sense	100	3.2	7.7	3.2	53	52	52	554	635	215	140
	300	3.4	6.7	2.9	52	51	51	642	619	218	123
	1000	2.7	3.5	3.6	52	49	51	491	421	346	111
Antisense	100	2.6	4.5	2.6	53	47	48	740	412	188	165
	300	2.1	5.1	2.7	52	44	48	595	397	183	181
	1000	2.7	3.3	4.8	52	44	49	503	230	279	273

[S]ODNs corresponding to murine *Myb* mRNA codons 2–9 were administered to BALB/c mice at various doses for 14 days by Alzet pumps. Blood cells were c unted in a hemocyt meter and hematocrit was determined by centrifugati n f heparinized blood on days 0, 14, and 21. Spleens were weighed immediately after death.

deprivation of MYB led to a persistent, though apparently nonlethal, growth-deprived state. Alternatively, MYB deprivation may have led to cell death in a sensitive subset of cells and to cytostasis in another which eventually recovered. Therefore, the protein probably exerts different functions within and between cells of a given type, and these functions most likely depend on the state of differentiation and cell cycle status. Unmasking these functions through inhibition studies of this type may provide useful clues to the function of MYB in nonhematopoietic cells and to the identity of potential protein partners in these effects.

That we obtained growth inhibition by targeting a gene expressed at such low levels may be viewed as surprising. However, recent reports suggest that low-level gene expression can have significant biological import (26, 27). For example, Burk *et al.* (27) reported that MYB protein cooperatively interacted with C/EBP transcription factor proteins, but only when *MYB* was expressed at a low level. High-level *MYB* expression abrogated this synergy. Accordingly, it is reasonable to hypothesize from all these studies that low-level *MYB* expression is of biological significance in melanoma cells.

The experiments reported herein serve as a paradigm of ODN-based therapeutics for human malignancies. Nevertheless, while it is clear that *MYB* is an effective target in human melanoma, it is not necessarily the best target for this strategy. It is equally straightforward that further development of the antisense strategy will be needed before the successful application of this technique in the clinic can be anticipated. Knowledge concerning DNA uptake mechanisms, intracellular ODN trafficking, mRNA disruption mechanisms, and, of equal importance, how apparent resistance develops will all contribute significantly to the effective pharmaceutical use of these compounds. Accordingly, while this area remains in its scientific infancy, these *in vivo* studies and those of our colleagues (28–30) convince us that modulation of gene expression with antisense DNA is a therapeutic strategy worth pursuing.

The editorial assistance of E. R. Bien is gratefully acknowledged. This work was supported in part by U.S. Public Health Service Grants CA54384 and CA51083 (A.M.G.) and CA25874 (M.H.). A.M.G. is the recipient of a Research Career Development Award from the National Cancer Institute.

1. American Cancer Society (1992) *American Cancer Society: Cancer Facts and Figures-1992* (ACS, Atlanta).
2. Mansour, S. L., Thomas, K. R. & Capecchi, M. R. (1988) *Nature (London)* 336, 348–352.
3. Prochownik, E. V., Kukowska, J. & Rodgers, C. (1988) *Mol. Cell. Biol.* 8, 3683–3695.
4. Zamecnik, P. C. & Stephenson, M. L. (1978) *Proc. Natl. Acad. Sci. USA* 75, 280–284.
5. Gewirtz, A. M. & Calabretta, B. (1991) in *Prospects for Antisense Nucleic Acid Therapy of Cancer and AIDS*, ed. Wickstrom, E. (Liss, New York), pp. 53–61.
6. Ratajczak, M. Z., Hijiya, N., Catani, L., DeRiel, K., Luger, S. M., MacGrave, P. & Gerwirtz, A. M. (1992) *Blood* 79, 1956–1961.
7. Ratajczak, M. Z., Kant, J. A., Luger, S. M., Hijiya, N., Zhang, J., Zon, G. & Gewirtz, A. M. (1992) *Proc. Natl. Acad. Sci. USA* 89, 11823–11827.
8. Gewirtz, A. M. & Calabretta, B. (1988) *Science* 242, 1303–1306.
9. Todokoro, K., Watson, R. J., Higo, H., Amanuma, H., Kuramochi, S., Yanagisawa, H. & Ikawa, Y. (1988) *Proc. Natl. Acad. Sci. USA* 85, 8900–8904.
10. Majello, B., Kenyon, L. C. & Dalla-Favera, R. (1986) *Proc. Natl. Acad. Sci. USA* 83, 9636–9640.
11. Linnenbach, A. J., Huebner, K., Reddy, E. P., Herlyn, M., Parmiter, A. H., Nowell, P. & Koprowski, H. (1988) *Proc. Natl. Acad. Sci. USA* 85, 74–78.
12. Trent, J. M., Thompson, F. H. & Meyskens, F. L. J. (1989) *Cancer Res.* 49, 420–423.
13. Meese, E., Meltzer, P. S., Witkowski, C. M. & Trent, J. (1989) *Genes Chromosomes Cancer* 1, 88–94.
14. Dasgupta, P., Linnenbach, A. J., Giaccia, A. J., Stamato, T. D. & Reddy, E. P. (1989) *Oncogene* 4, 1201–1205.
15. Zon, G. & Stec, W. J. (1991) in *Oligonucleotides and Analogues: A Practical Approach*, ed. Eckstein, F. (Oxford Univ. Press, Oxford), pp. 87–108.
16. Promega Corporation (1991) in *Technical Bulletin #112* (Promega, Madison, WI).
17. Coligan, J. E., Kruisbeek, A. M., Margulies, D. H., Shevach, E. M. & Strober, W. (1993) *Current Protocols in Immunology* (Greene Associates, New York), pp. 2.1.2–2.1.22.
18. Morrison, S. D. (1983) *J. Natl. Cancer Inst.* 71, 407–408.
19. Sambrook, J., Fritsch, E. F. & Maniatis, T. (1989) *Molecular Cloning: A Laboratory Manual* (Cold Spring Harbor Lab. Press, Plainview, NY).
20. Nakajima-Iijima, S., Hamada, H., Reddy, P. & Kakunaga, T. (1985) *Proc. Natl. Acad. Sci. USA* 82, 6133–6137.
21. Kacker, R. K., Giovanella, B. C. & Pathak, S. (1990) *Anticancer Res.* 10, 859–871.
22. Fumagalli, S., Doneda, L., Nomura, N. & Larizza, L. (1993) *Melanoma Res.* 3, 23–27.
23. Husein, Z., FitzGerald, G. B. & Wick, M. M. (1990) *J. Invest. Dermatol.* 95, 571–575.
24. Leprince, D., Saule, S., de Taisne, C., Gegonne, A., Begue, A., Righi, M. & Stehelin, D. (1983) *EMBO J.* 2, 1073–1078.
25. Trent, J. M., Stanbridge, E. J., McBride, H. L., Meese, E. U., Cassey, G., Araujo, D. E., Witkowski, C. M. & Nagel, R. B. (1990) *Science* 247, 568–571.
26. Sims, J. E., Gayle, M. A., Slack, J. L., Alderson, M. R., Bird, T. A., Giri, J. G., Colotta, F., Re, F., Mantovani, A., Shanebeck, K., Grabstein, K. H. & Dower, S. K. (1993) *Proc. Natl. Acad. Sci. USA* 90, 6155–6159.
27. Burk, O., Mink, S., Ringwald, M. & Klempnauer, K.-H. (1993) *EMBO J.* 12, 2027–2038.
28. Agrawal, S., Goodchild, J., Civeira, M. P., Thornton, A. H., Sarin, P. S. & Zamecnik, P. C. (1988) *Proc. Natl. Acad. Sci. USA* 85, 7079–7083.
29. Bayever, E., Iversen, P., Smith, L., Spinolo, J. & Zon, G. (1992) *Antisense Res. Dev.* 2, 109–110.
30. Kitajima, I., Shinohara, T., Bilakovics, J., Brown, D. A., Xu, X. & Nerenberg, M. (1992) *Science* 258, 1792–1795.